

UNCLASSIFIED

~~CONFIDENTIAL~~

Copy 48  
NACA  
RM-A51A12

C-1

NACA RM A51A12

NACA

GROUP 4  
Downgraded at 3 year intervals; declassified after 12 years

# RESEARCH MEMORANDUM CASE FILE COPY

THE TRANSONIC CHARACTERISTICS OF 17 RECTANGULAR,  
SYMMETRICAL WING MODELS OF VARYING  
ASPECT RATIO AND THICKNESS

By Warren H. Nelson and John B. McDevitt

Ames Aeronautical Laboratory  
Moffett Field, Calif.

JPL LIBRARY  
CALIFORNIA INSTITUTE OF TECHNOLOGY  
MAY 21 1951

CLASSIFIED DOCUMENT

This document contains classified information affecting the National Defense of the United States within the meaning of the Espionage Act, USC 50:31 and 32. Its transmission or the revelation of its contents in any manner to an unauthorized person is prohibited by law.

Information so classified may be imparted only to persons in the military and naval services of the United States, appropriate civilian officers and employees of the Federal Government who have a legitimate interest therein, and to United States citizens of known loyalty and discretion who of necessity must be informed thereof.

## NATIONAL ADVISORY COMMITTEE FOR AERONAUTICS

WASHINGTON

May 10, 1951

~~CONFIDENTIAL~~  
UNCLASSIFIED



~~UNCLASSIFIED~~

## NATIONAL ADVISORY COMMITTEE FOR AERONAUTICS

RESEARCH MEMORANDUMTHE TRANSONIC CHARACTERISTICS OF 17 RECTANGULAR,  
SYMMETRICAL WING MODELS OF VARYING  
ASPECT RATIO AND THICKNESS

By Warren H. Nelson and John B. McDevitt

## SUMMARY

An investigation to determine the aerodynamic characteristics of a series of thin, rectangular wings was conducted in the Ames 16-foot high-speed wind tunnel, utilizing the transonic-bump technique over a Mach number range from 0.40 to 1.10, corresponding to a Reynolds number range from 1.25 to 2.05 million. The lift, drag, and pitching-moment data are presented for wings having aspect ratios of 6, 4, 2, and 1, and NACA 63AOXX sections with thickness-to-chord ratios of 10, 8, 6, 4, and 2 percent.

## INTRODUCTION

The purpose of this investigation was to provide comprehensive data on the effects of aspect ratio and thickness on the aerodynamic characteristics of a family of symmetrical, straight wings through the transonic speed range.

Seventeen wings in all were investigated, with aspect ratios of 6, 4, 2, and 1. Rectangular plan forms were used, and the profiles were NACA 63AOXX sections having thickness-to-chord ratios of 10, 8, 6, 4, and 2 percent.

In order to obtain an indication of the reliability of the bump data, a semispan scale model of the larger, full-span, aspect-ratio-2 wing reported in reference 1 was also constructed and tested on the bump.

The results are presented without analysis to expedite publication.

~~UNCLASSIFIED~~

## NOTATION

$C_D$	drag coefficient $\left( \frac{\text{twice semispan drag}}{qS} \right)$
$\Delta C_D$	total drag coefficient minus drag coefficient at zero lift
$C_L$	lift coefficient $\left( \frac{\text{twice semispan lift}}{qS} \right)$
$C_m$	pitching-moment coefficient, referred to $0.25 \bar{c}$ $\left( \frac{\text{twice semispan pitching moment}}{qS\bar{c}} \right)$
$A$	aspect ratio $\left( \frac{b^2}{S} \right)$
$\frac{L}{D}$	lift-drag ratio
$\left( \frac{L}{D} \right)_{\max}$	maximum lift-drag ratio
$M$	Mach number
$R$	Reynolds number based on mean aerodynamic chord
$S$	total wing area (twice wing area of semispan model), square feet
$V$	velocity, feet per second
$b$	twice span of semispan model, feet
$c$	local wing chord, feet
$\bar{c}$	mean aerodynamic chord $\left( \frac{\int_0^{b/2} c^2 dy}{\int_0^{b/2} c dy} \right)$ , feet
$q$	dynamic pressure $\left( \frac{1}{2} \rho V^2 \right)$ , pounds per square foot
$\frac{t}{c}$	thickness-to-chord ratio
$y$	spanwise distance from plane of symmetry, feet
$\alpha$	angle of attack, degrees
$\rho$	air density, slugs per cubic foot
$\frac{dC_L}{d\alpha}$	slope of lift curve measured at zero lift, per degree

$\frac{dC_m}{dC_L}$  slope of pitching-moment curve measured at zero lift

## APPARATUS

### Wind Tunnel and Equipment

These tests were conducted on a transonic bump in the Ames 16-foot high-speed wind tunnel. The bump is described in detail in reference 2. The aerodynamic forces and moments were measured by means of a strain-gage balance mounted inside the bump.

### Models

The sting-supported full-span model mounted centrally in the wind tunnel and the similar reduced-scale, semispan model mounted on the bump are shown in figure 1. These wings, used to provide a comparison of the results obtained with the two testing techniques, had NACA 65<sub>1</sub>-210 sections, aspect ratios of 2, and taper ratios of 0.4.

A typical mounting of the rectangular wings on the bump is shown in figure 2. The principal dimensions and plan forms of the rectangular wings are shown in figure 3. Five aspect-ratio-6 wings of the various thicknesses used were constructed and the aspect ratios of 4, 2, and 1 were obtained by successively cutting off the tips. The profiles were NACA 63AOXX sections having thickness-to-chord ratios of 10, 8, 6, 4, and 2 percent (fig. 4).

A fence located 3/16 inch from the bump surface was used to keep leakage, originating inside the bump, from affecting the flow over the model. This leakage is the result of clearance between the wing and bump surface required for this type of mounting.

## TESTS AND PROCEDURE

### Range of Test Variables

The characteristics of the rectangular wings were investigated for a Mach number range from 0.4 to 1.10. The variation of Reynolds number with Mach number for the rectangular wings is shown in figure 5. The angle-of-attack range was limited from -2° to 20° by the balance mechanism, and for some of the thinner wings it was limited to a smaller angle-of-attack range by the bending stress at the root. No data were

obtained for the aspect-ratio-6 wings with thickness ratios of 0.04 and 0.02 and the aspect-ratio-4 wing with a thickness ratio of 0.02 because of structural weakness and susceptibility to flutter at high subsonic speeds.

#### Reduction of Data

The test data have been reduced to standard NACA coefficient form. A drag correction was applied to account for an interaction between the lift and drag components of the balance. A tare correction to the drag of the rectangular wings to account for the drag of the fence was evaluated by cutting the wing off flush with the fence and testing the fence alone. The tare corrections applied and the areas of the fence and wings are given in the following list:

Aspect ratio	Semispan wing area (sq ft)	Fence area (sq ft)	Fence area		Fence tare-drag coefficient
				Semispan wing area	
6	0.750	0.159		0.21	0.0014
4	.500	.159		.32	.0022
2	.250	.159		.64	.0043
1	.125	.159		1.27	.0085

The measured fence tare-drag coefficient did not change appreciably with Mach number or with changes in angle of attack. The interference effects of the fence and the effects of leakage around the fence are unknown; corrections for these effects have not been made. These effects would be greatest on the lower aspect-ratio wings since they have the smaller area.

An angle-of-attack correction of  $-0.4^{\circ}$  was included due to the cross flow over the bump.

The models investigated on the transonic bump are mounted in a local, high-velocity region. Typical contours of local Mach number in the bump flow field are shown in figure 6. Outlines of the rectangular wings have been superimposed on these diagrams to indicate the Mach number gradients which existed across the wings during the tests. No attempt has been made to evaluate the effects of these gradients. The test Mach numbers presented in this report are the average Mach numbers over the wings.

## RESULTS

The results are presented without analysis to expedite publication.

The drag data presented herein should be used with caution, particularly that for the lower Mach numbers or aspect ratios where the measured loads were small compared to the capacity of the balance. For this reason, only data above 0.70 Mach number have been used in the cross plots involving drag measurements. Other factors which contribute to the uncertainty of the drag data are the large drag tares (for the lower aspect ratios), the fact that the lift-drag interaction mentioned previously may have varied slightly with time, and the Mach number gradients existing throughout the flow field of the bump. However, it is believed that the trends shown throughout the transonic speed range are qualitatively correct.

Figure 7 presents a comparison of the lift, drag, and pitching-moment data for the tapered, aspect-ratio-2, NACA 65<sub>1</sub>-210 wings for the full-span model mounted on a sting in the center of the wind tunnel, and for the semispan model mounted on the bump. The Reynolds number range was about 2 to 3 million for the bump test, and it was about 6 to 9 million for the sting test.

The basic lift, drag, and pitching-moment data from the bump tests of the rectangular wings are presented in figures 8 through 10.

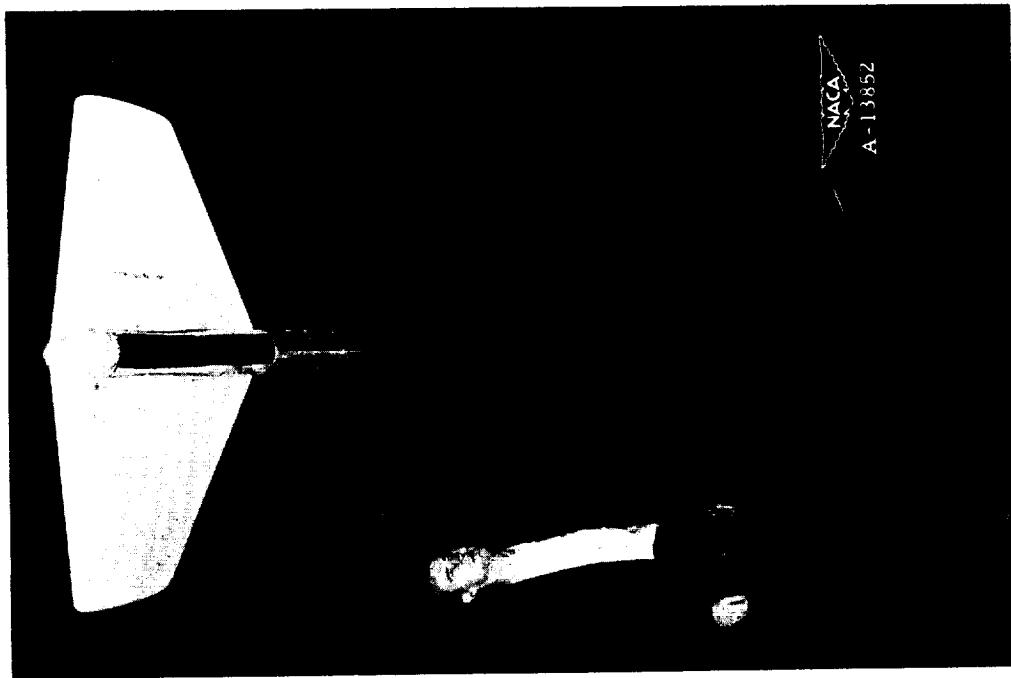
The variation of lift-drag ratio with lift coefficient is shown in figure 11. The maximum lift-drag ratios and the lift coefficients at which they occurred are shown as functions of Mach number in figures 12 and 13, respectively. The maximum lift-drag ratios appear erratic for some of the wings (especially the aspect-ratio-1 wings), particularly at the lower transonic Mach numbers. However, it is believed that the trends shown at the higher Mach numbers are correct. Phenomena of flow separation and reattachment as well as changes in the boundary layer may occur as the Mach number changes, so that it seems probable that some of the irregularities indicated do actually exist. In particular, a dip in the L/D maximum curve near 0.8 Mach number may appear for thin wings of low aspect ratios (reference 3).

The variations with Mach number of the lift-curve slopes, the drag coefficients, and the pitching-moment-curve slopes are shown in figures 14 through 16 for rectangular wings. All the slopes shown in these summary curves were measured at zero lift. It should be noted that slopes are shown even for those cases in which the curves were nonlinear.

Ames Aeronautical Laboratory,  
National Advisory Committee for Aeronautics,  
Moffett Field, Calif.

## REFERENCES

1. Nelson, Warren H., and Erickson, Albert L.: The Effect of Aspect Ratio on the Subsonic Aerodynamic Characteristics of Wings with NACA 65<sub>1</sub>-210 Sections. NACA RM A9K18, 1949.
2. Axelsohn, John A., and Taylor, Robert A.: Preliminary Investigation of the Transonic Characteristics of an NACA Submerged Inlet. NACA RM A50C13, 1950.
3. Reese, David E., Jr., and Phelps, E. Ray: Lift, Drag and Pitching Moment of Low-Aspect-Ratio Wings at Subsonic and Supersonic Speeds - Plane Tapered Wing of Aspect Ratio 3.1 With 3-Percent-Thick, Biconvex Section. NACA RM A50K28, 1950.

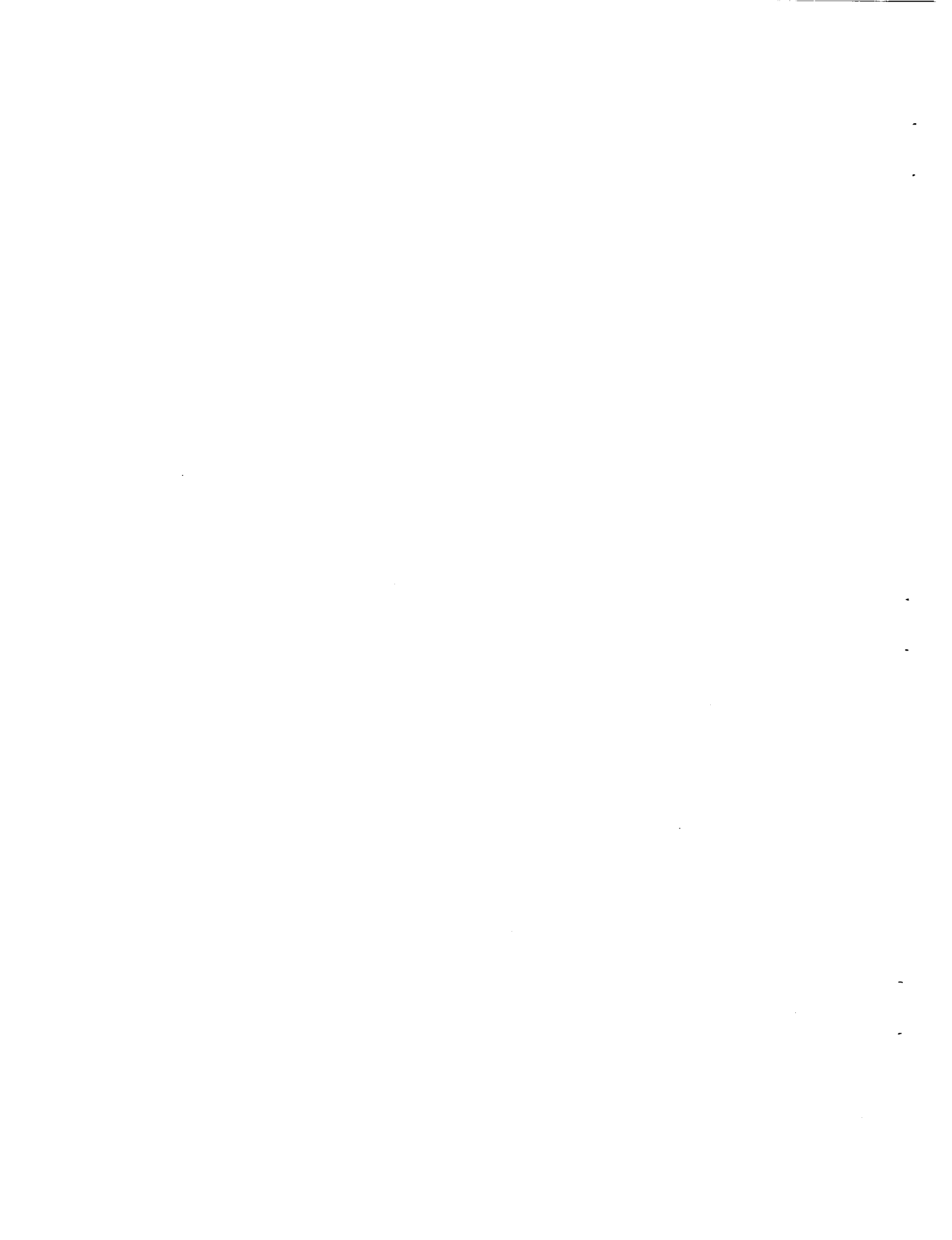


(a) Full-span model.



(b) Semispan model.

Figure 1.—The two methods of mounting the tapered, aspect-ratio-2, NACA 65<sub>1</sub>-210 wing models.



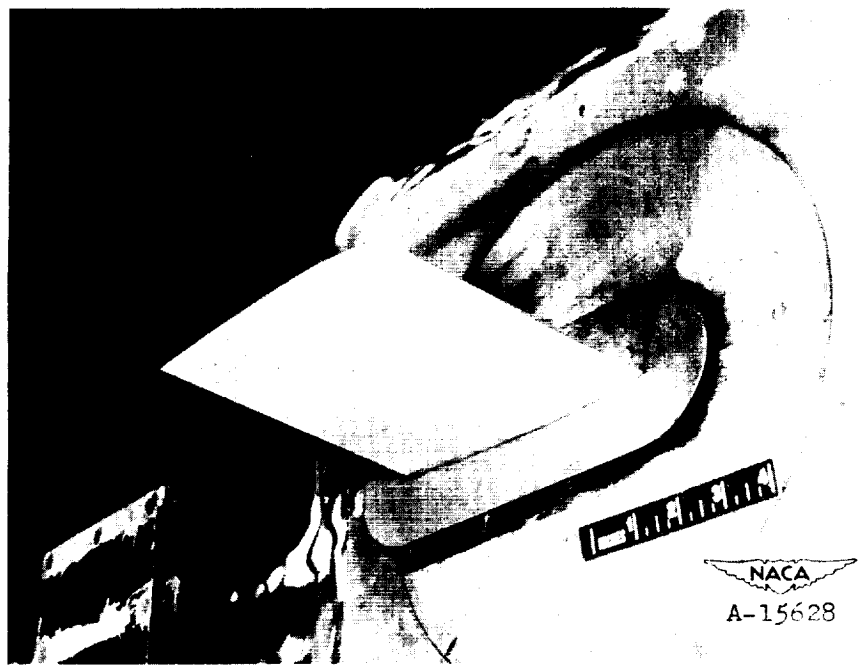
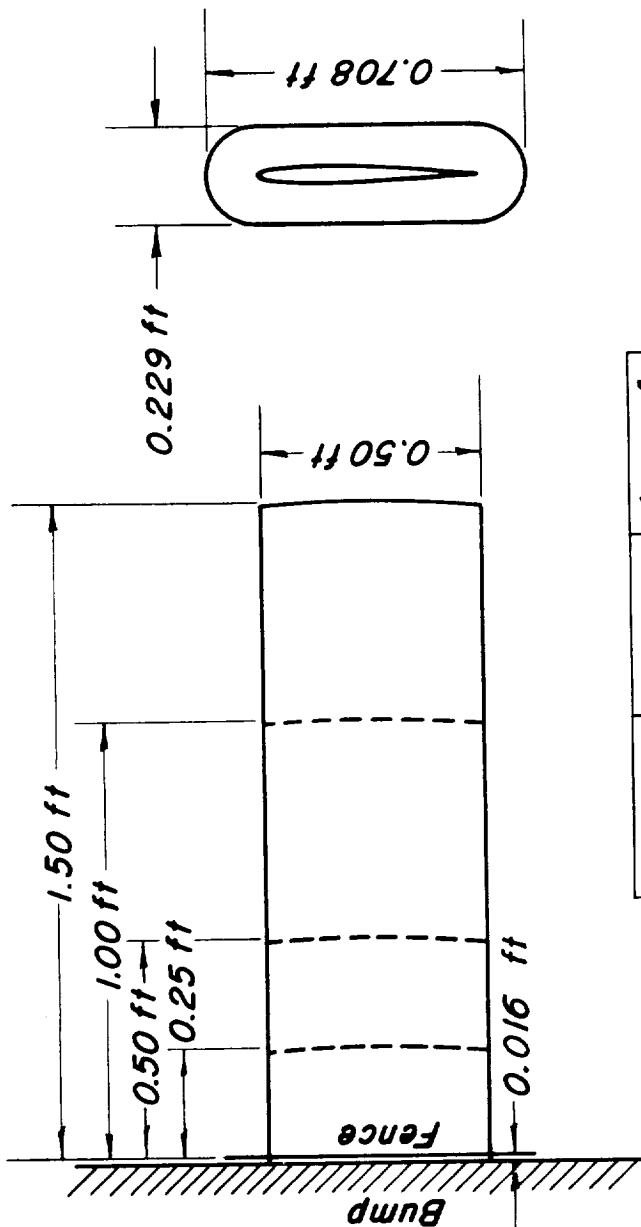


Figure 2.— An aspect-ratio-2, rectangular wing model with an NACA 63A004 section mounted on the transonic bump in the 16-foot high-speed wind tunnel.

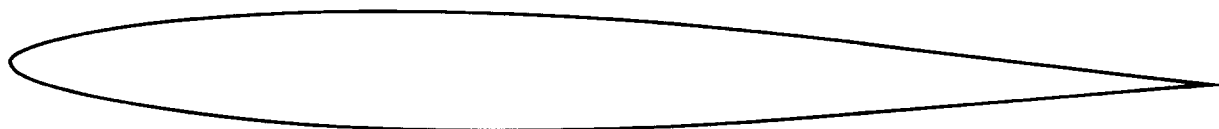
CONFIDENTIAL



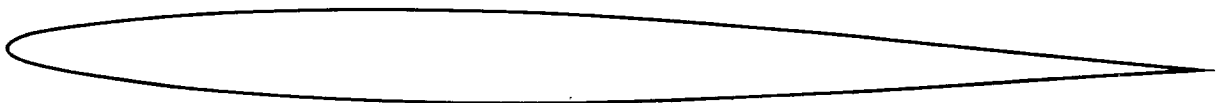


Aspect Ratio	Semispan, ft	Area of Semispan, sq ft
1	0.25	.125
2	0.50	.250
4	1.00	.500
6	1.50	.750

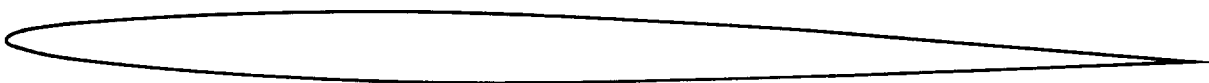
Figure 3.—Dimensions and plan forms of the rectangular wings.



NACA 63A010



NACA 63A008



NACA 63A006



NACA 63A004



NACA 63A002



Figure 4.- Airfoil profiles used for the rectangular wings.

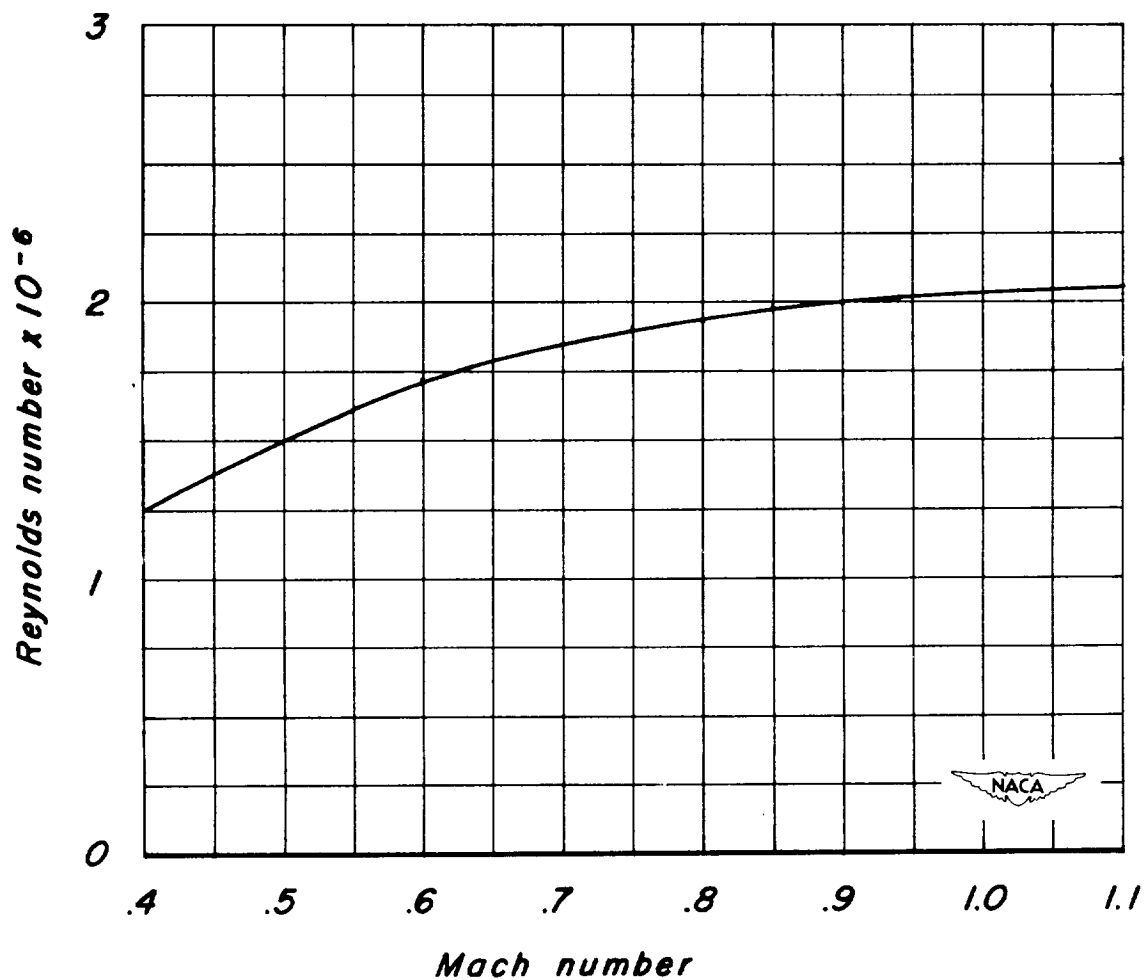


Figure 5.—The variation of Reynolds number with Mach number for the rectangular wings.

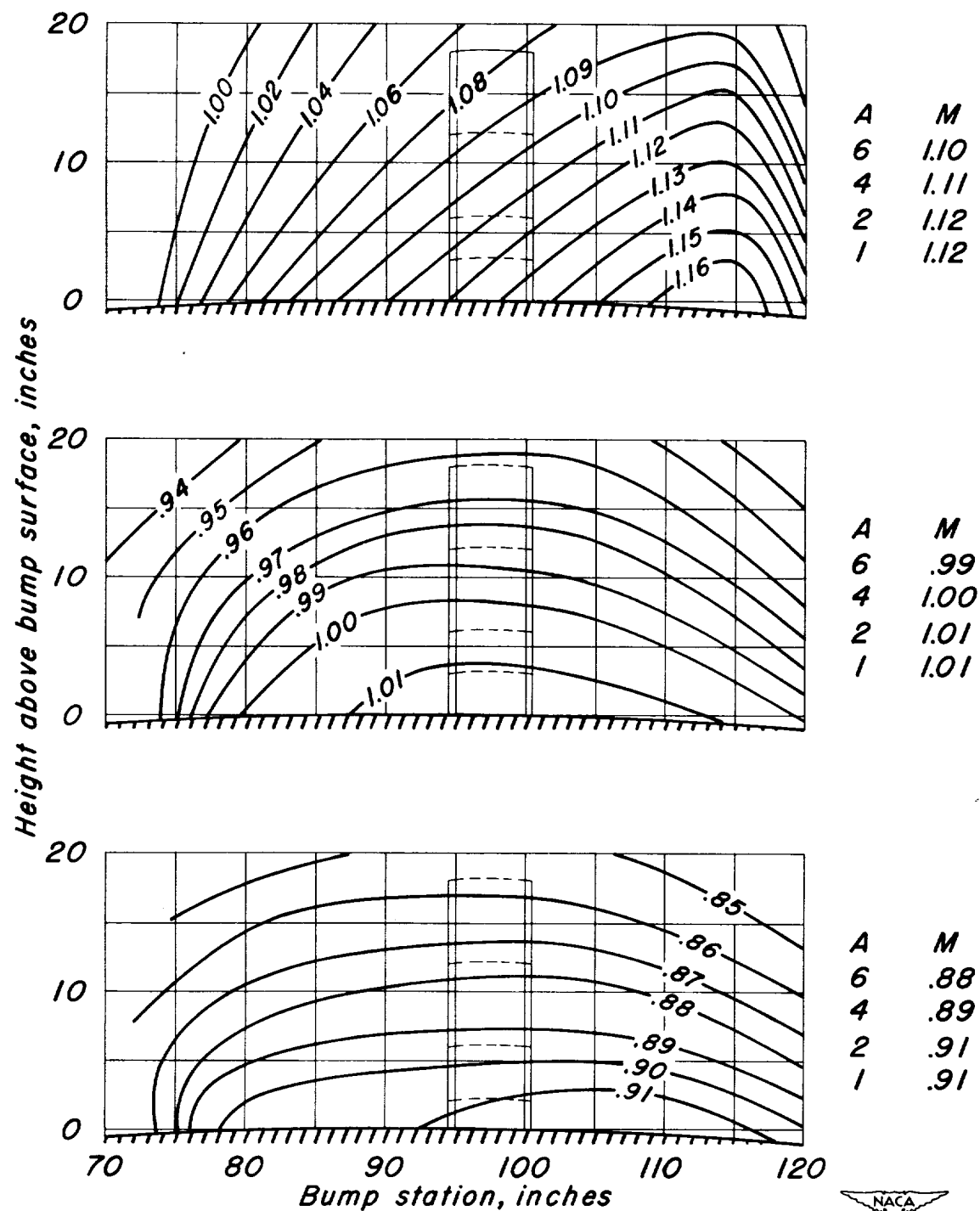
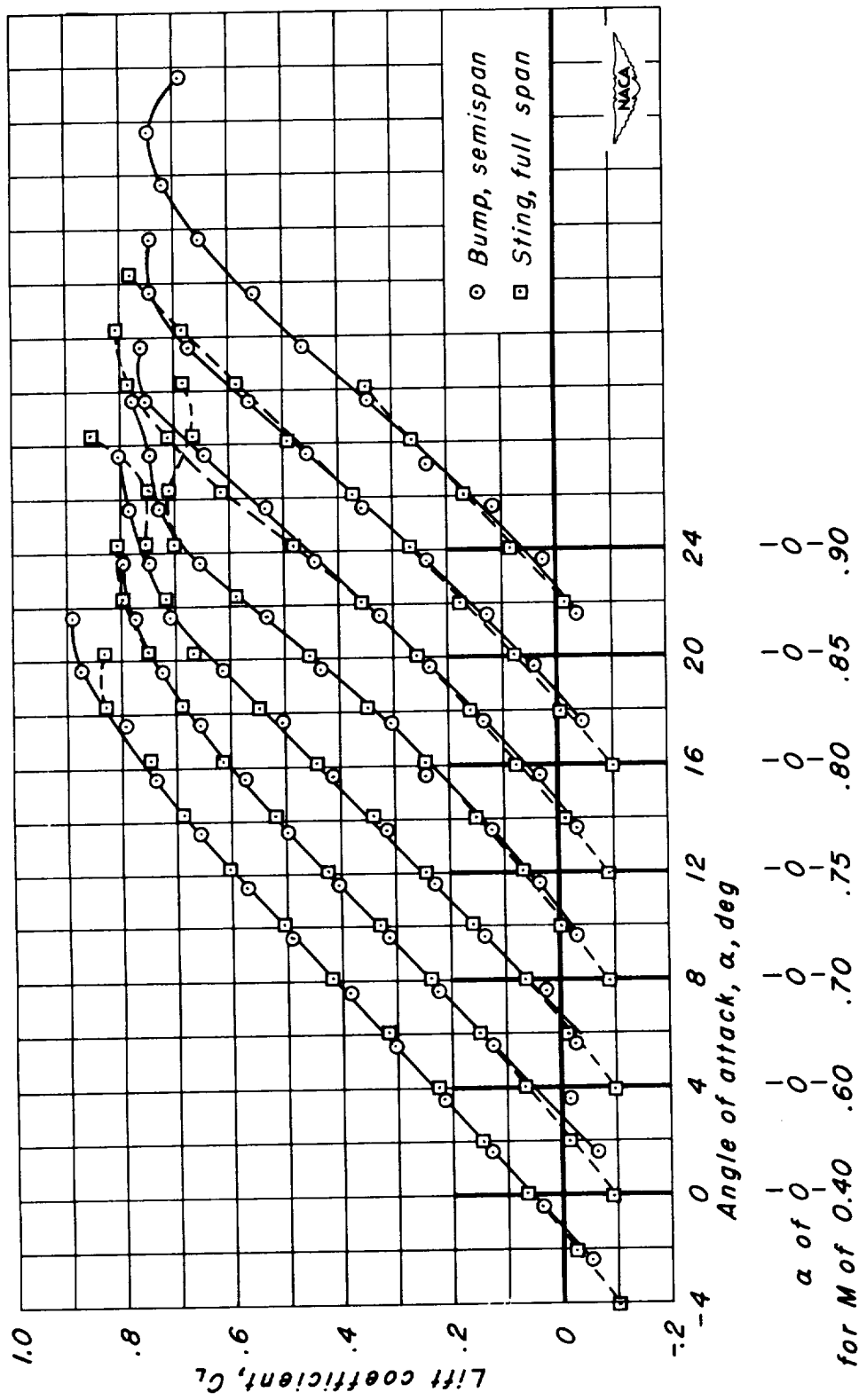
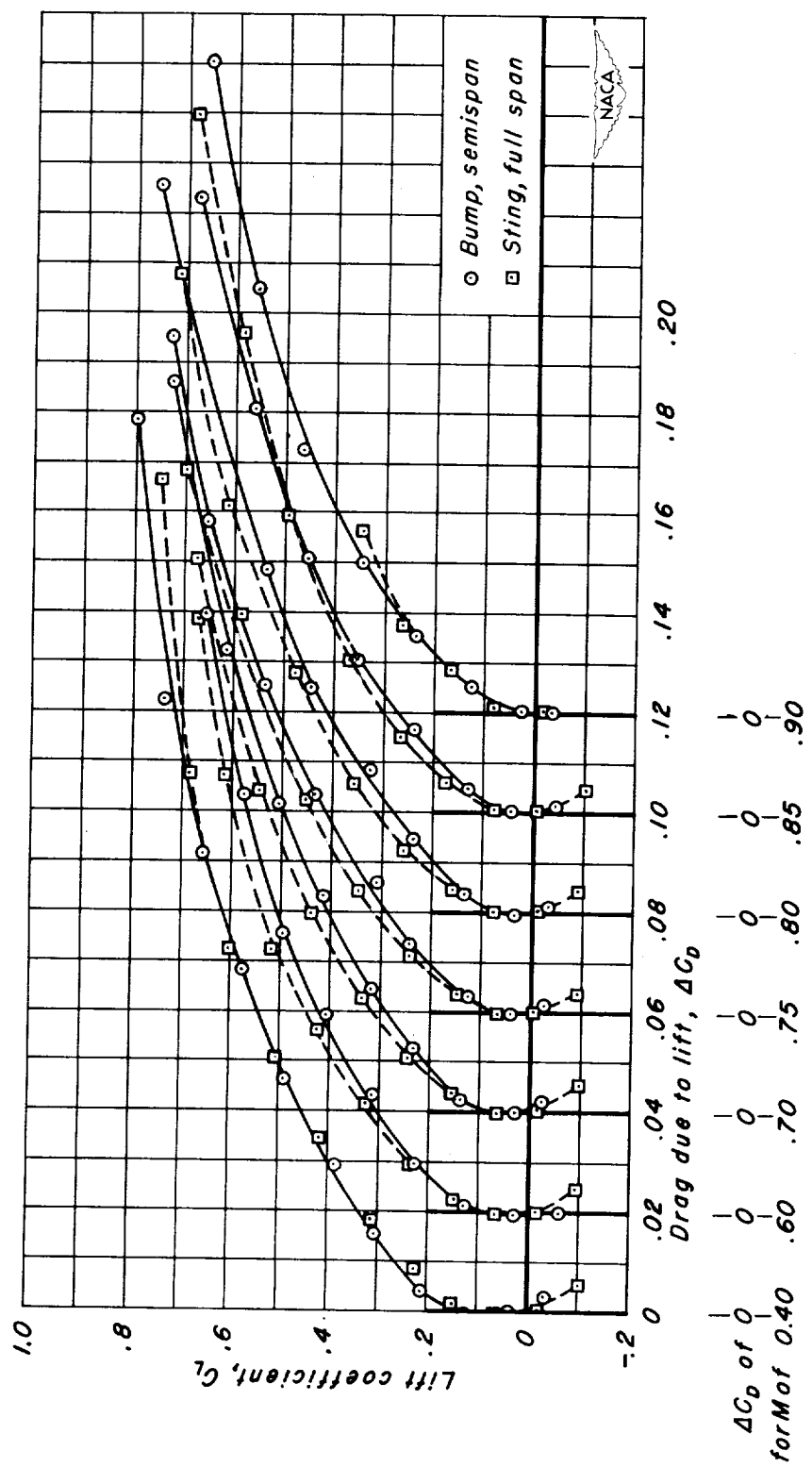


Figure 6.- Typical Mach number contours over the transonic bump in the Ames 16-foot high-speed wind tunnel.

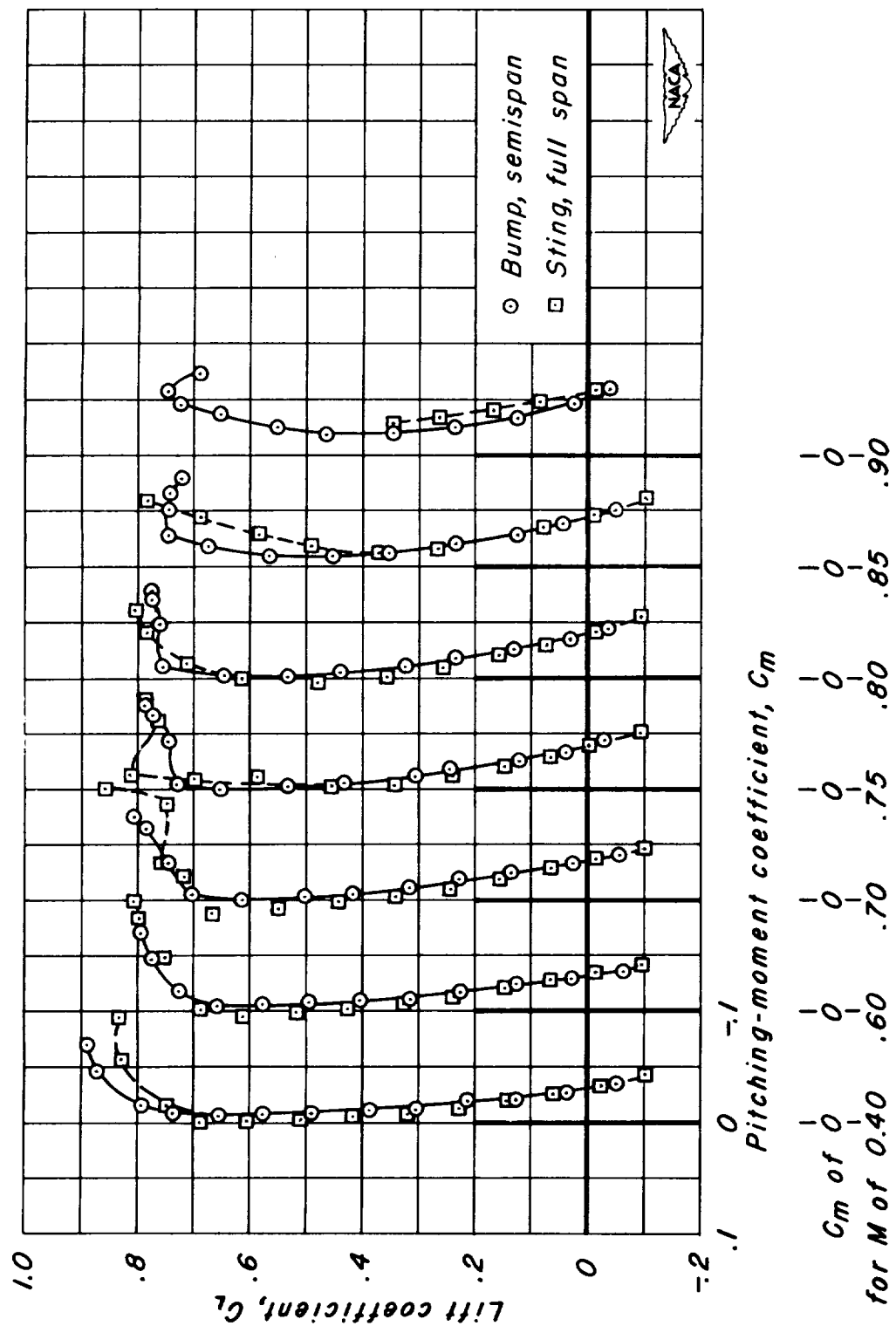


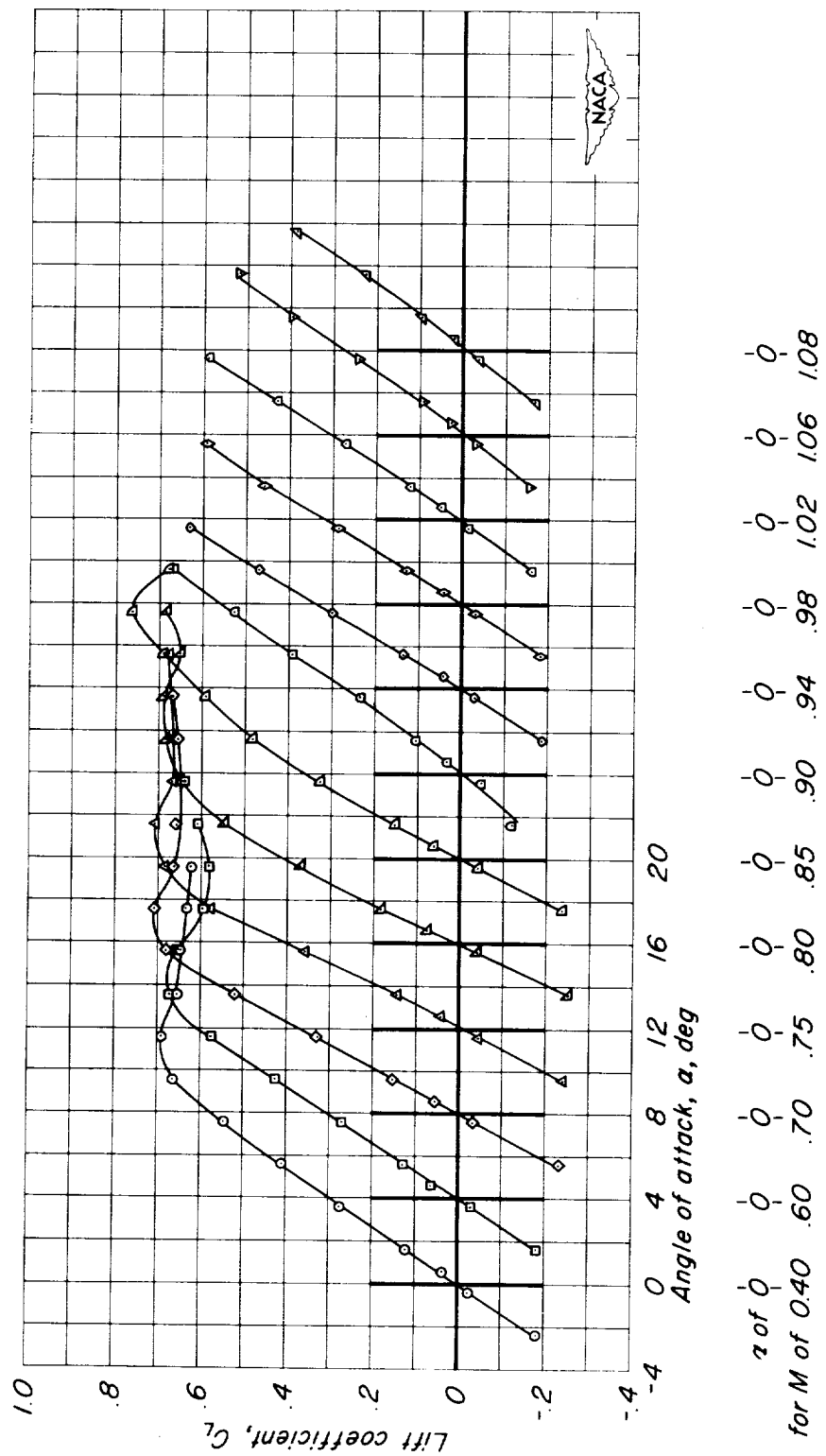
(a)  $C_L$  vs  $\alpha$ .

Figure 7.—Comparison of the aerodynamic characteristics of the tapered, aspect-ratio-2, NACA 65-210 wings, as obtained with a sting-mounted model and a bump-mounted model.

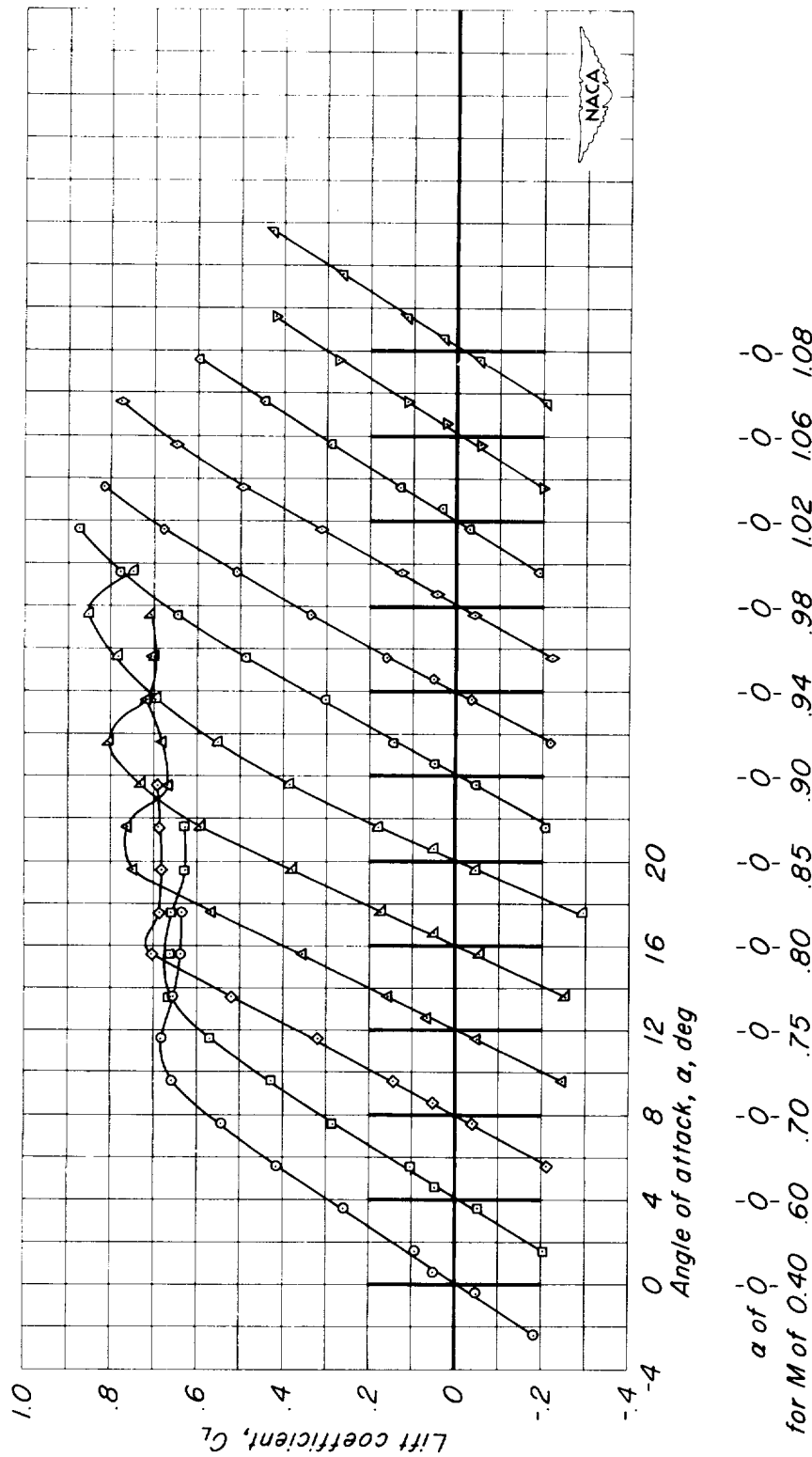


(b) Drag due to lift,  $\Delta C_D$  vs  $C_L$ :  
Figure 7. - Continued.

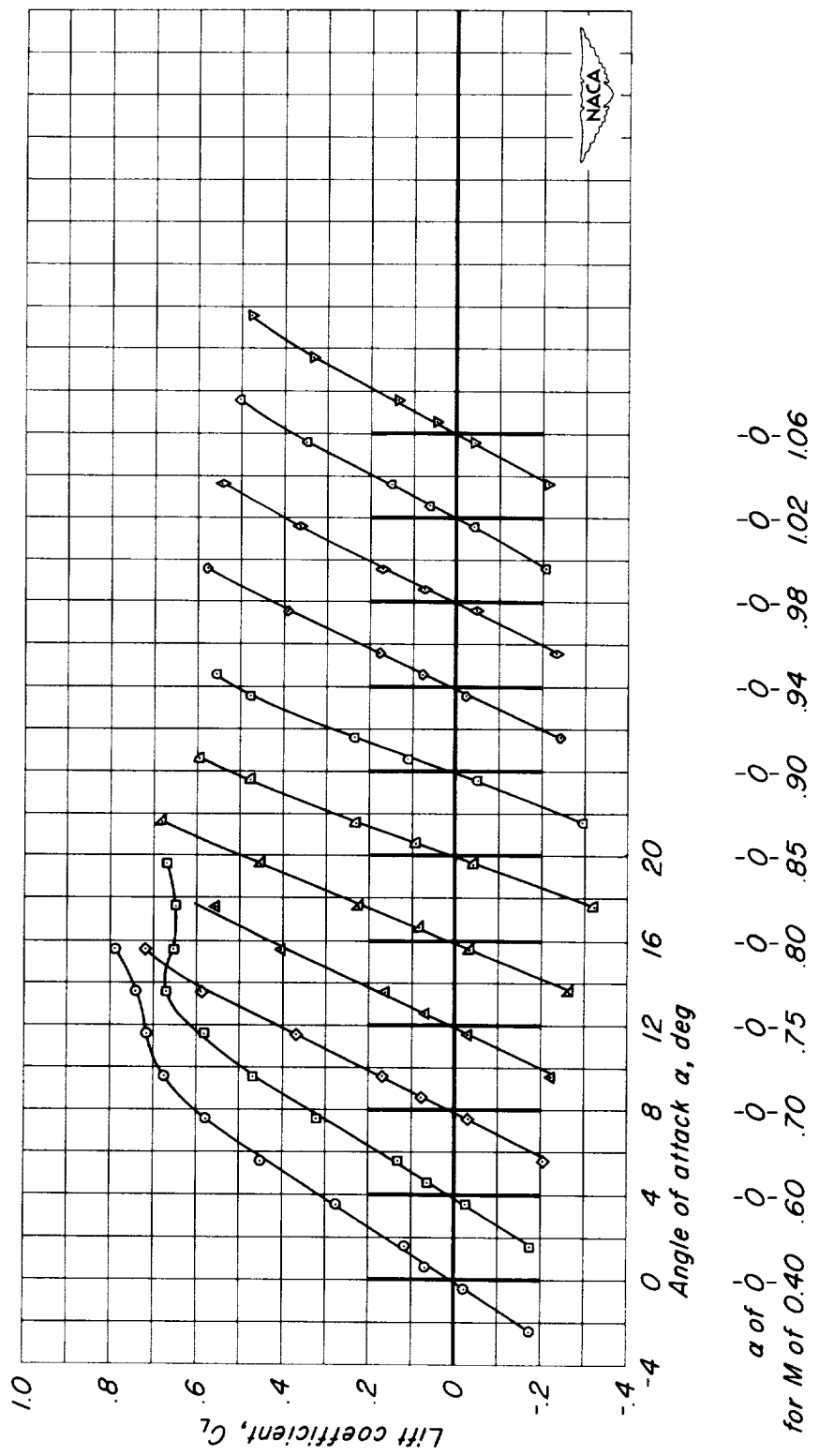




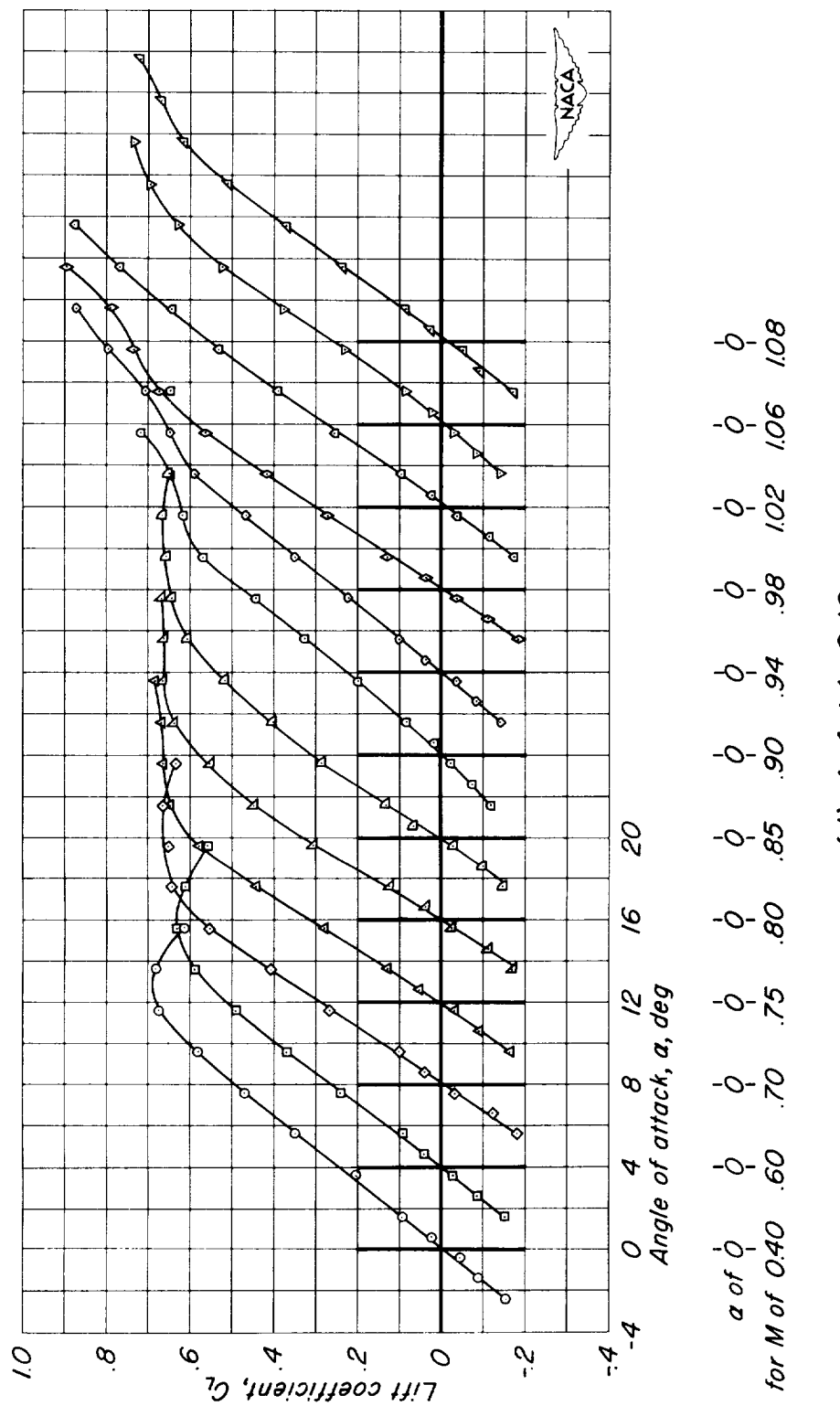
(a)  $A, t/c, C_L$ .  
*Figure 8.-The variation of lift coefficient with angle of attack for the rectangular wings with NACA 63AOXX sections.*



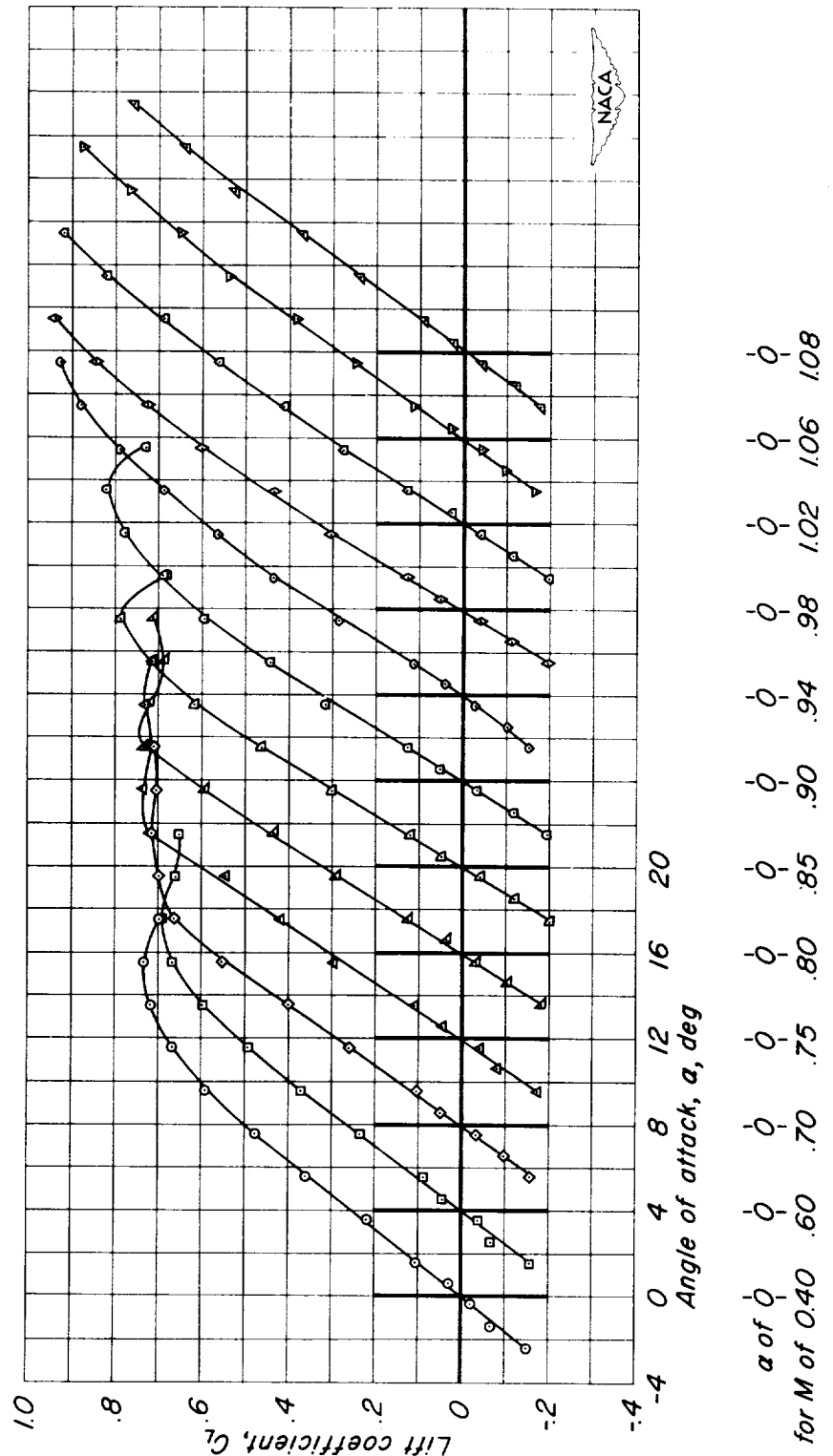
(b) A, 6;  $t/c$ , 0.08.  
Figure 8.-Continued.

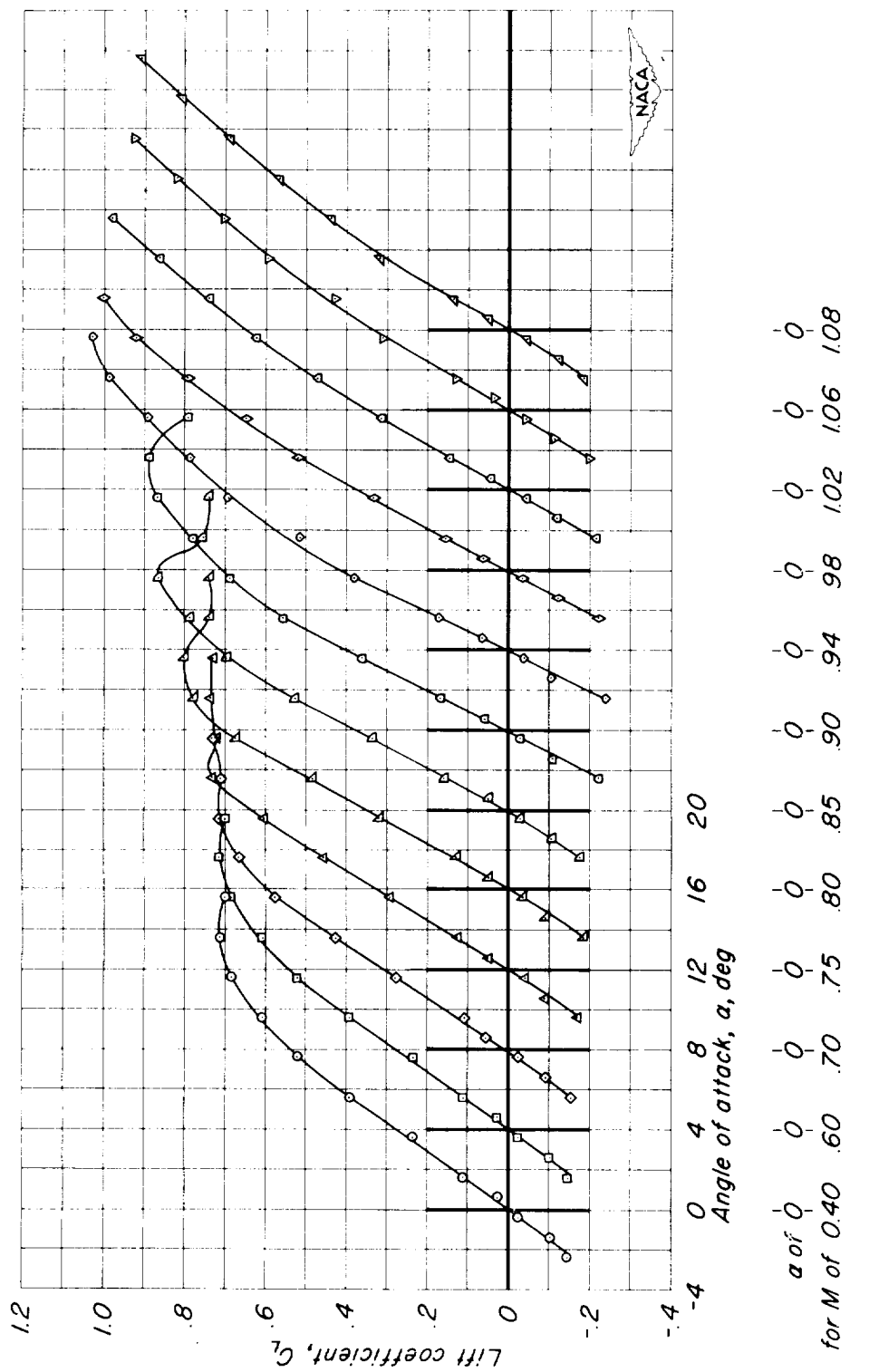


(c)  $A_6; 1/c, 0.06$ .  
Figure 8.-Continued.

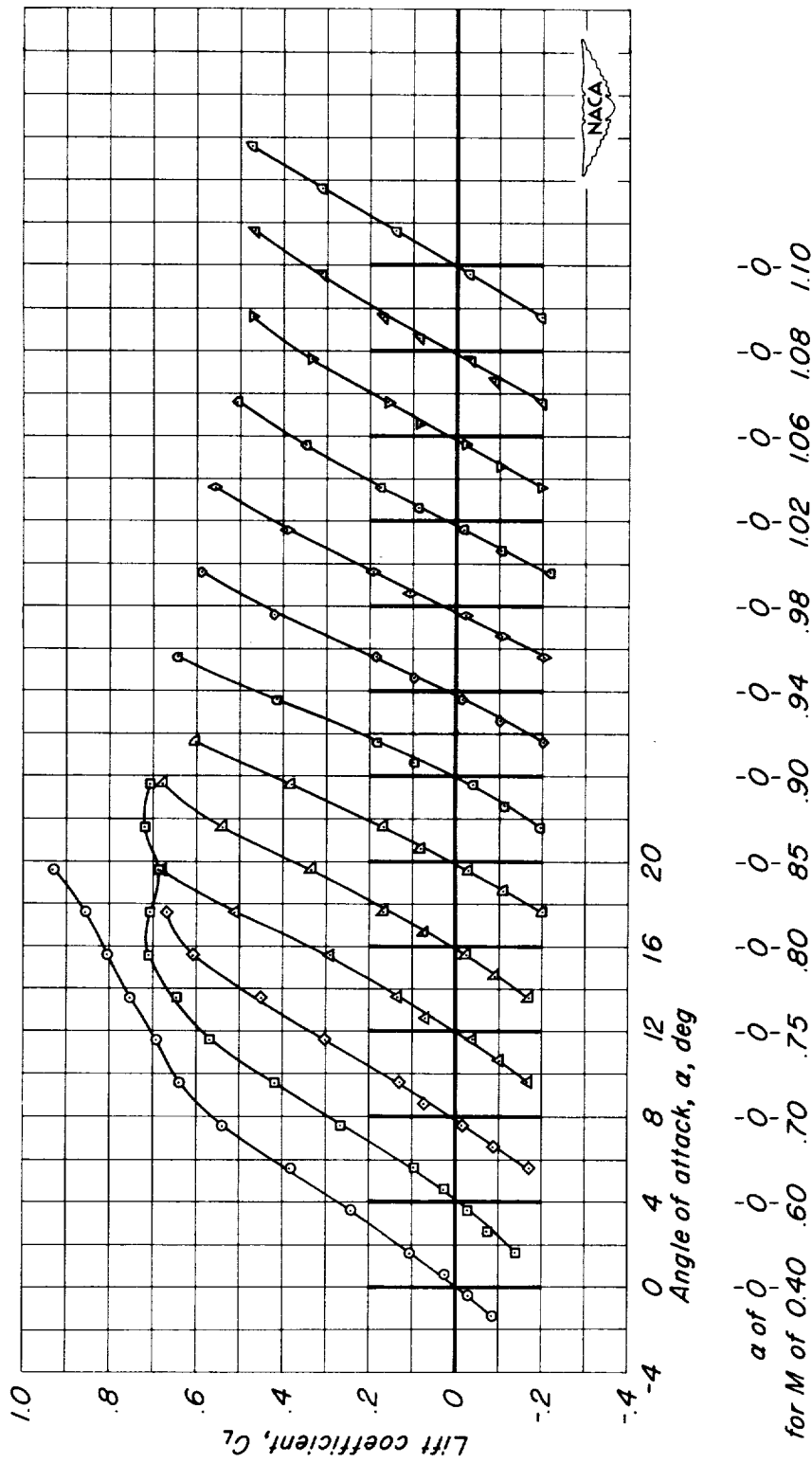


(d)  $A, 4; t/c, 0.10$ .  
Figure 8.-Continued.

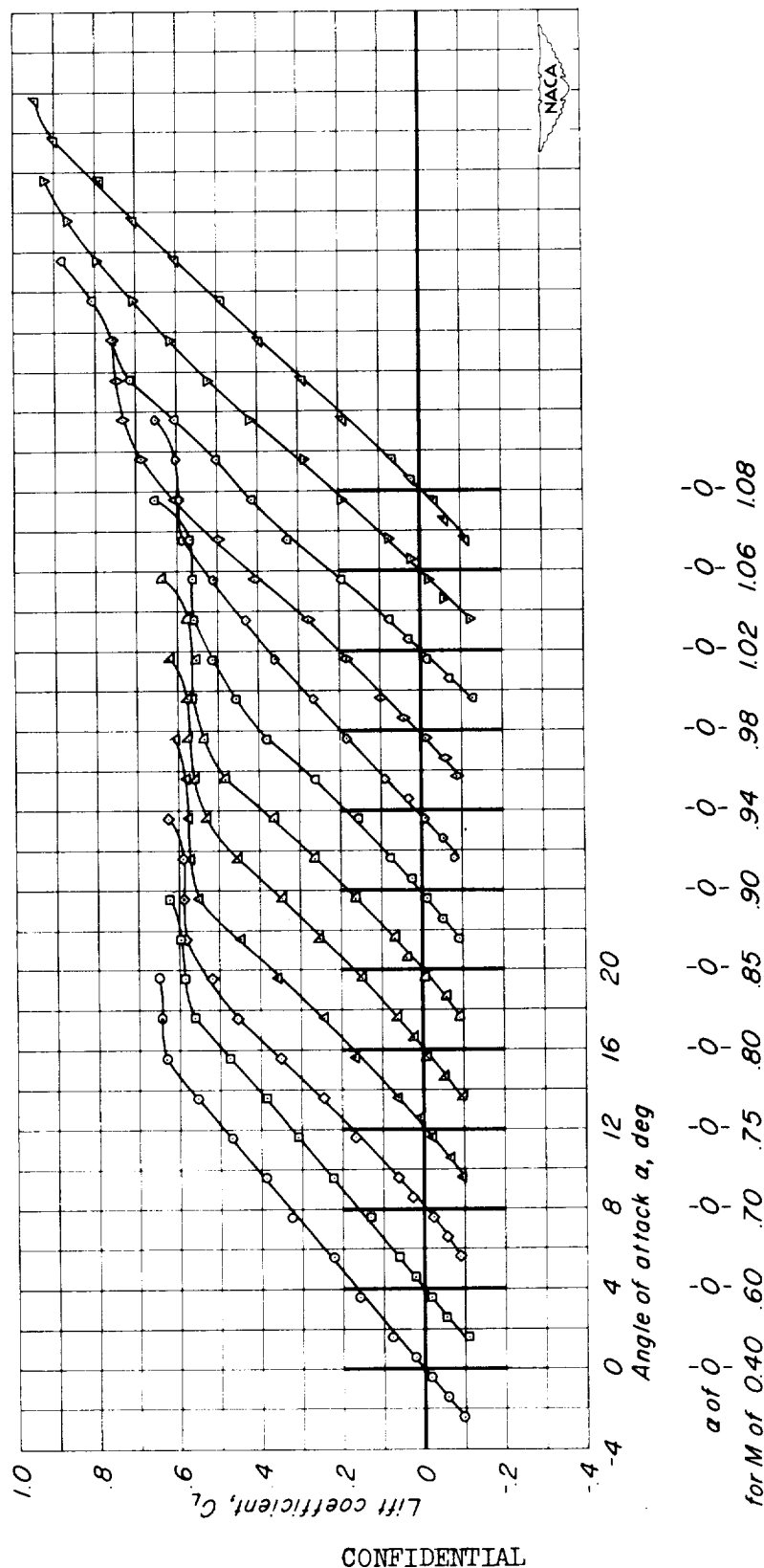




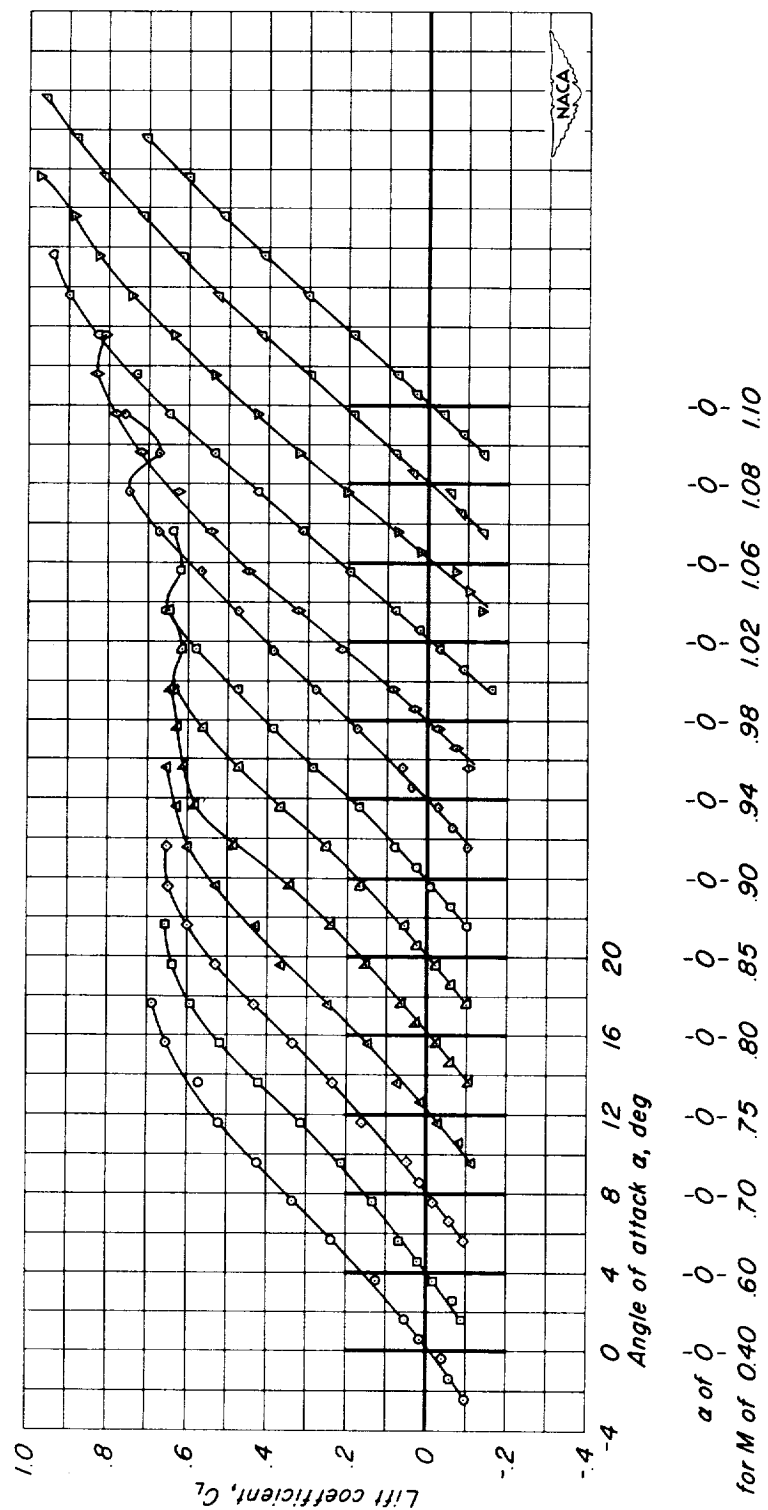
(f)  $A, 4; t/c, 0.06$ .  
Figure 8.-Continued.



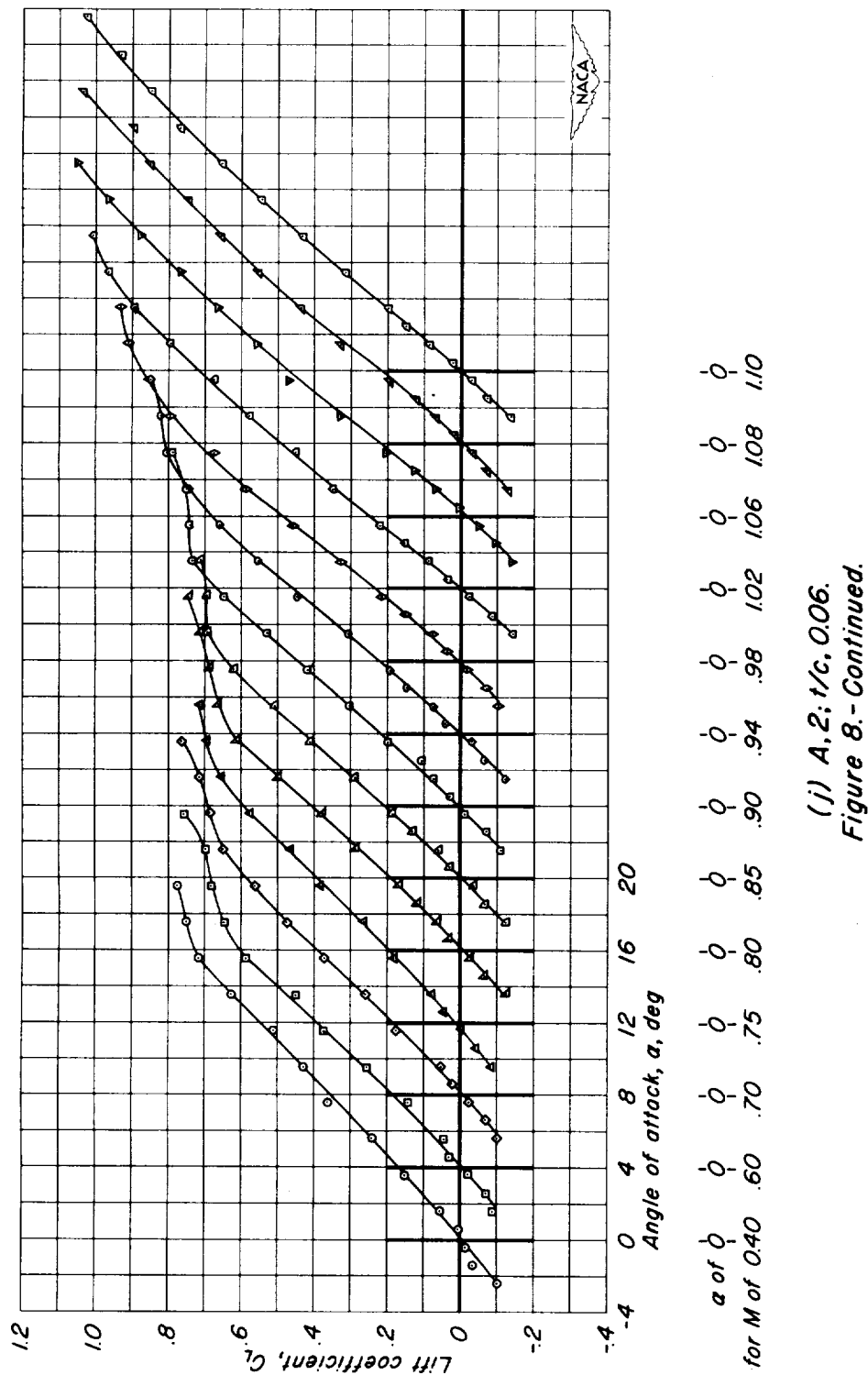
(g)  $A, 4; 1/c, 0.04$ .  
Figure 8.-Continued.



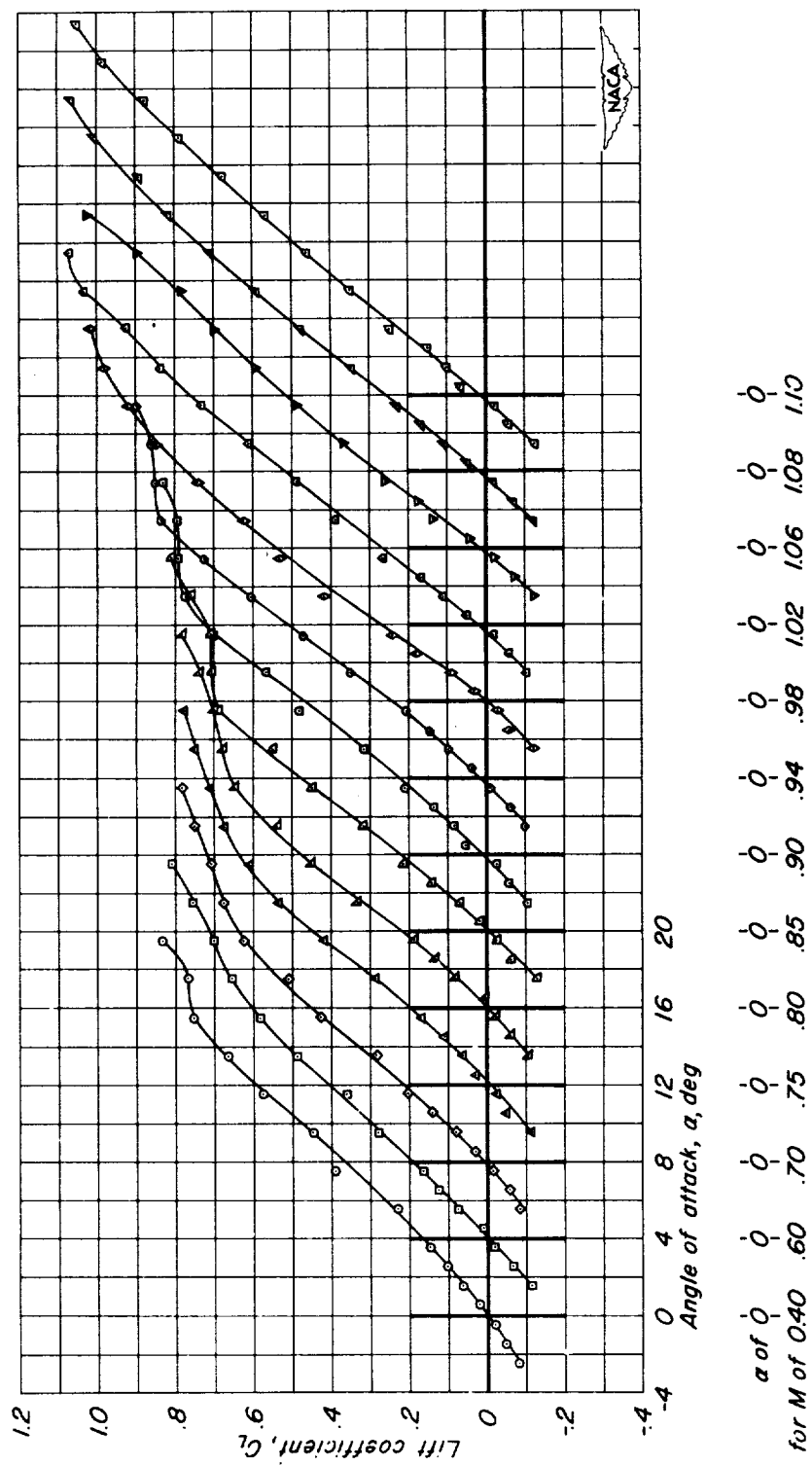
(h) A, 2; 1/c, 0.10.  
Figure 8.-Continued.



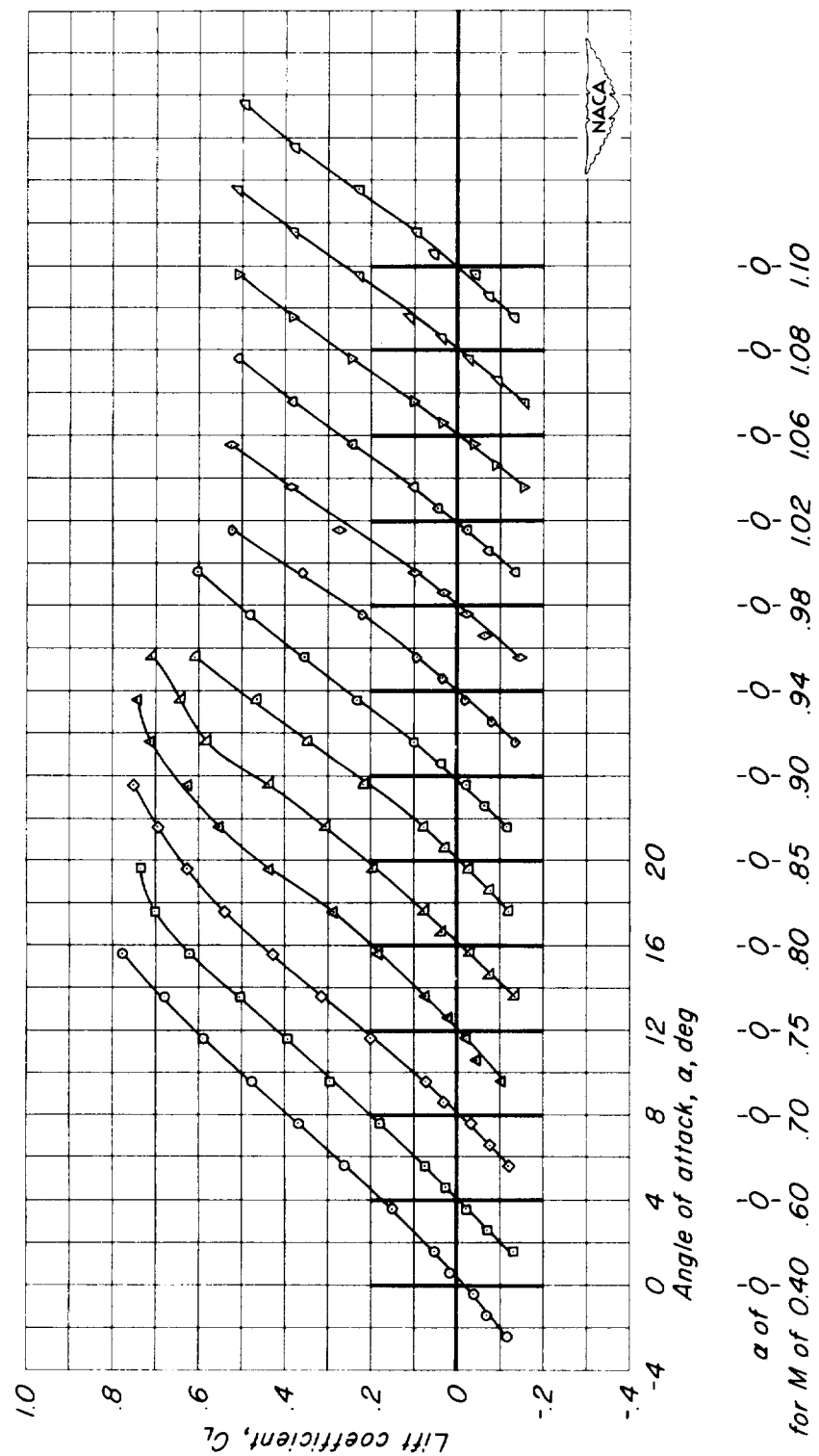
(i)  $A, 2; t/c, 0.08$ .  
Figure 8.-Continued.



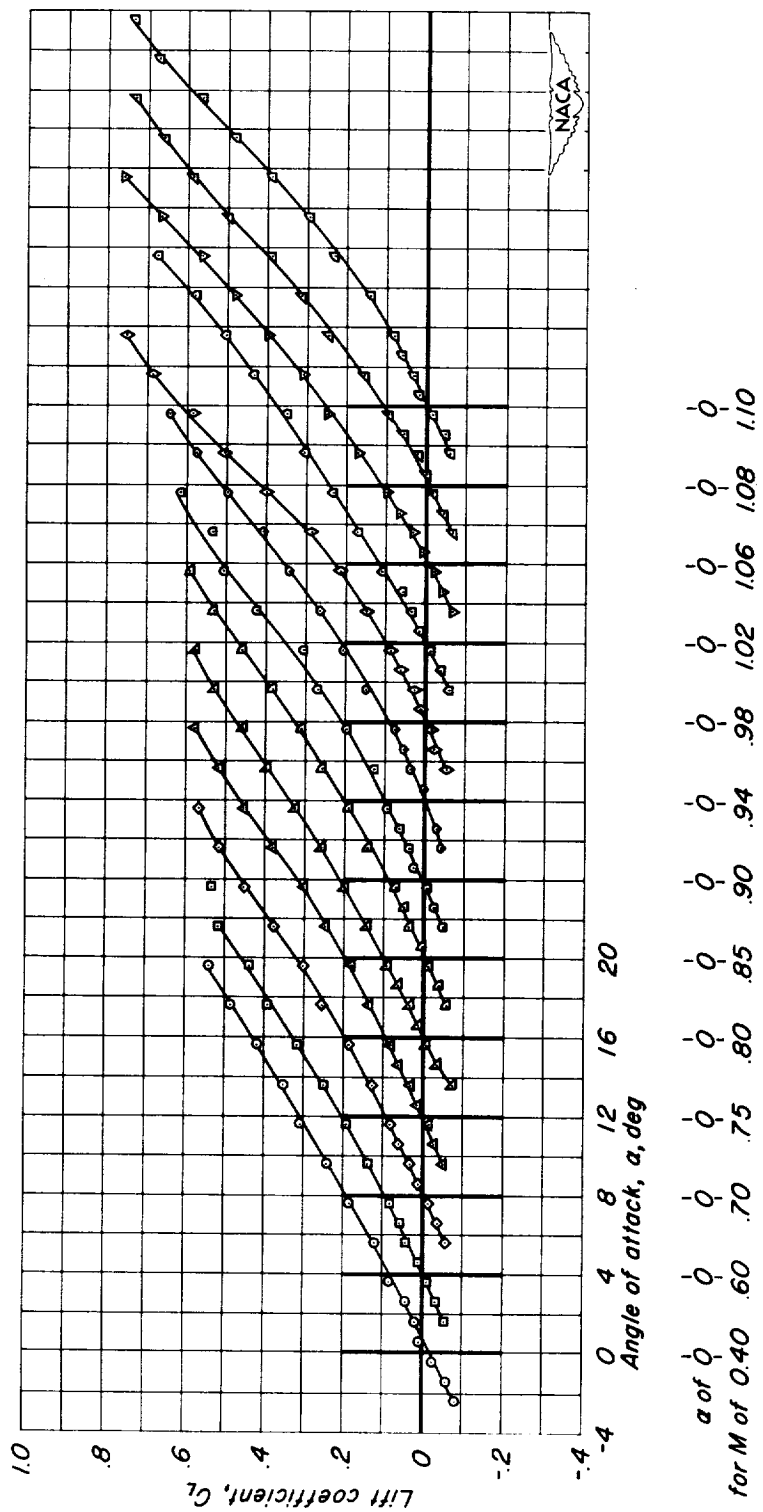
(j)  $A, 2; t/c, 0.06$   
Figure 8 - Continued.

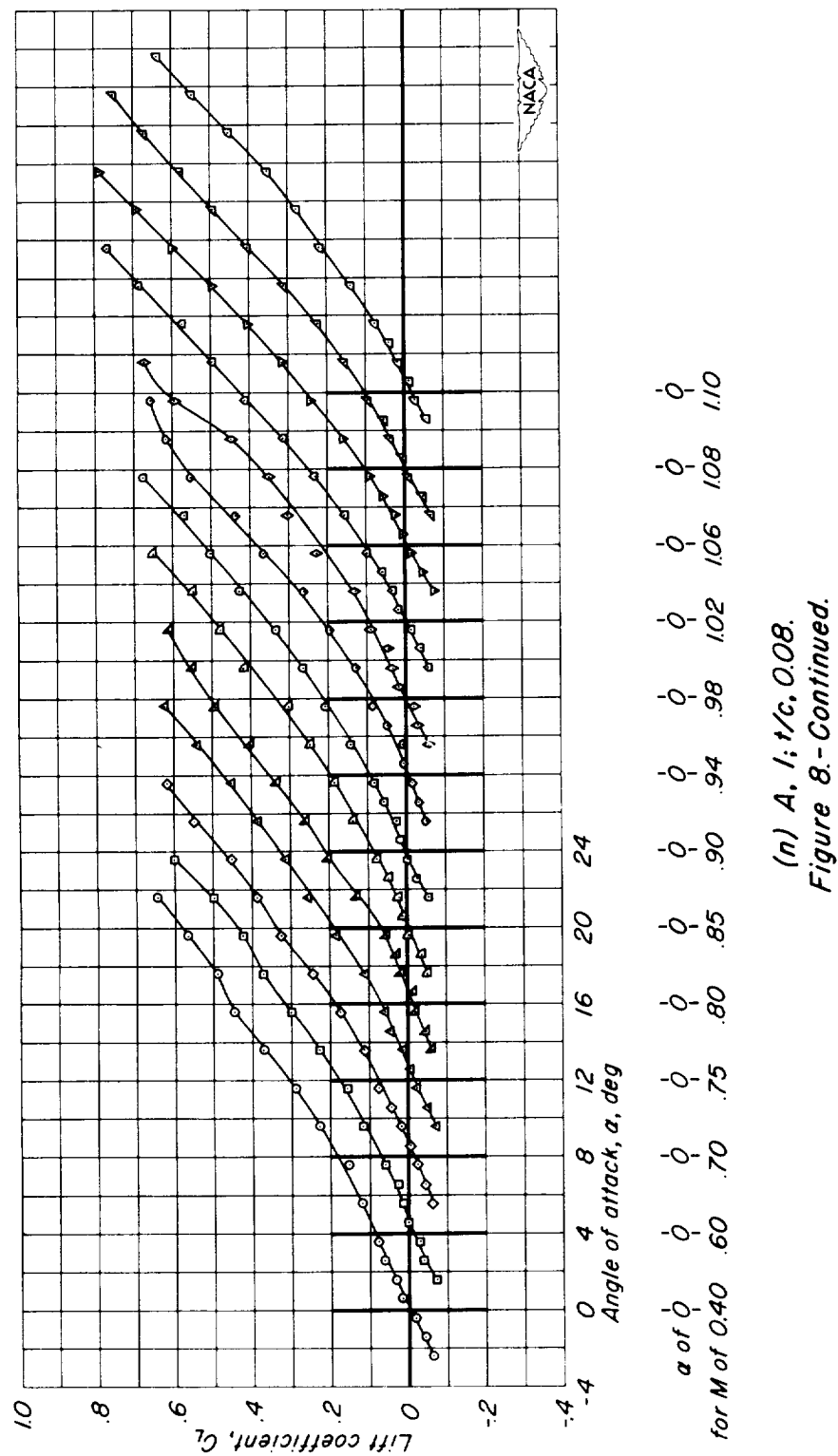


(k) A.2, 1/c, 0.04.  
Figure 8.-Continued.

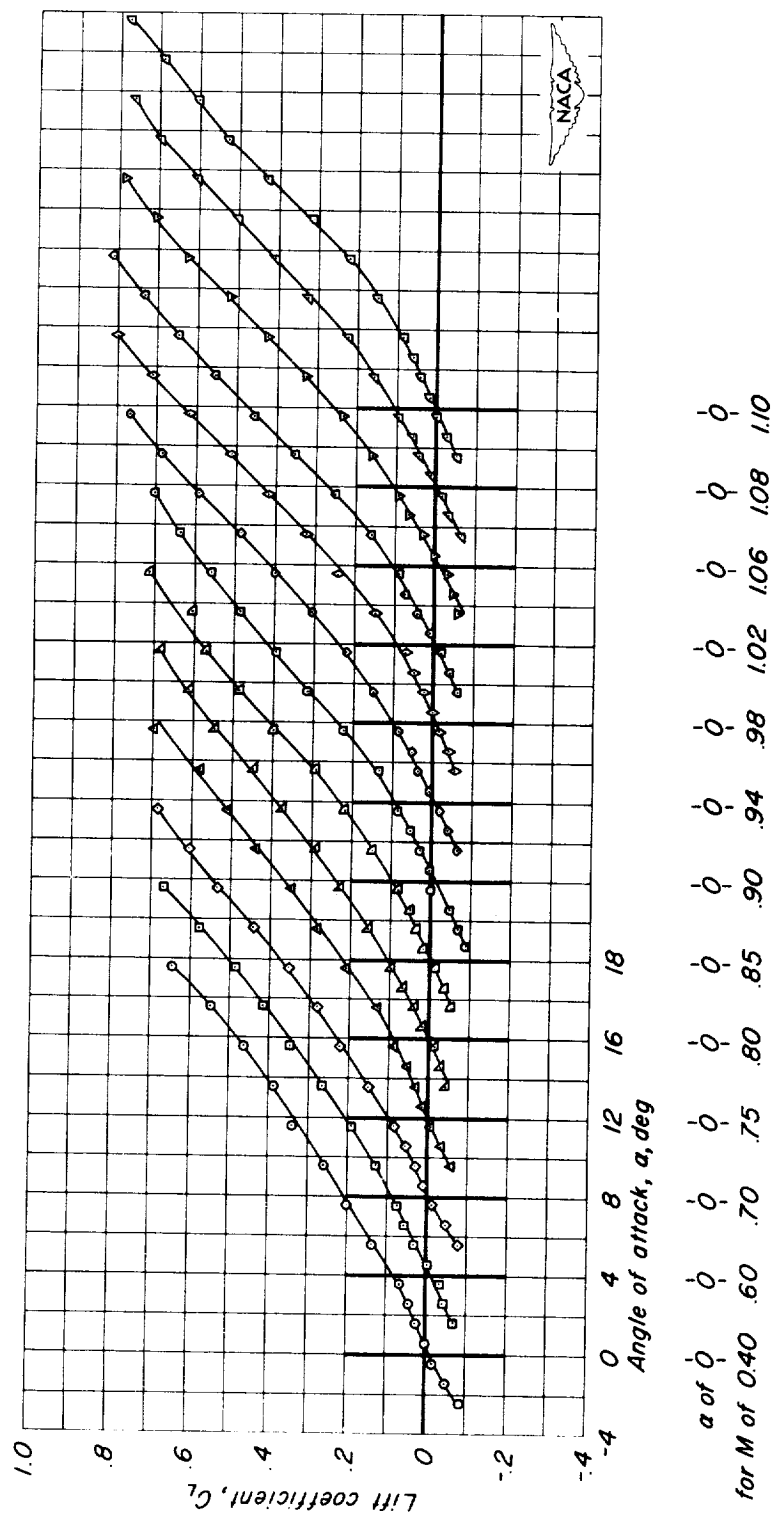


(I)  $A, 2; t/c, 0.02$ .  
Figure 8.-Continued.





(n)  $A, t/c, 0.08$ .  
Figure 8.-Continued.



(o)  $A, l; t/c, 0.06$   
*Figure 8 - Continued.*

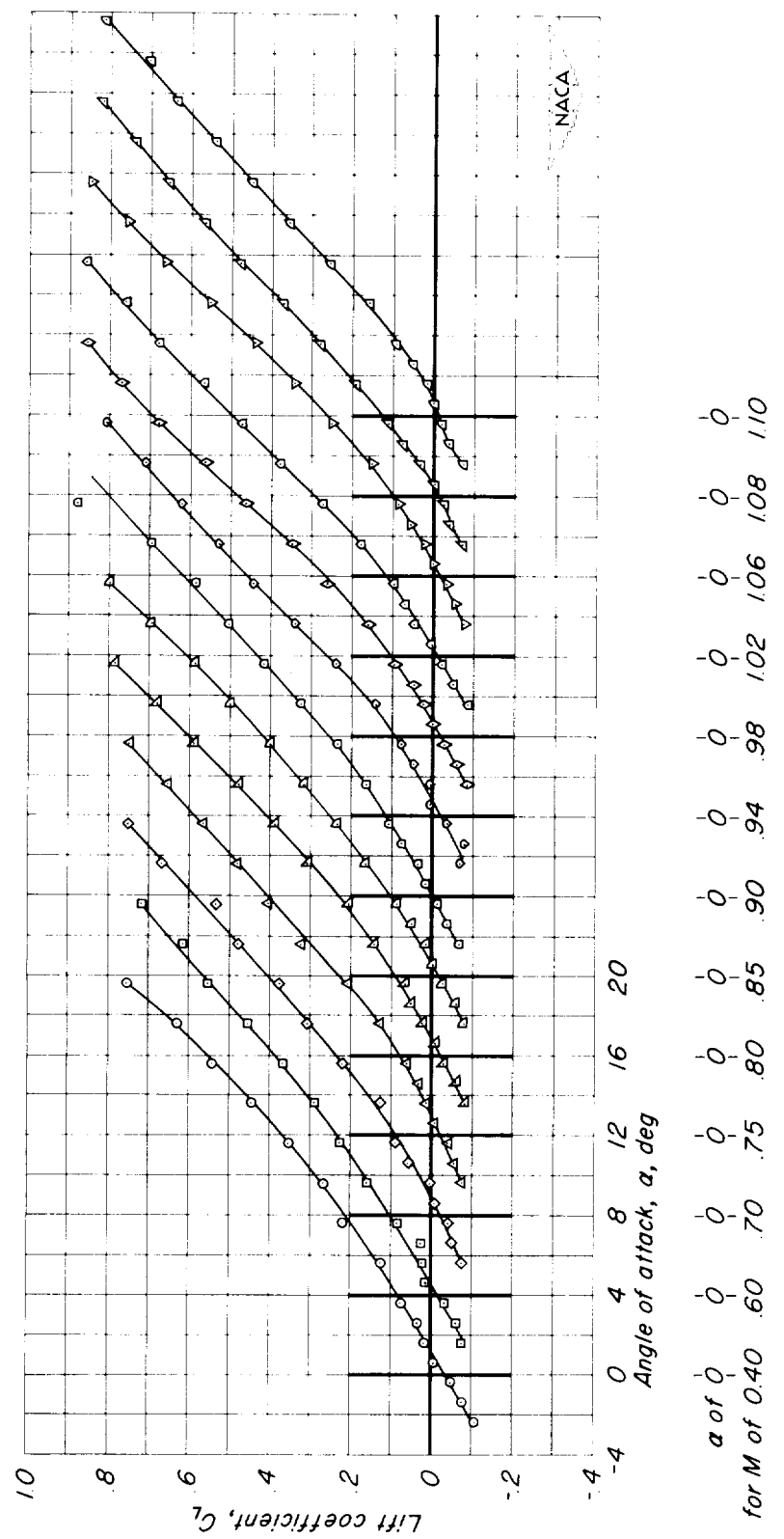
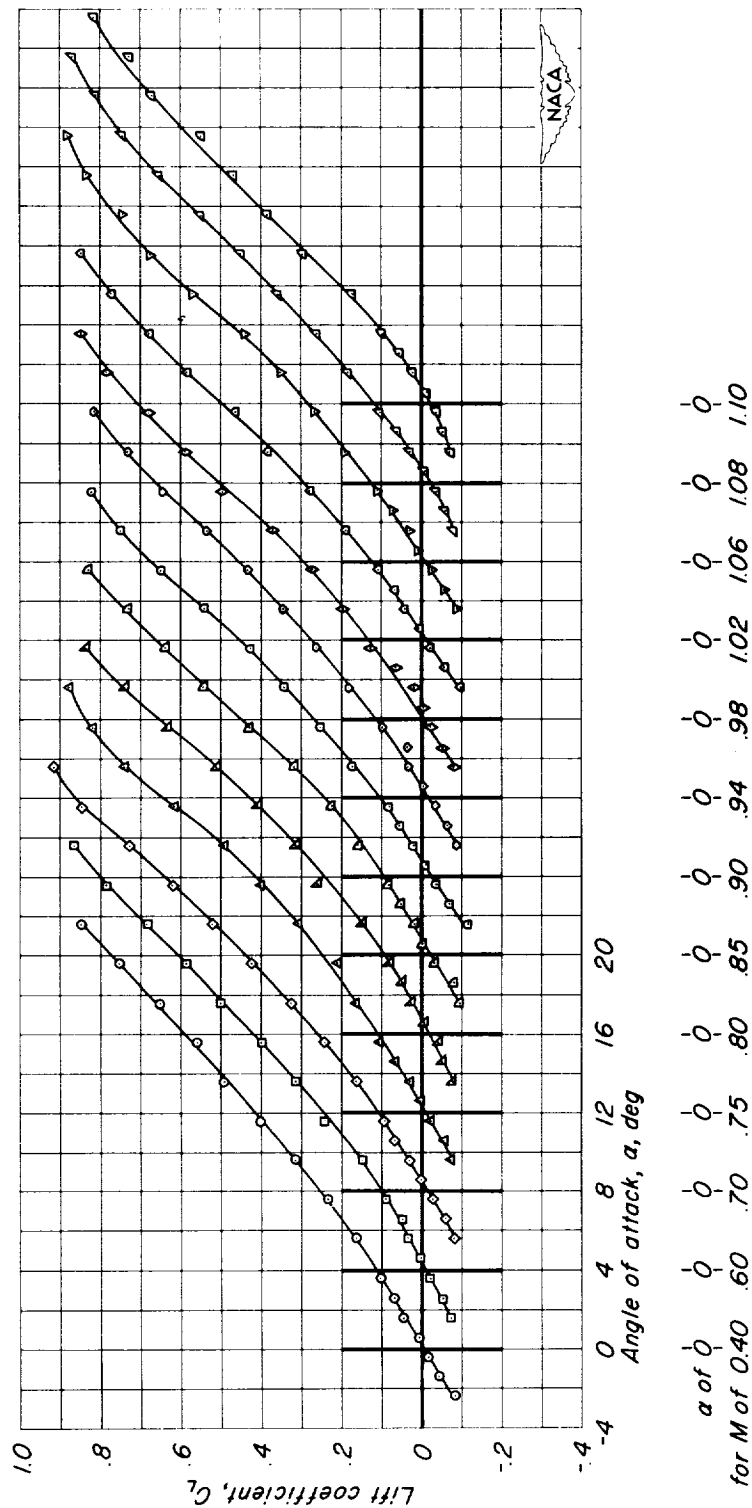
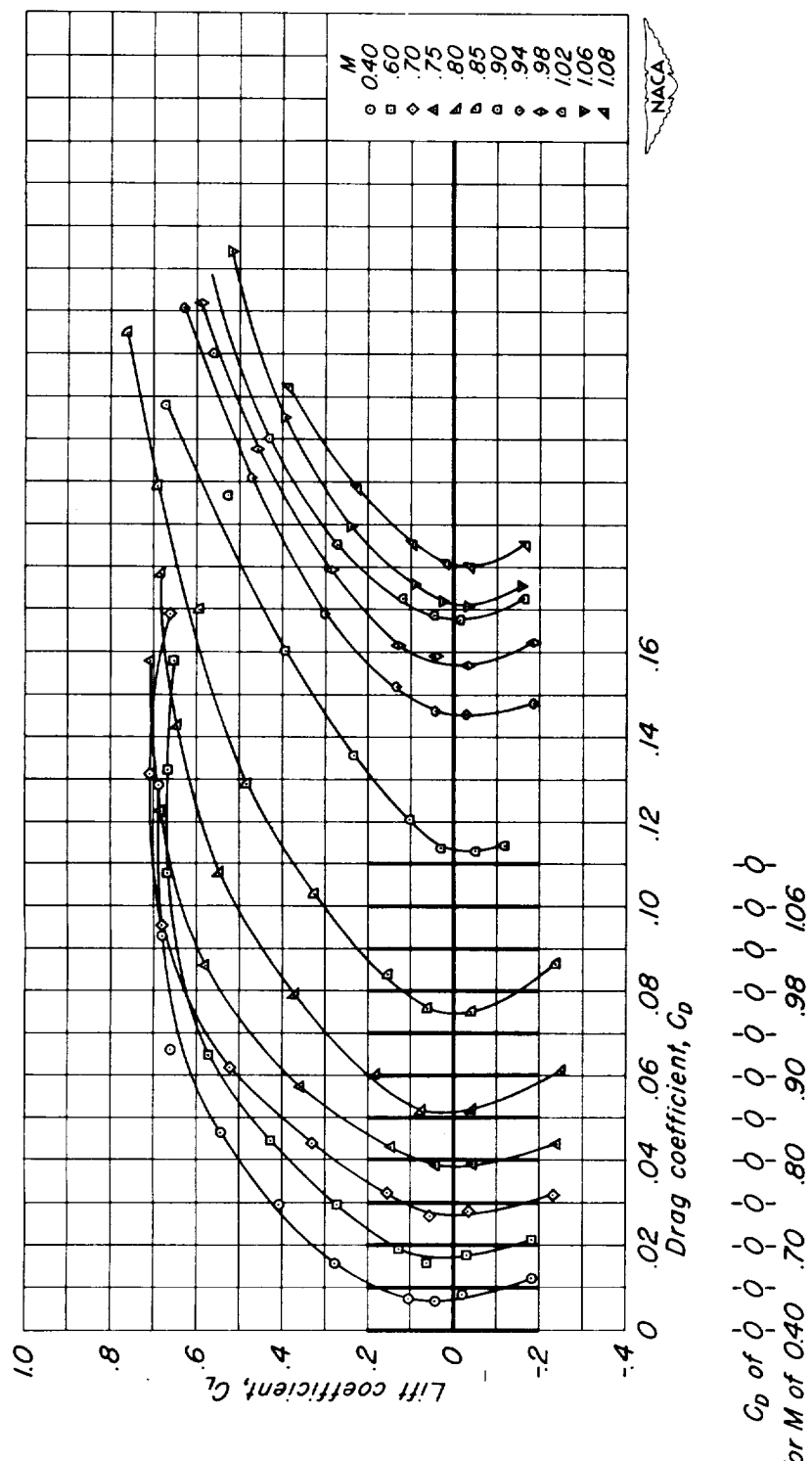
(p)  $A_1, 1/c, 0.04$ .

Figure 8.-Continued.

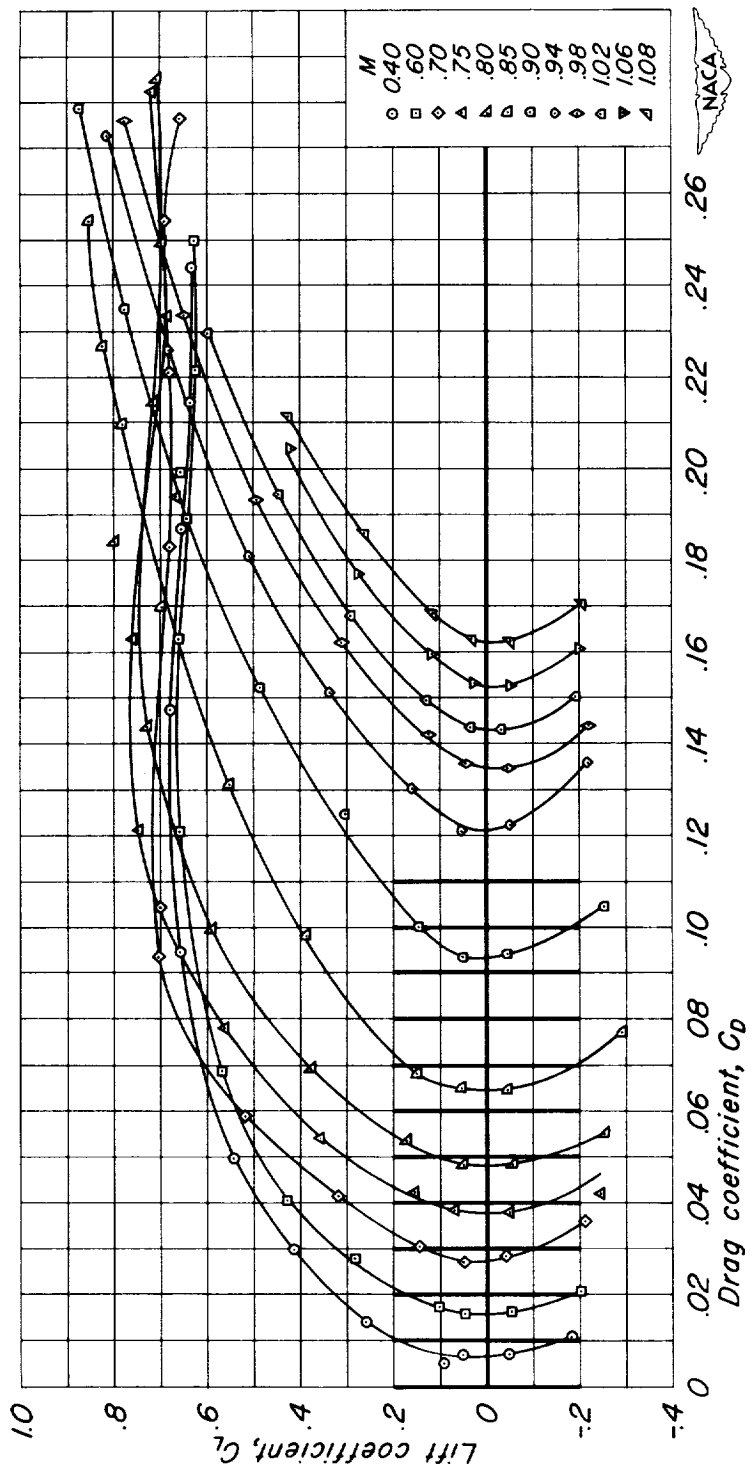


(q)  $A/l; t/c, 0.02$ .  
Figure 8 - Concluded.



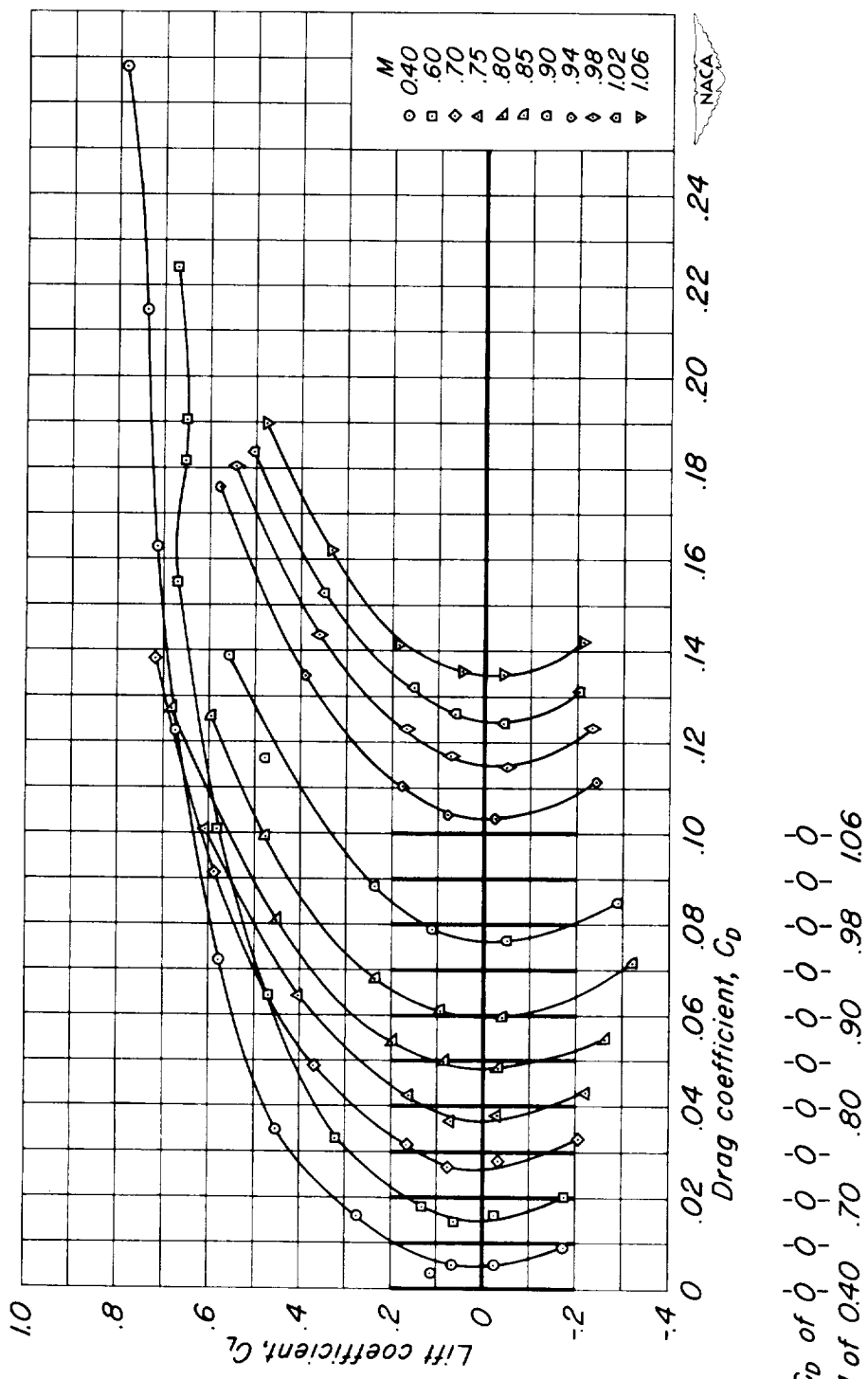
*Figure 9.-The variation of drag coefficient with lift coefficient for the rectangular wings with NACA 6340XX sections.*

CONFIDENTIAL



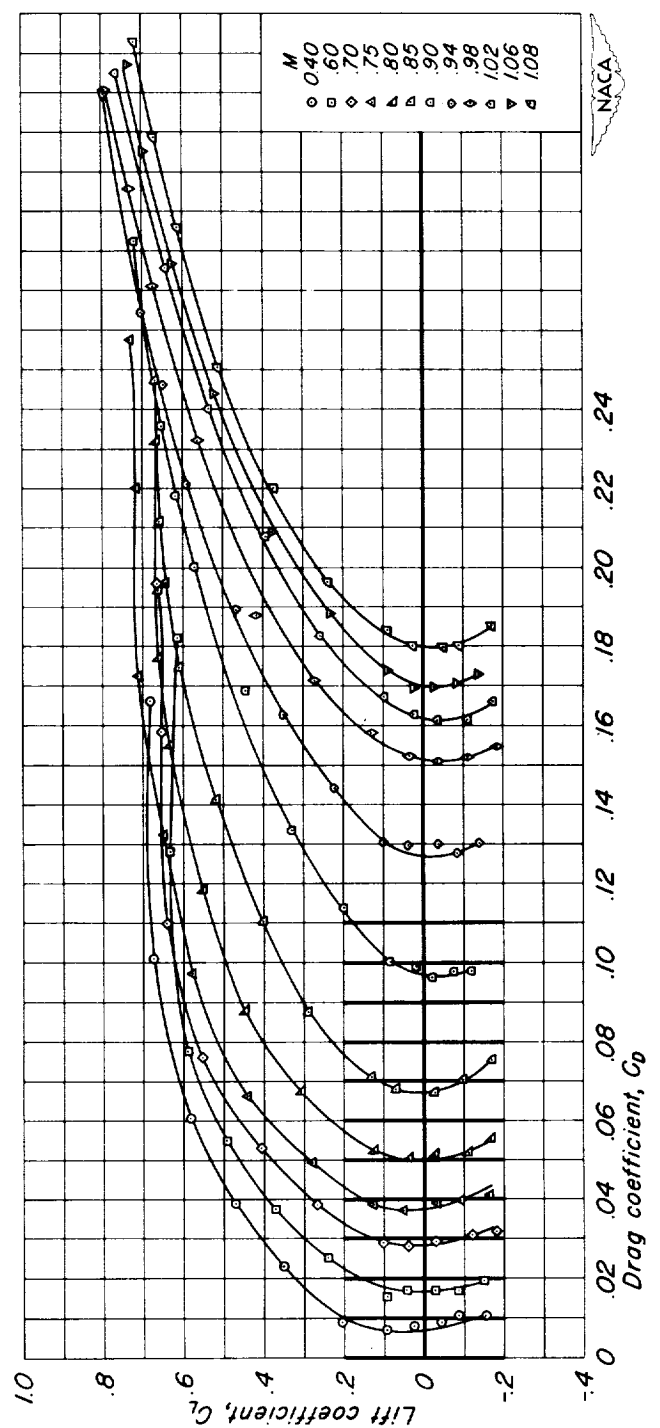
$C_D$  of  $\phi$     $\phi$     $\phi$     $\phi$     $\phi$     $\phi$     $\phi$     $\phi$     $\phi$   
for  $M$  of 0.40 .70 .80 .90 .98 1.06

(b)  $A, 6; t/c, 0.08$ .  
Figure 9.- Continued.



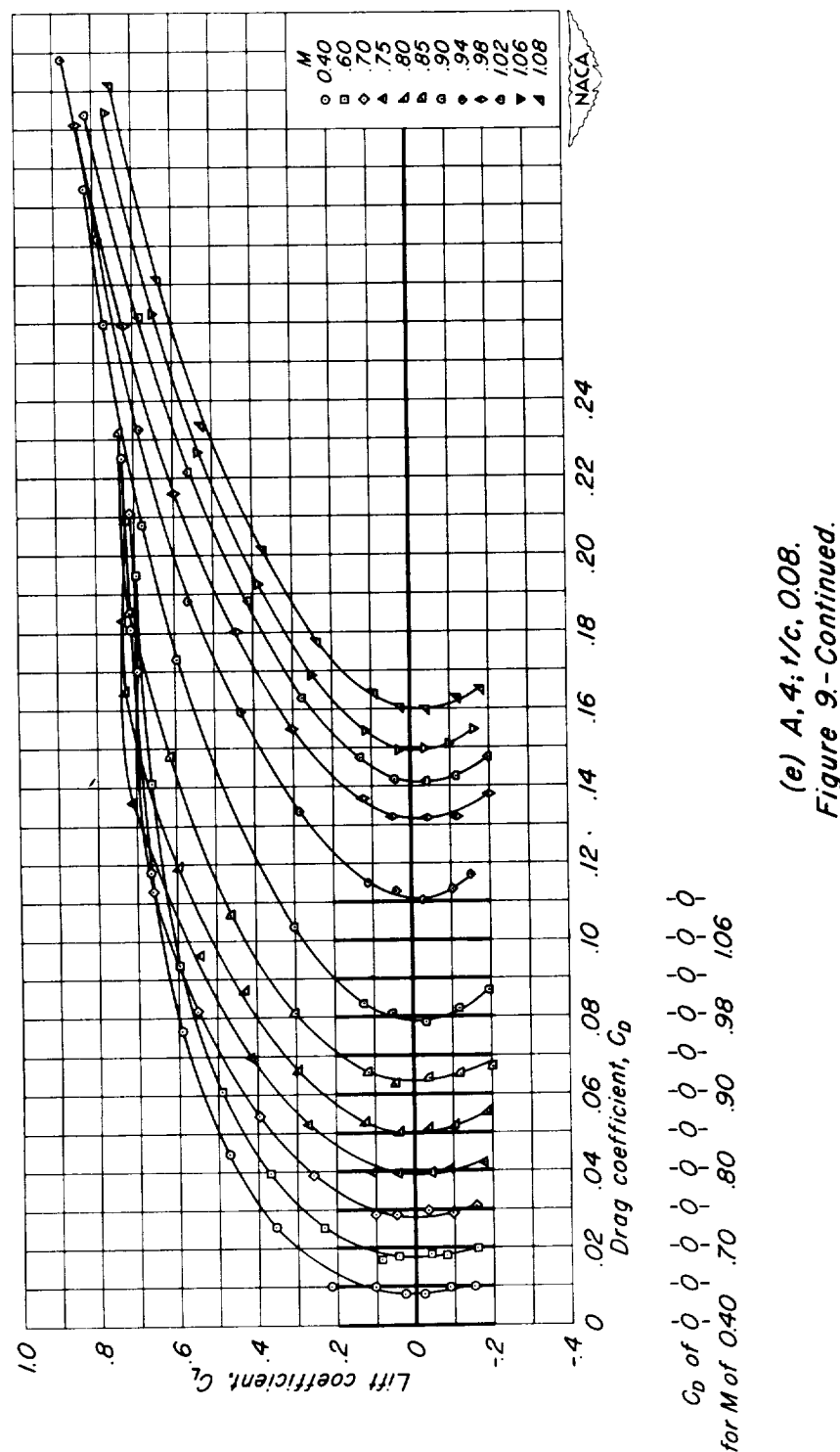
(c) A, 6; 1/c, 0.06.  
*Figure 9-Continued.*

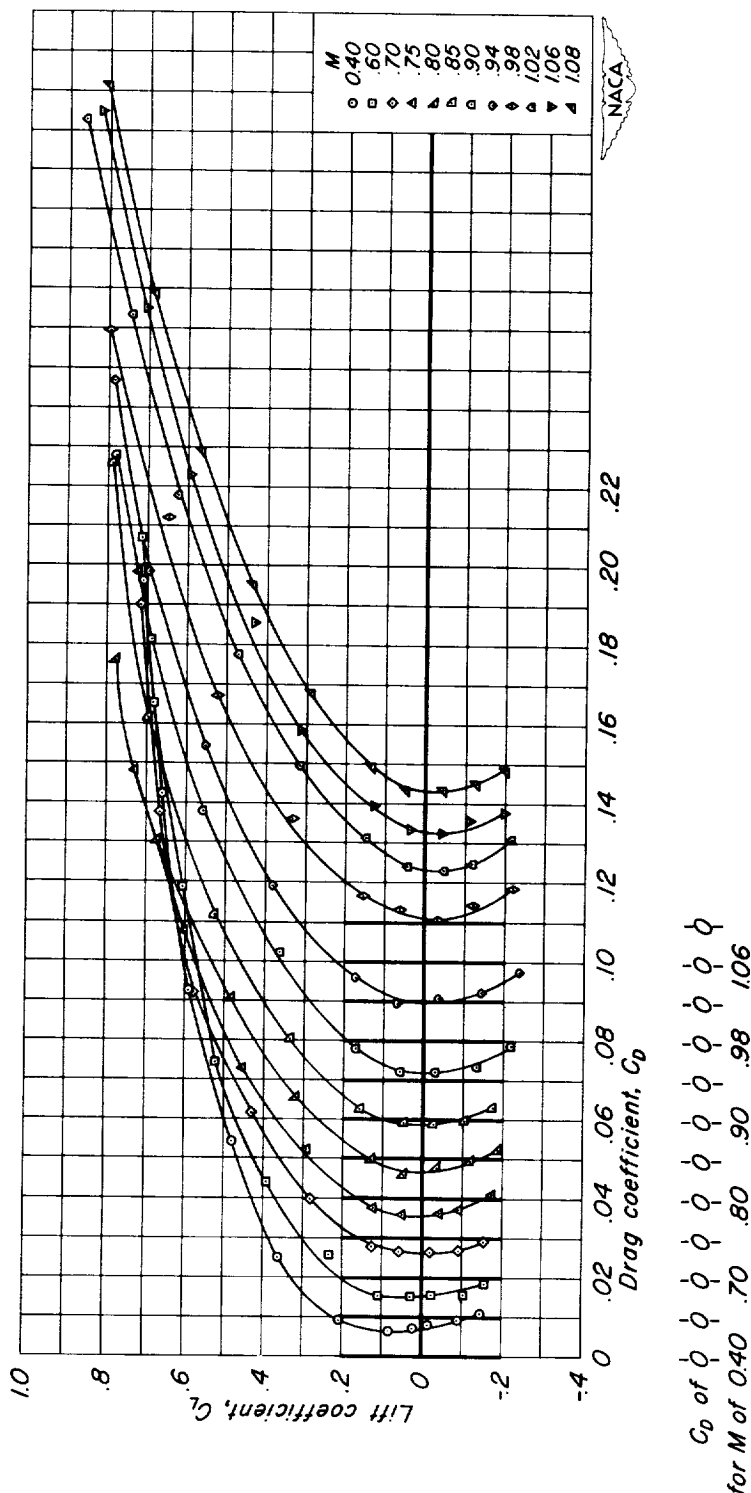
**CONFIDENTIAL**



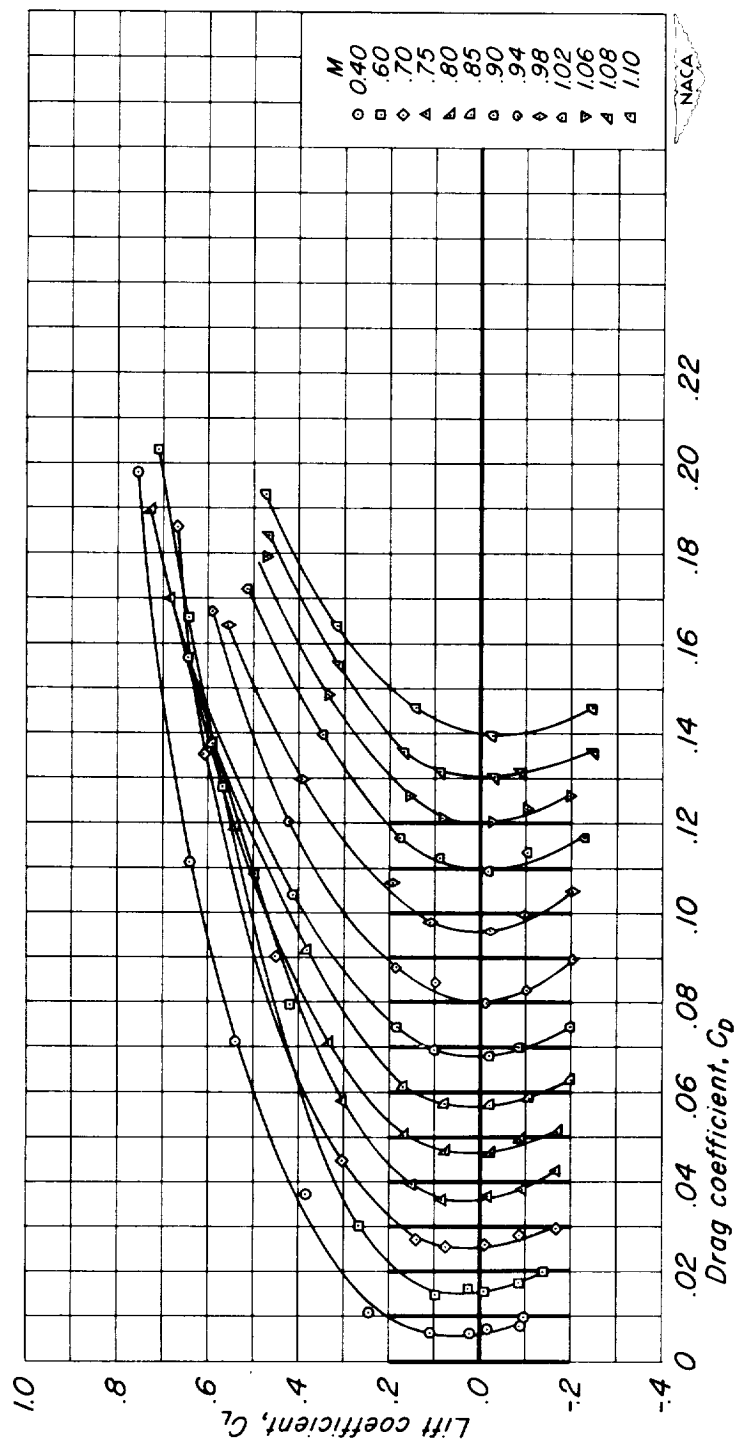
(d)  $A, 4; 1/c, 0/10$ .  
Figure 9.-Continued.

$C_d$  of  $\varnothing$   $\varnothing$   $\varnothing$   $\varnothing$   $\varnothing$   $\varnothing$   $\varnothing$   $\varnothing$   
for  $M$  of 0.40 .70 .80 .90 .98 1.06



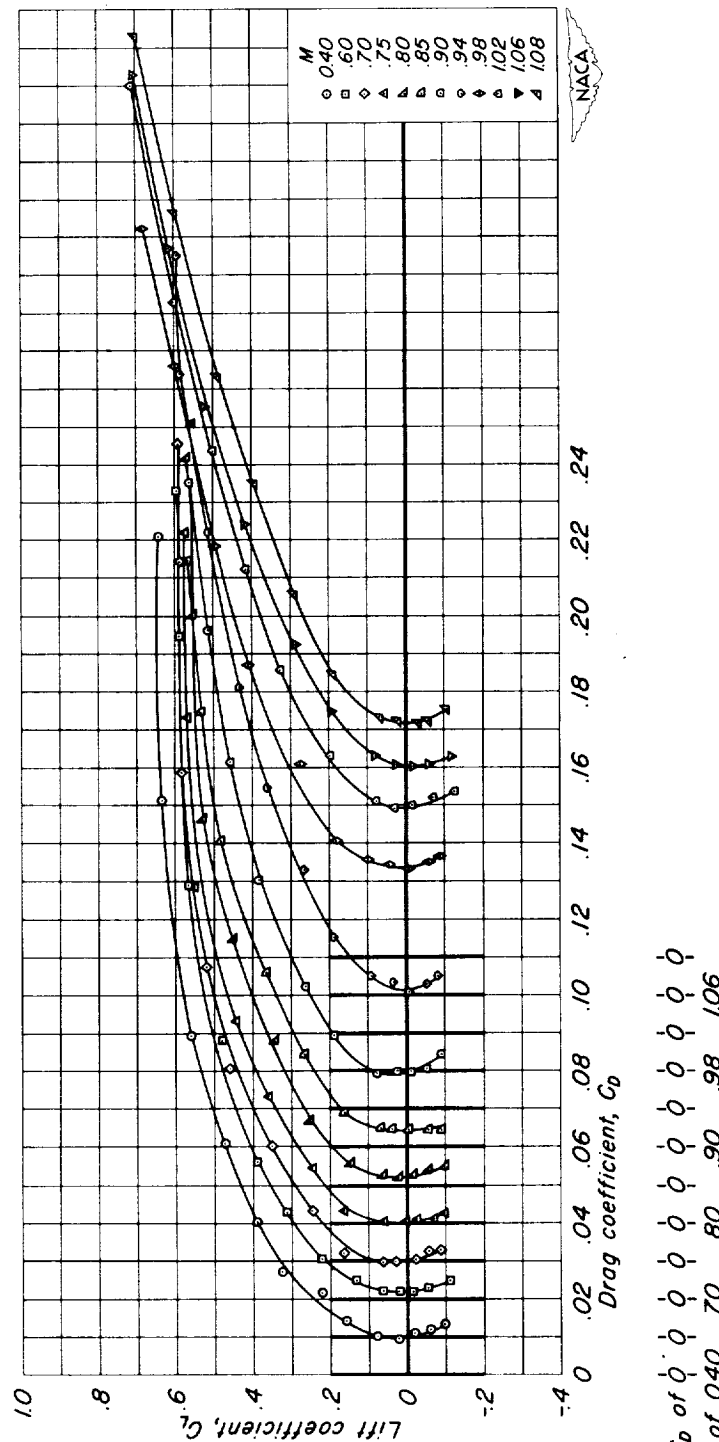


(f) A, 4;  $t/c$ , 0.06.  
Figure 9.-Continued.

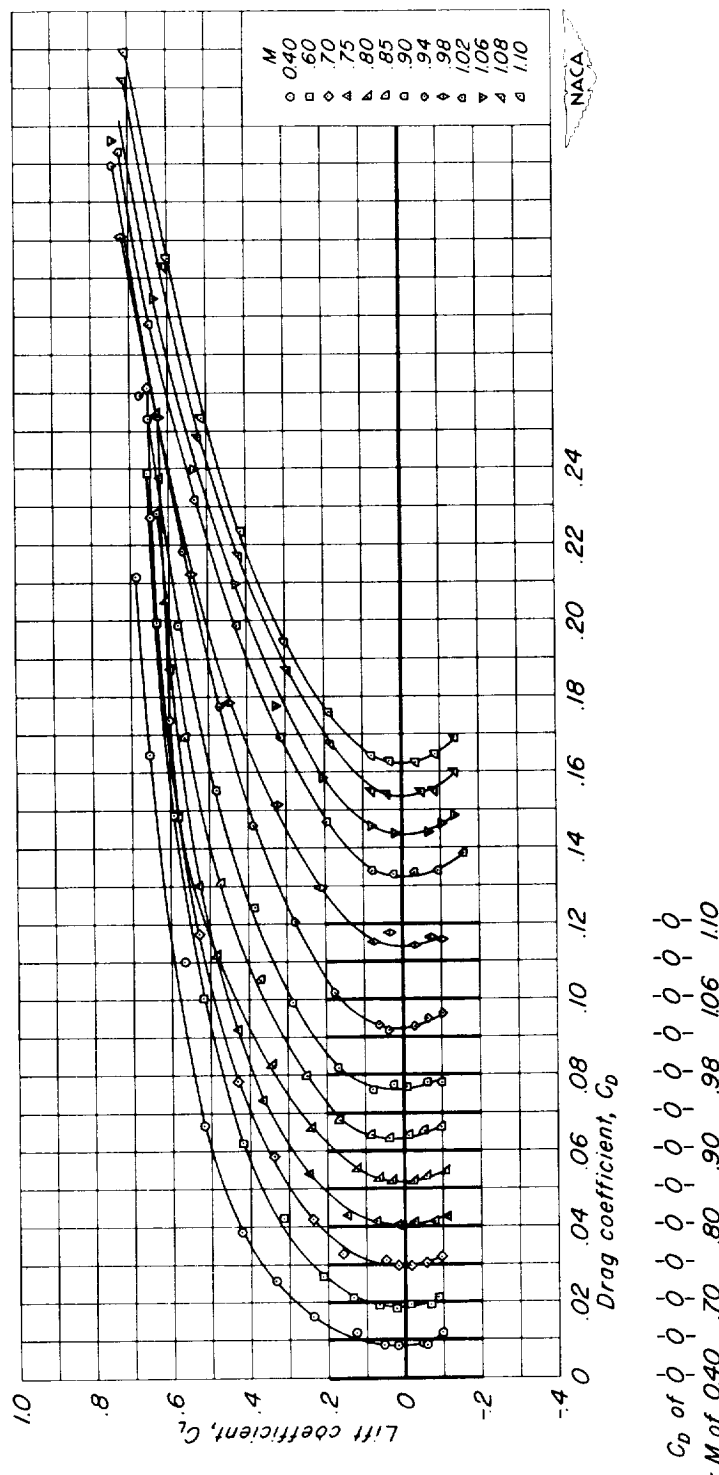


(g) A, 4; 1/c, 0.04.  
Figure 9.-Continued.

$C_D$  of  
for  $M$  of 0.40 .70 .80 .90 .98 1.06 1.10



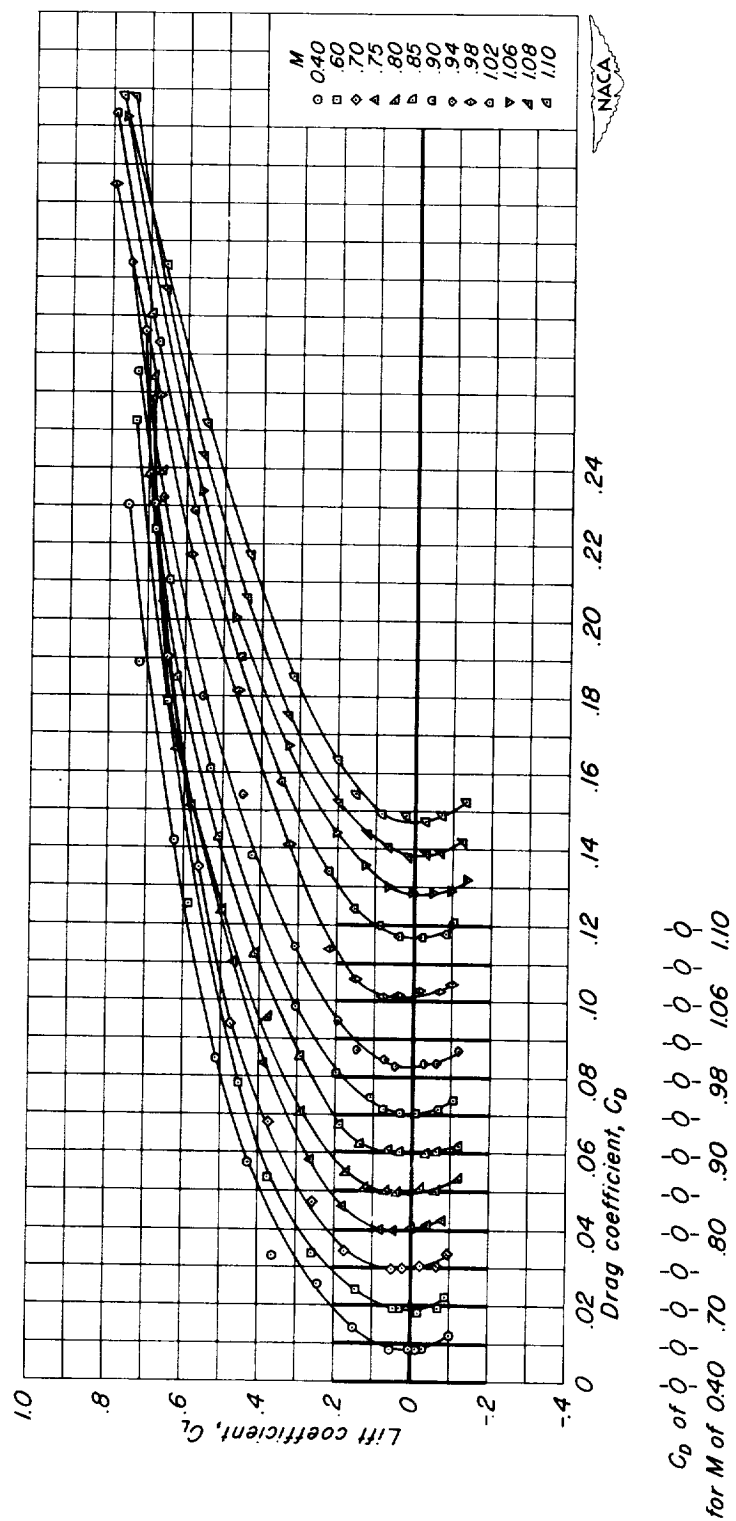
(h) A.2;  $t/c$ , 0.10.  
Figure 9.-Continued.



(i)  $A, 2; t/c, 0.08$ .  
Figure 9-Continued.

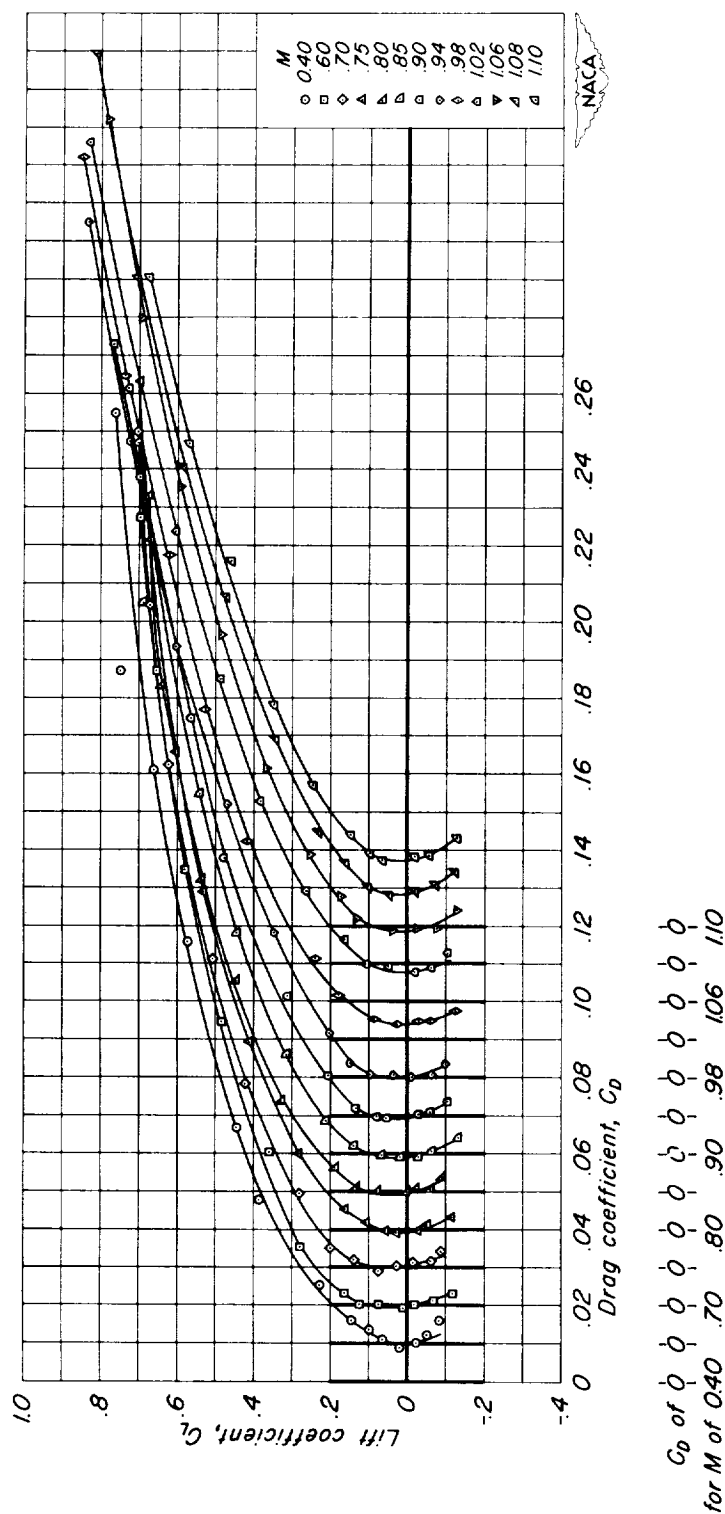
CONFIDENTIAL

NACA RM A51A12

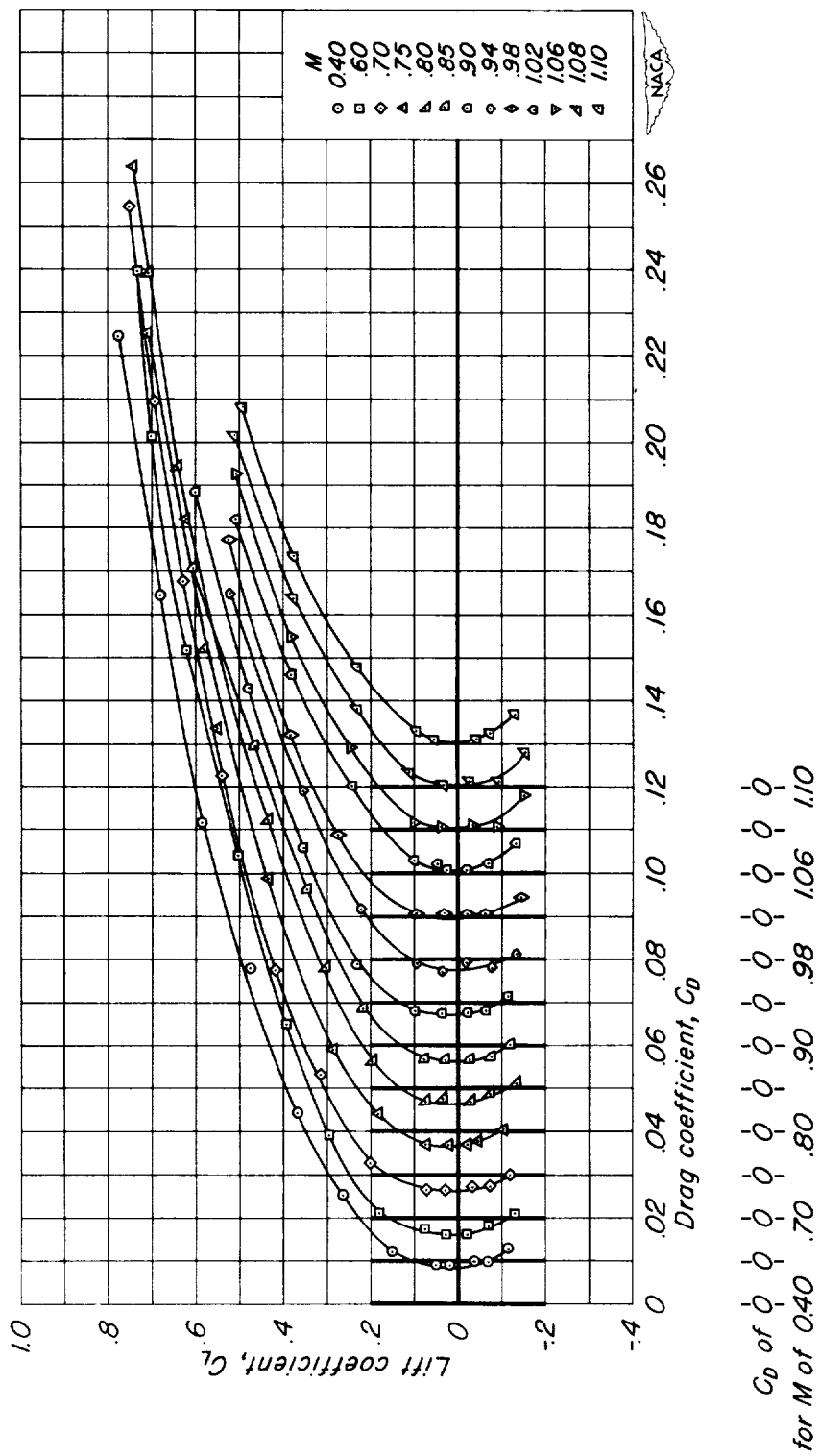


(j) A, 2; *t/c*, 0.06.  
*Figure 9-Continued.*

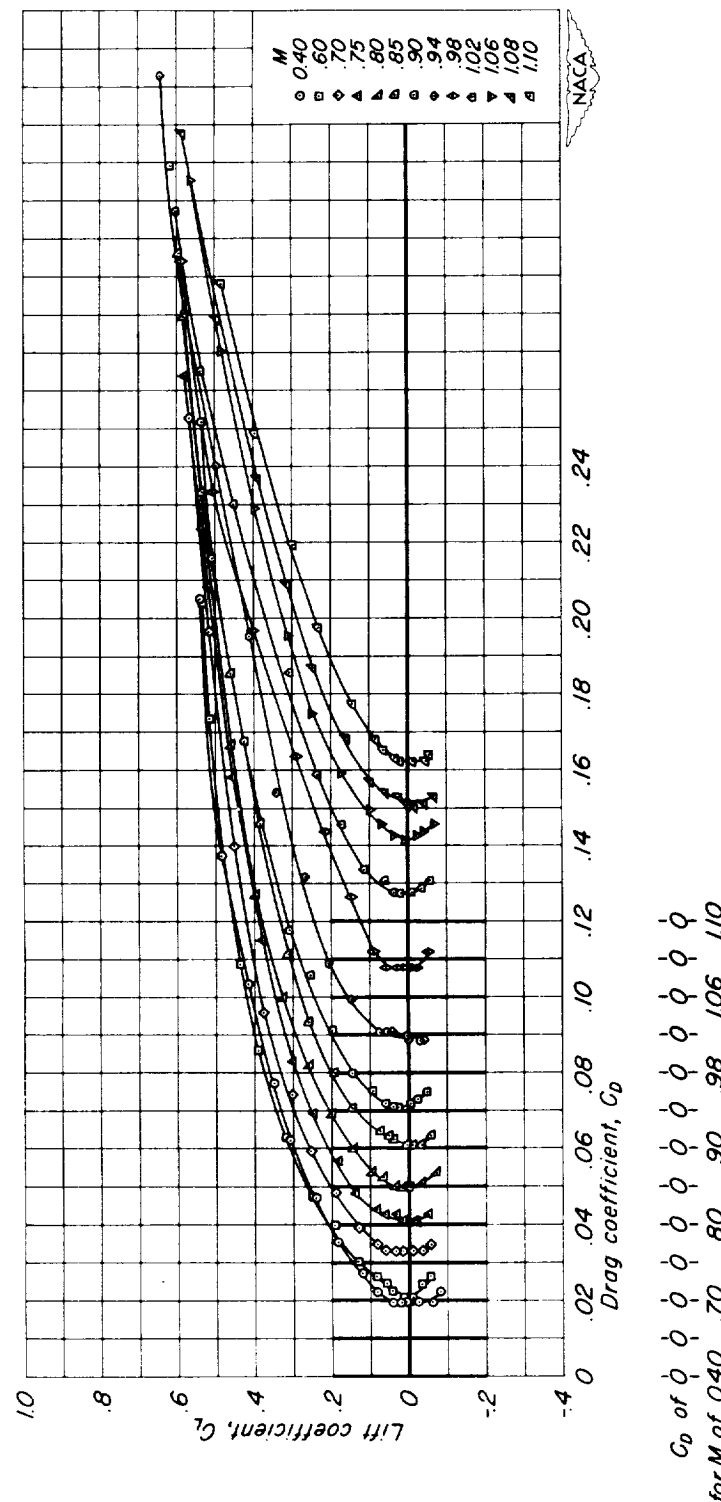
CONFIDENTIAL



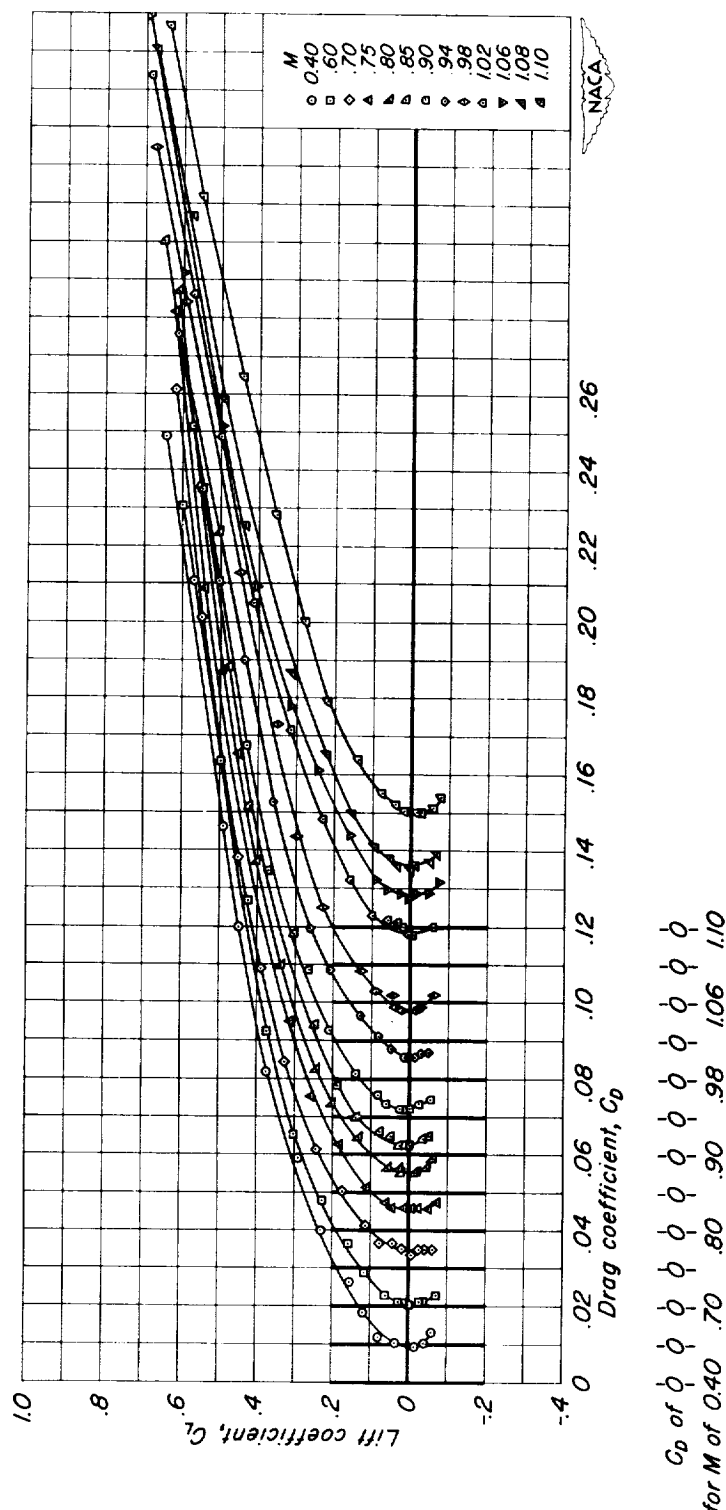
(k) A, 2;  $1/c$ , 0.04.  
Figure 9.-Continued.



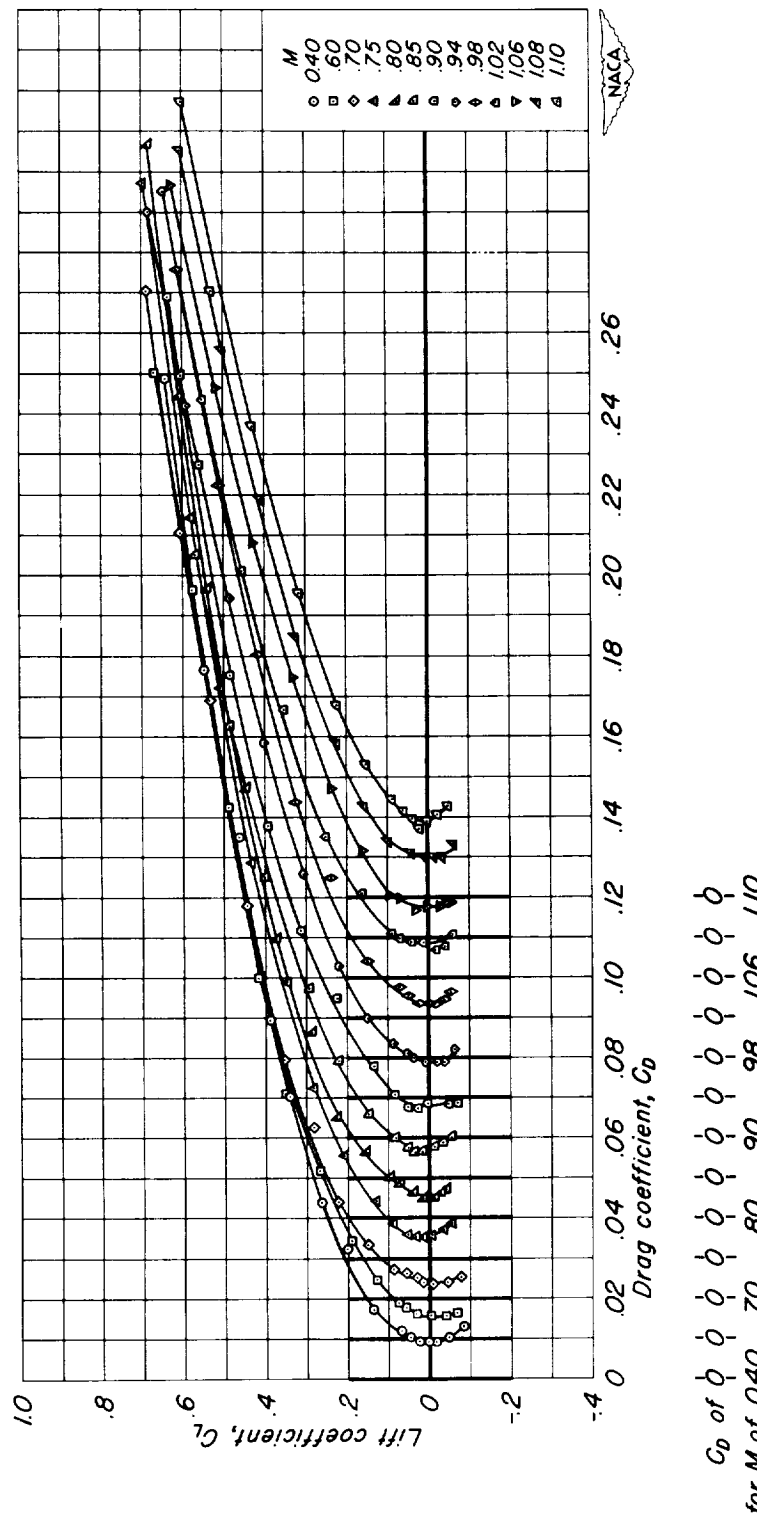
(1) A,2;  $t/c$ , 0.02.  
Figure 9.-Continued.



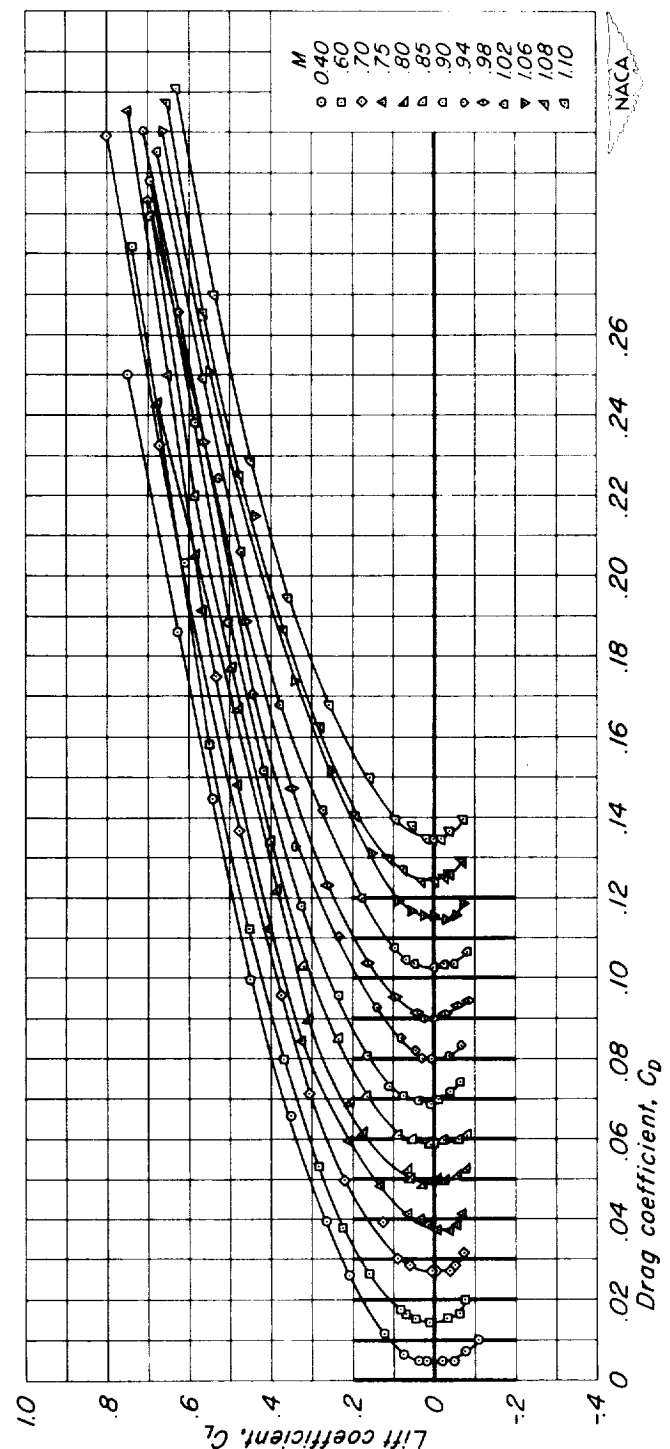
(m)  $A, l; 1/c, 0.10$ .  
Figure 9.-Continued.



(n)  $A, l; t/c, 0.08$ .  
Figure 9.-Continued.



(o)  $A, 1; t/c, 0.06.$   
*Figure 9-Continued.*



(P) A, 1;  $t/c$ , 0.04.  
Figure 9.-Continued.

$C_d$  or  $\frac{1}{2} \rho V^2 S C_d$   
for  $M$  of 0.40 .70 .80 .90 .98 1.06 1.10

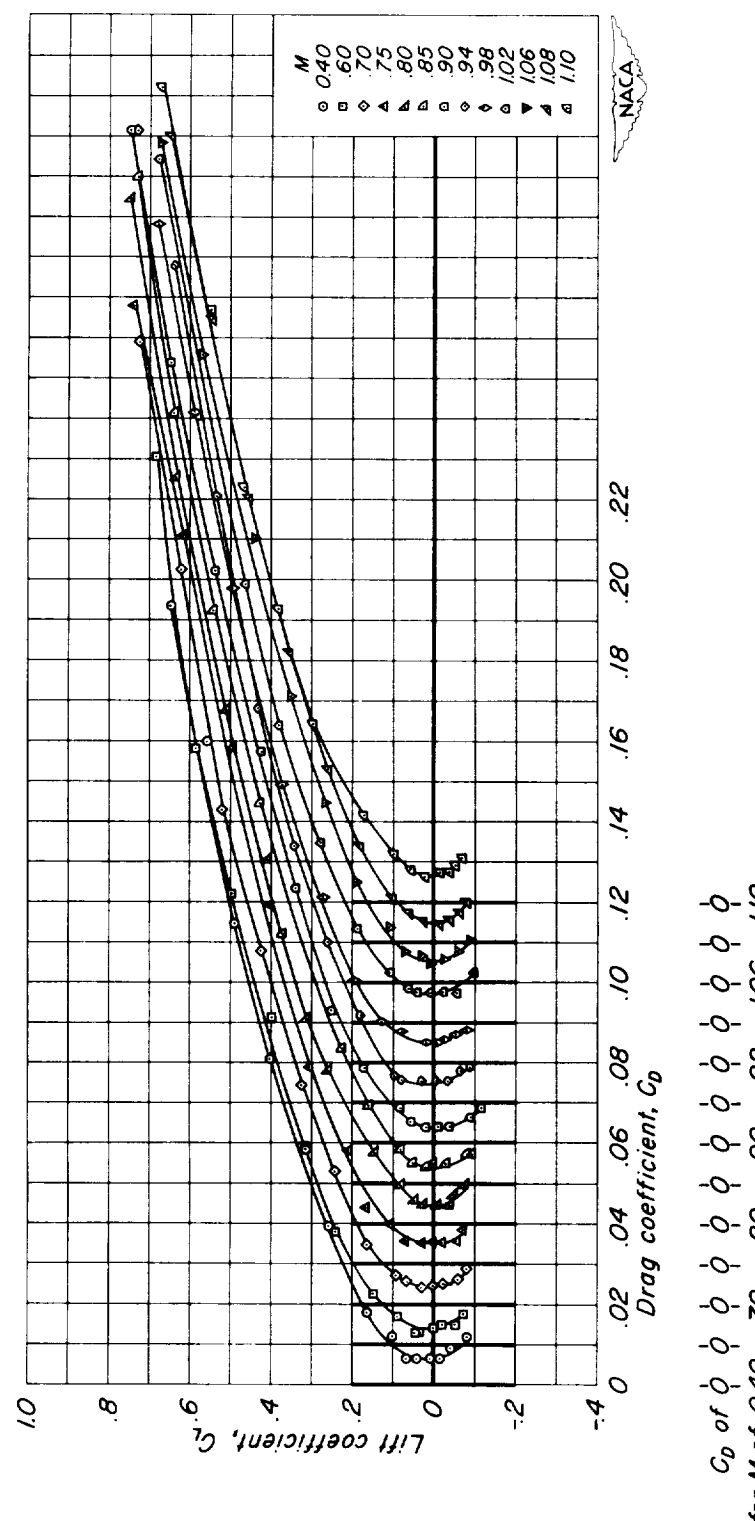
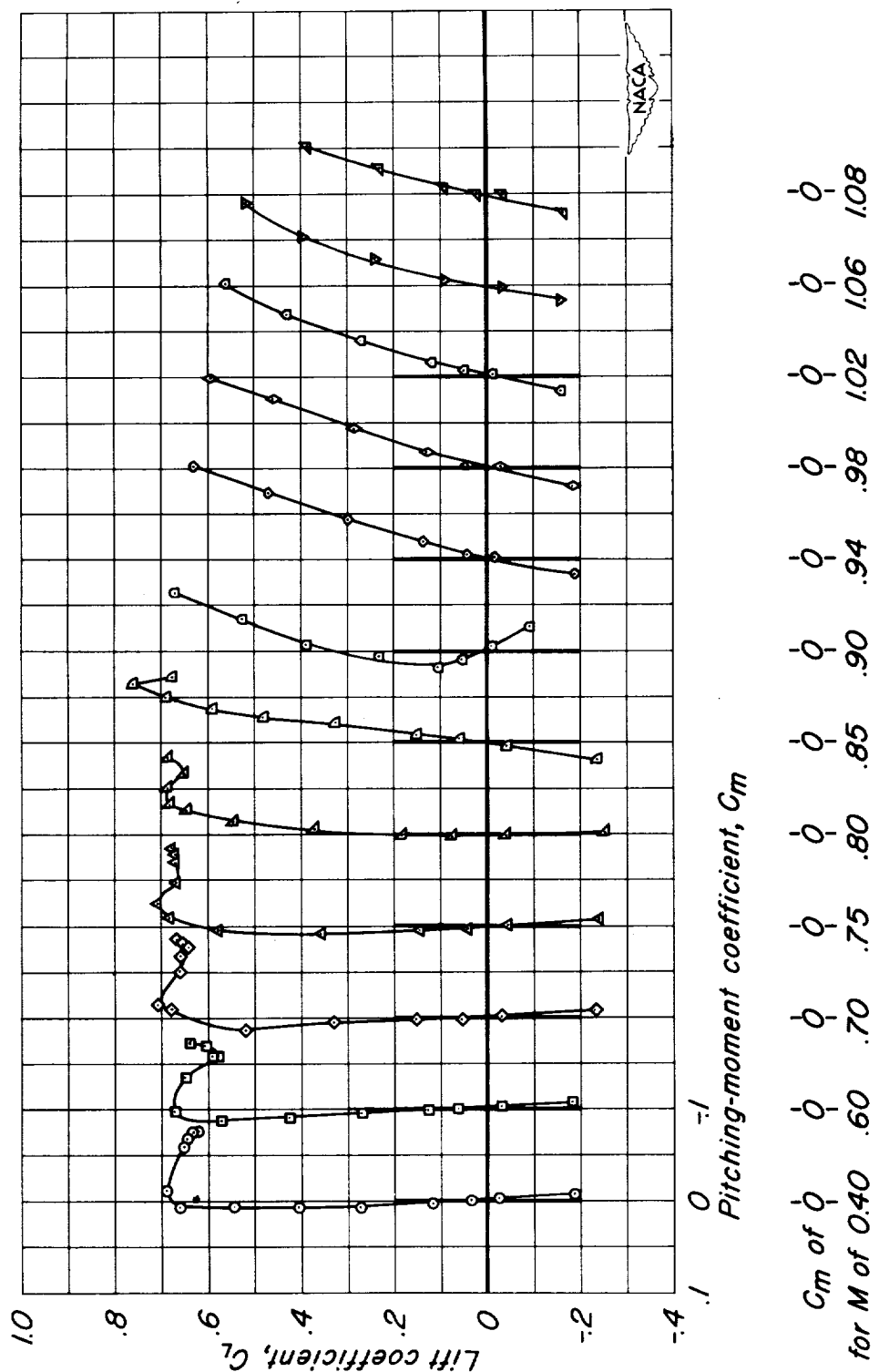
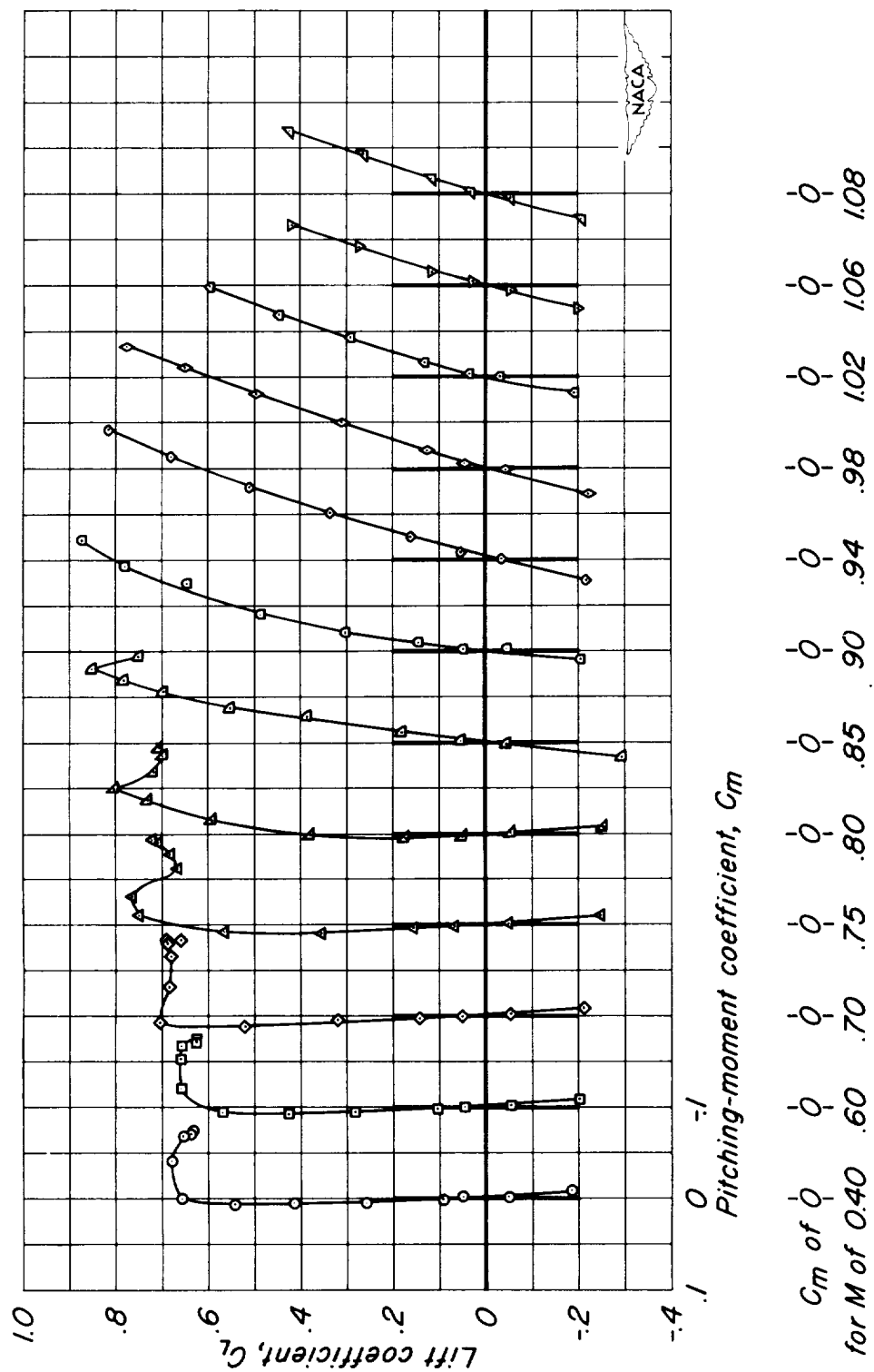


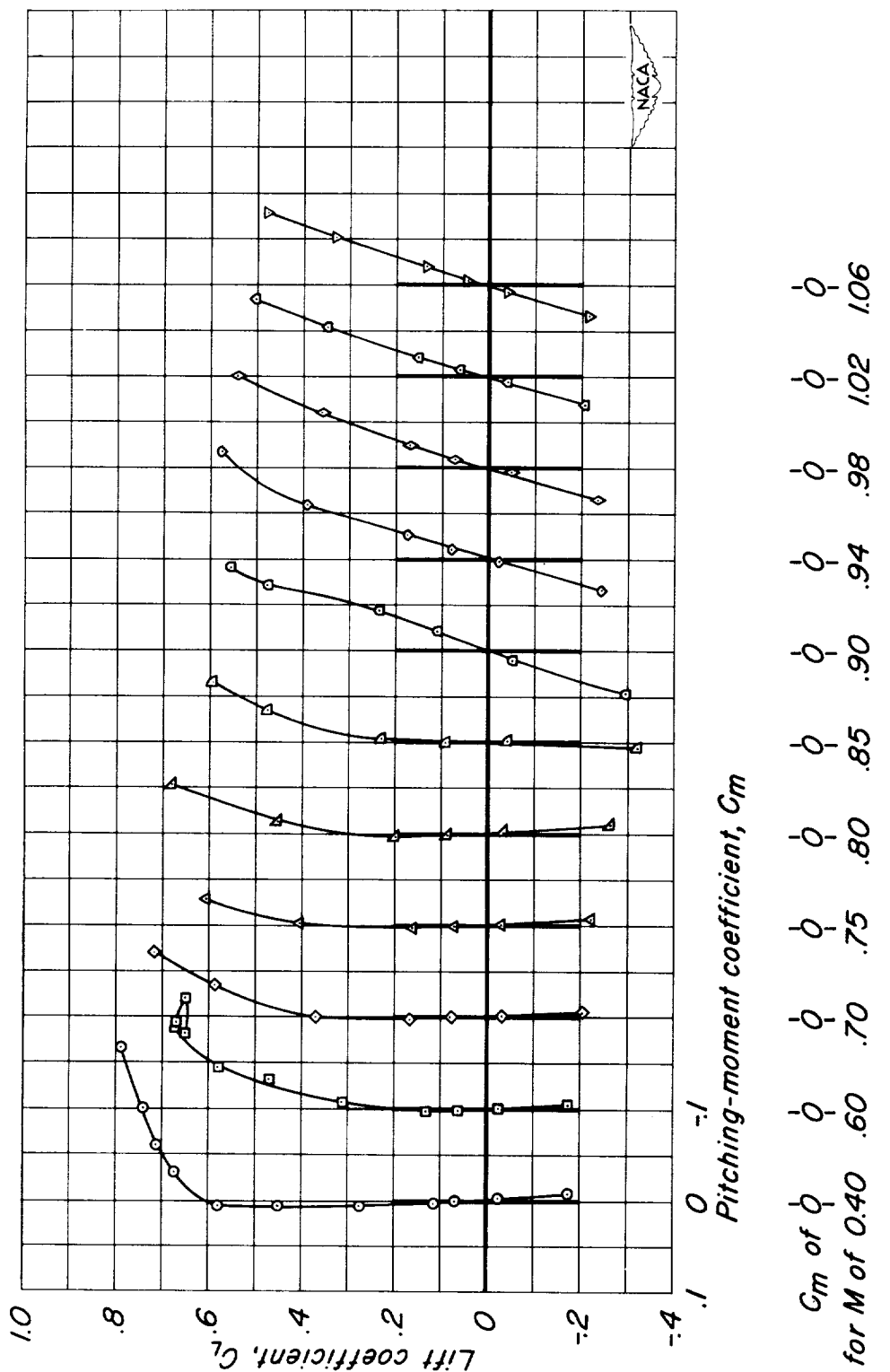
Figure 9.-Concluded.  
(a)  $A/l = t/c = 0.02$ .



(a)  $A = 6; t/c = 0.10.$   
*Figure 10.-The variation of pitching-moment coefficient with lift coefficient for the rectangular wings with NACA 63AOXX sections.*

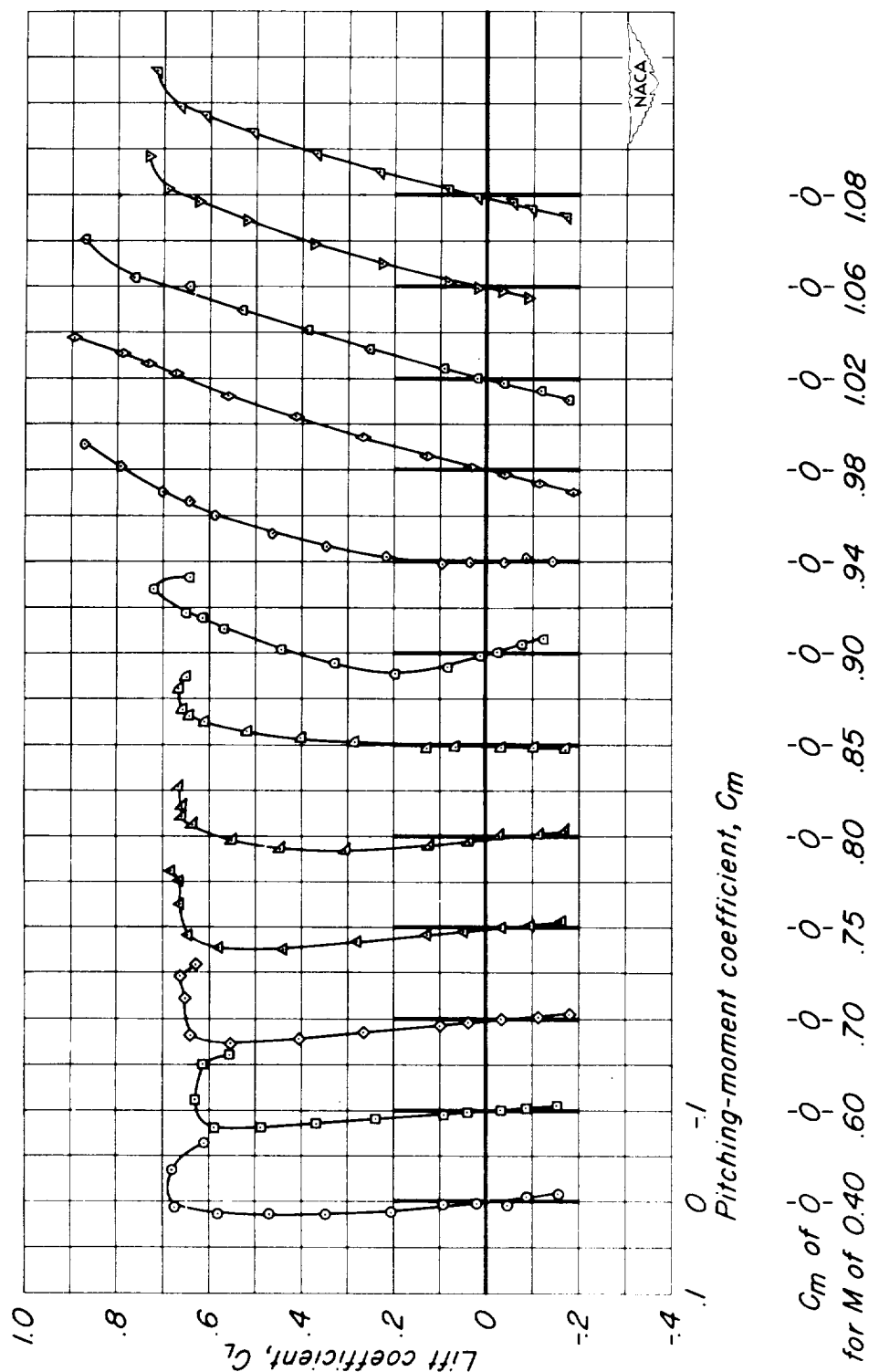


(b)  $A,6; t/c, 0.08$ .  
Figure 10.-Continued.

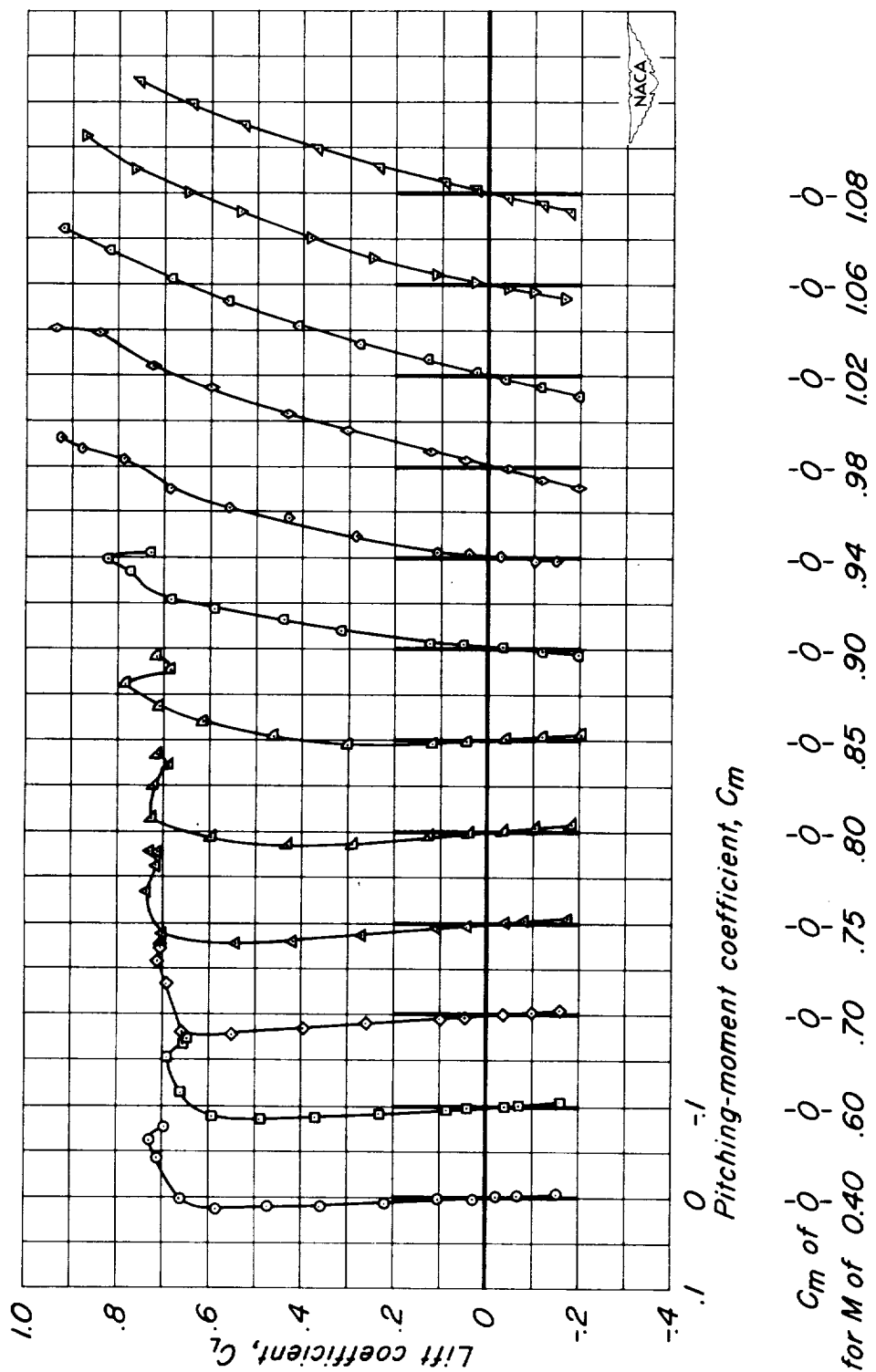


(c) A, 6;  $t/c$ , 0.06.  
*Figure 10-Continued.*

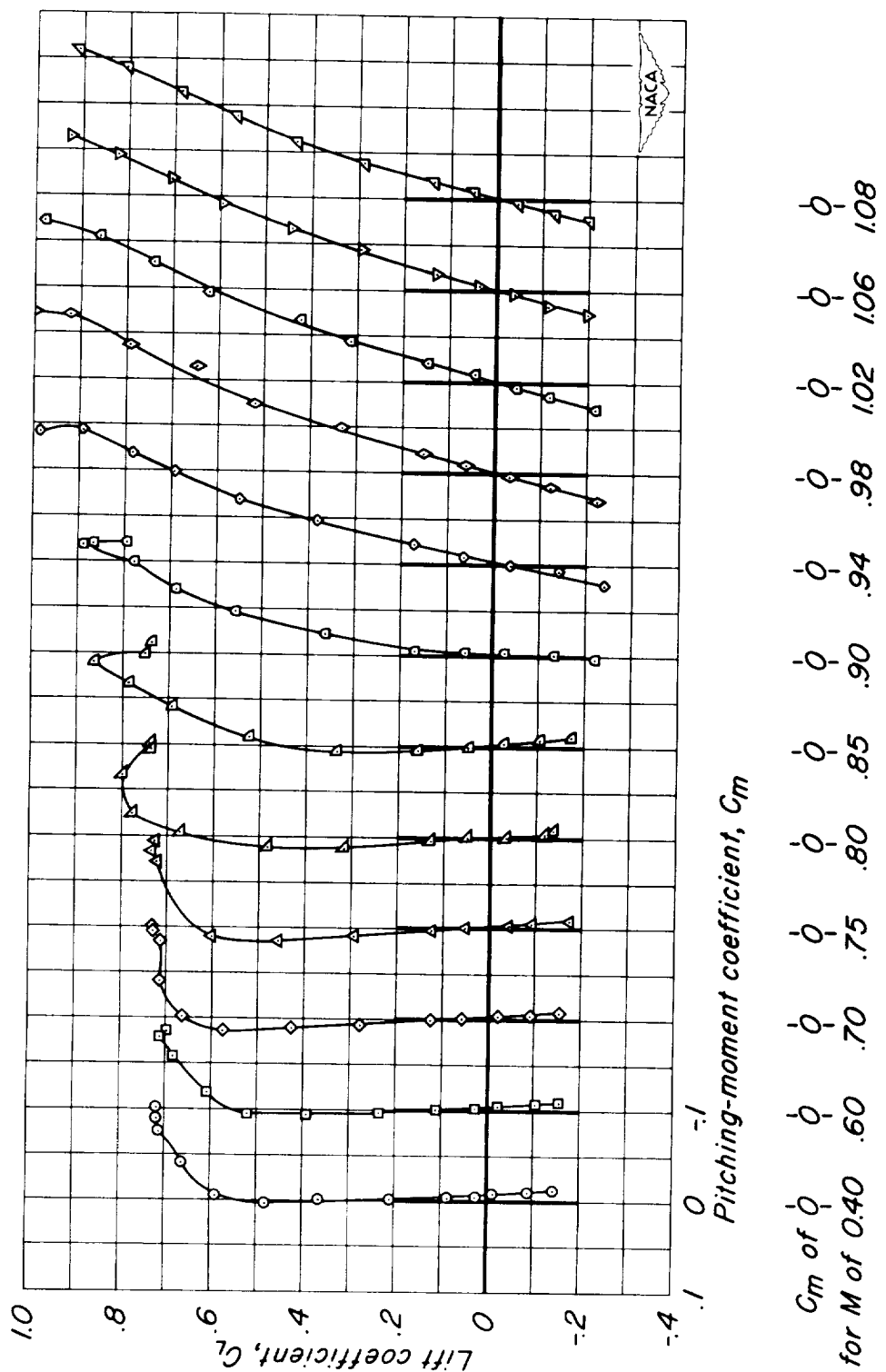
CONFIDENTIAL



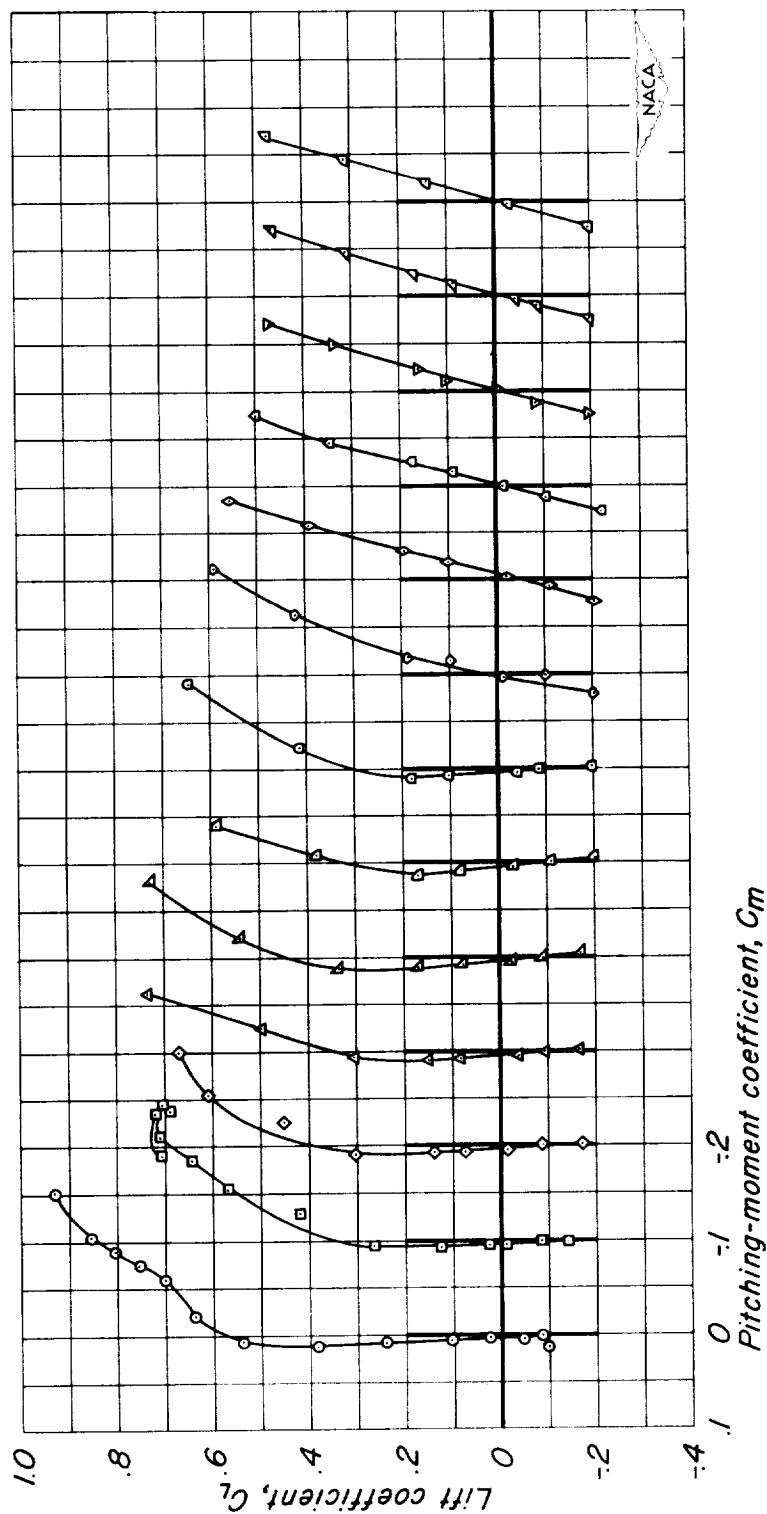
(d)  $A, 4; t/c, 0, 10$ .  
Figure 10.-Continued.



(e) A, 4;  $t/c$ , 0.08.  
Figure 10-Continued.



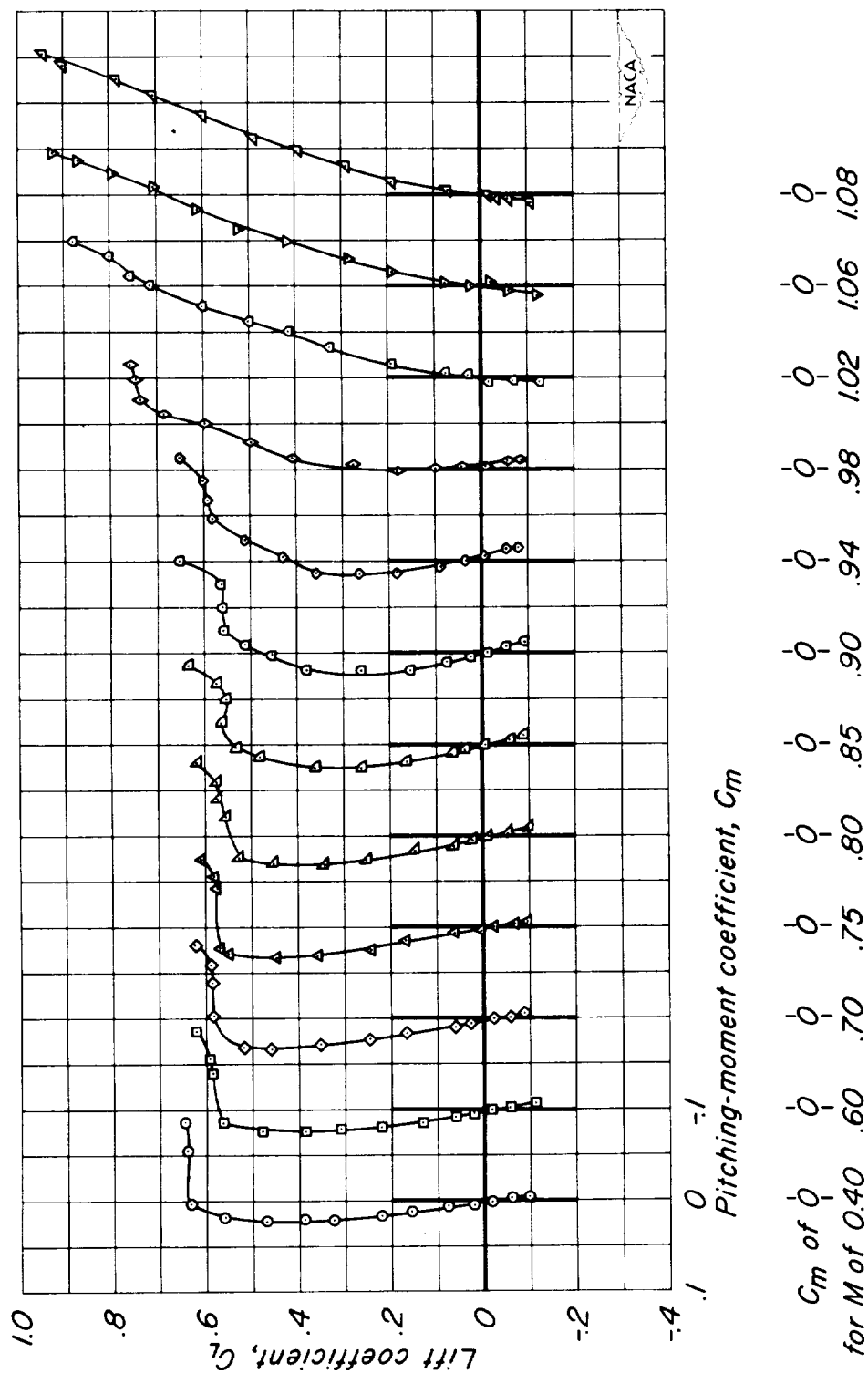
(f)  $A, 4; t/c, 0.06$ .  
Figure 10-Continued.



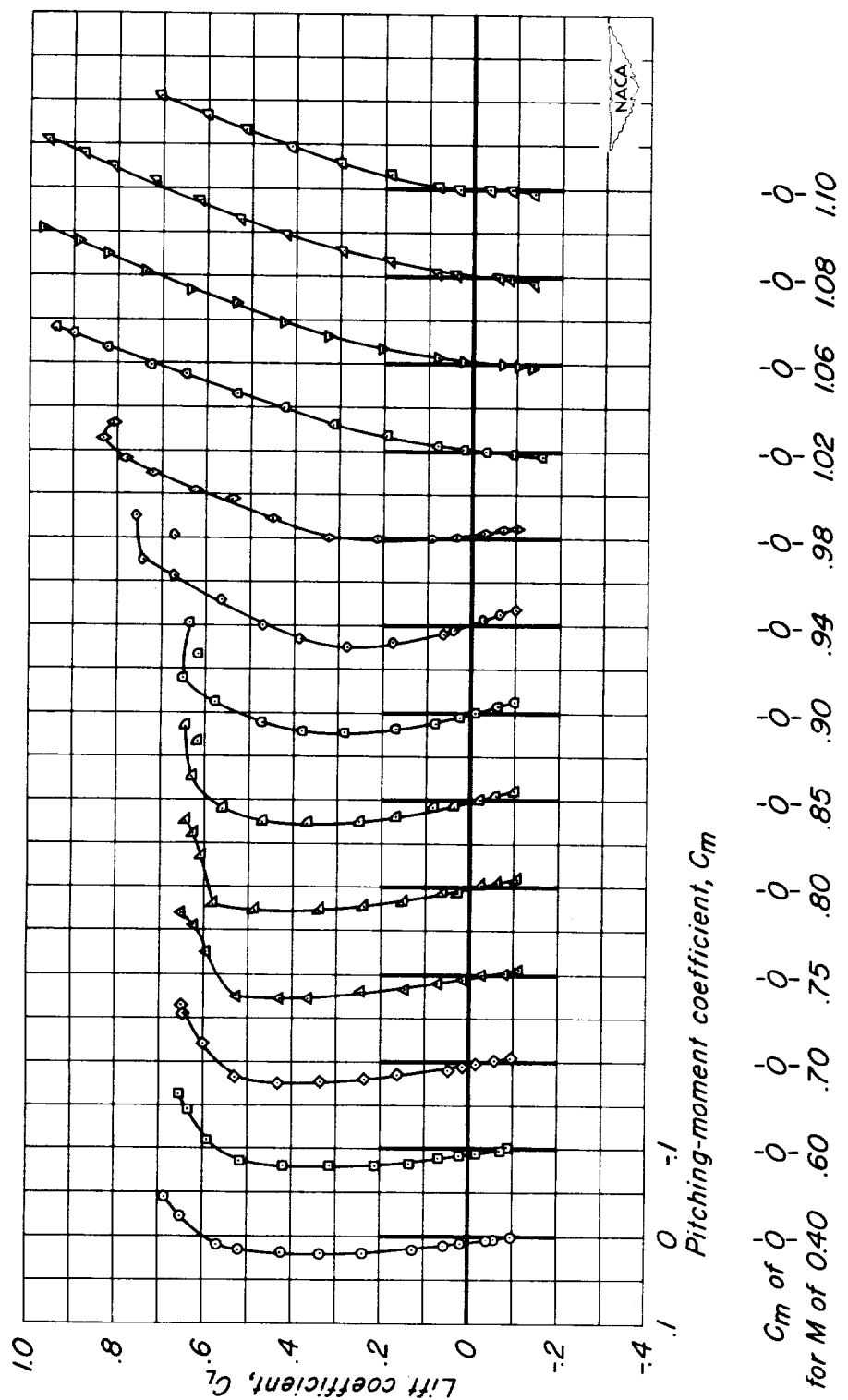
$C_m$  of  $\phi$   
for  $M$  of 0.40    0    0    0    0    0    0    0  
                     .60    .70    .75    .80    .85    .90    .94    .98    1.02    1.06    1.08    1.10

$\int \quad 0 \quad -1 \quad -2$   
*Pitching-moment coefficient,  $C_m$*

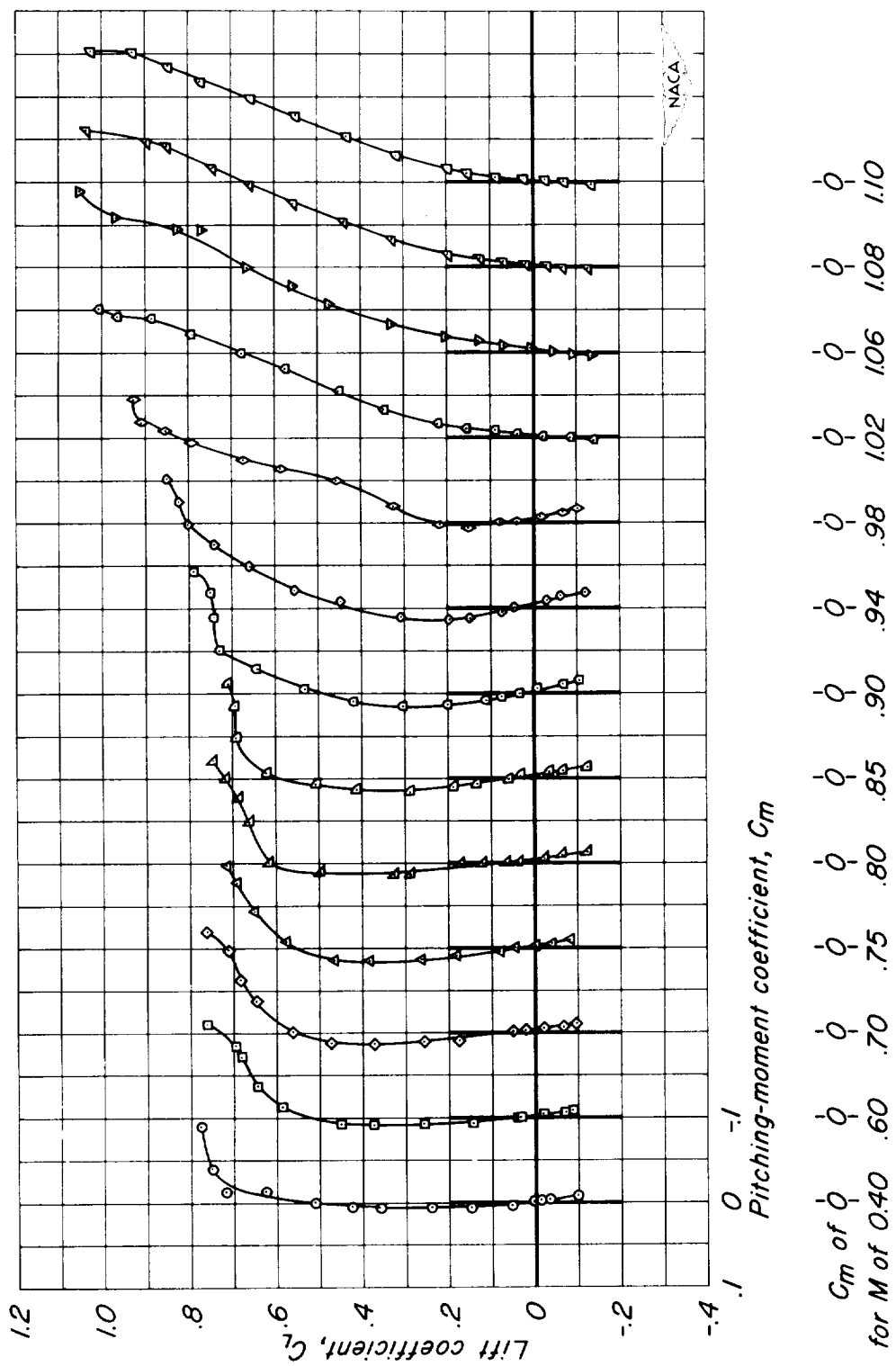
(g)  $A, 4; t/c, 0.04$ .  
Figure 10.-Continued.



(h)  $A, 2; t/c, 0.10$ .  
*Figure 10 - Continued.*



(i)  $A, 2; t/c, 0.08$ .  
Figure 10.-Continued.



(j) A,2;  $t/c$ , 0.06.  
Figure 10.-Continued.

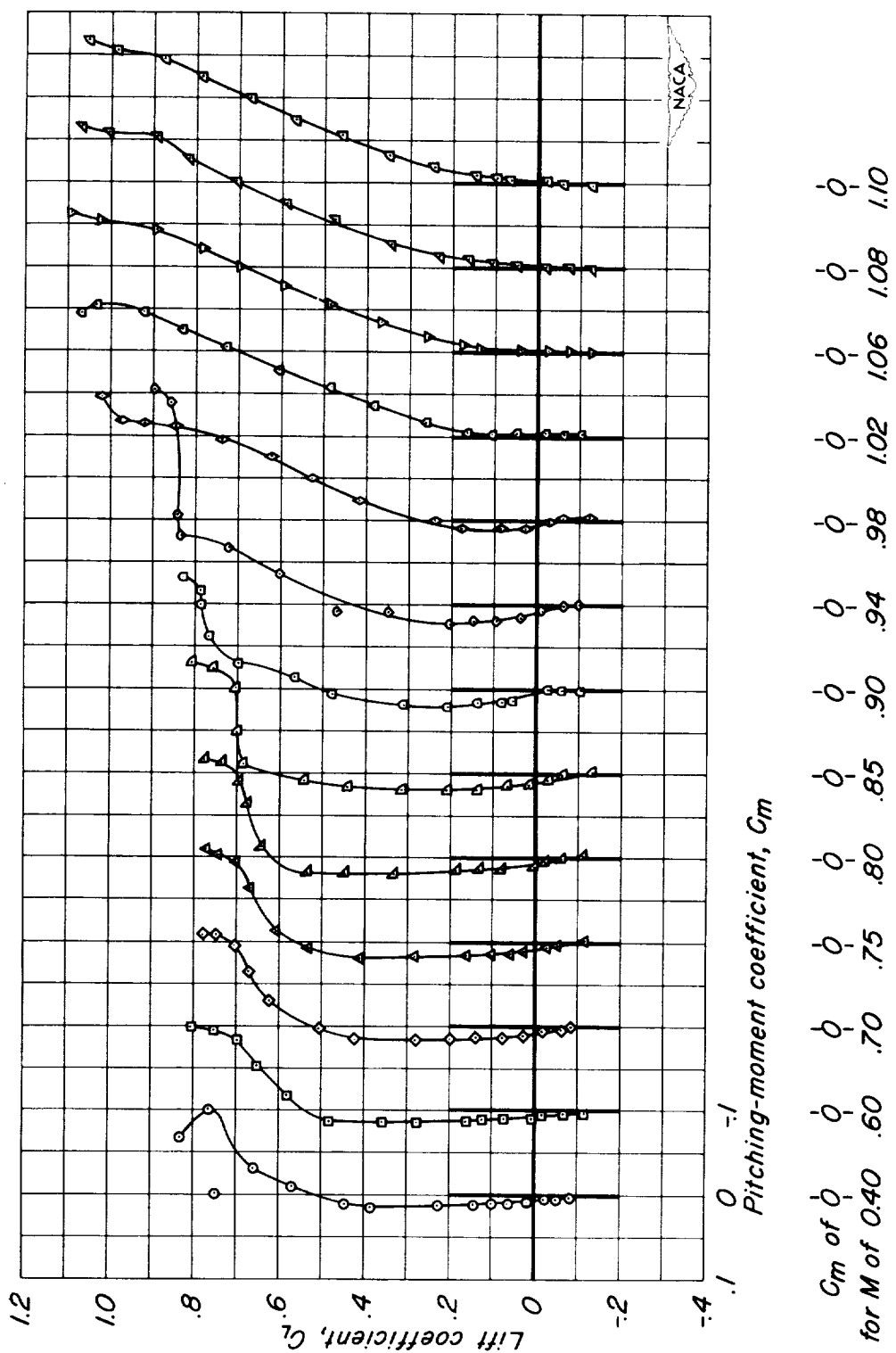
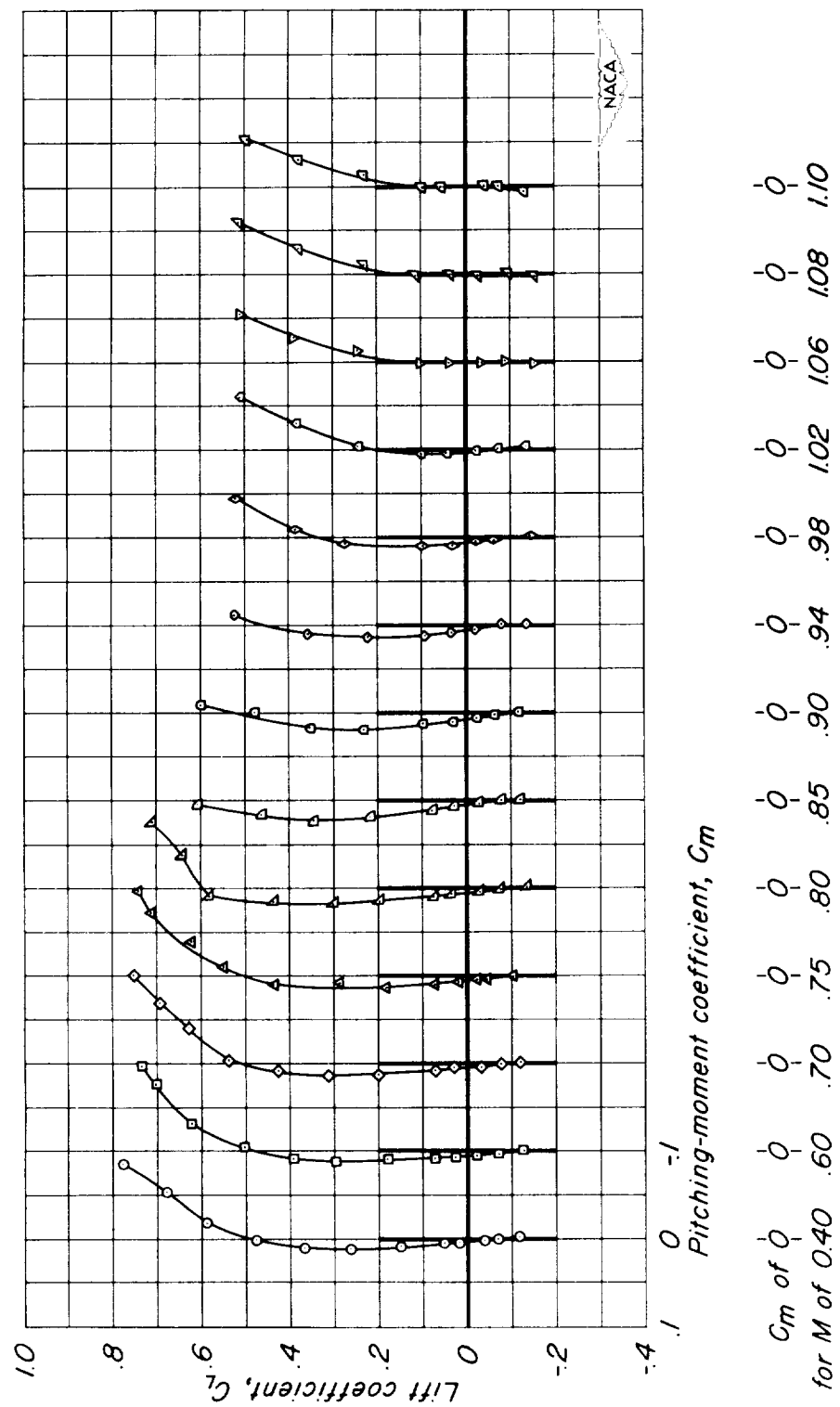
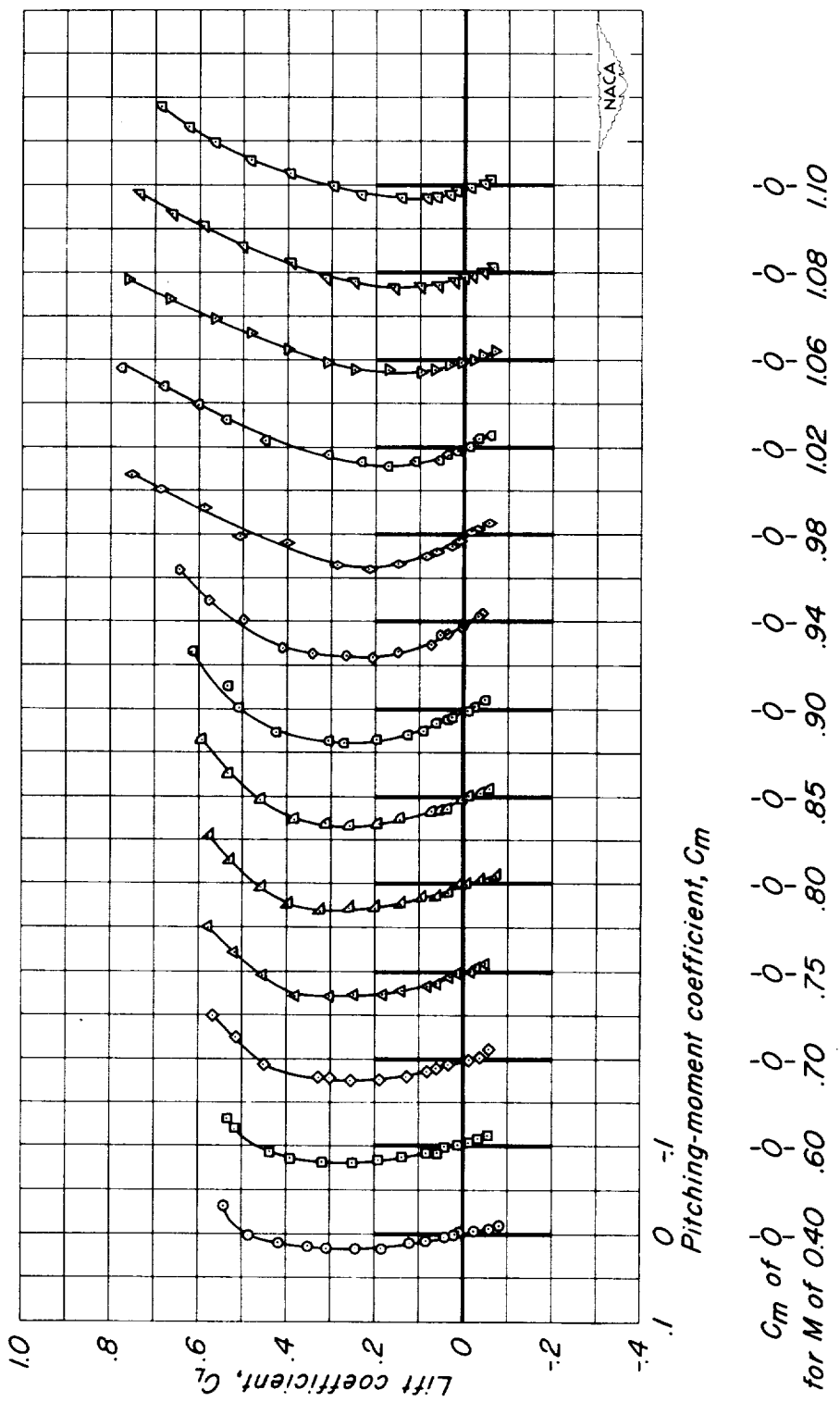


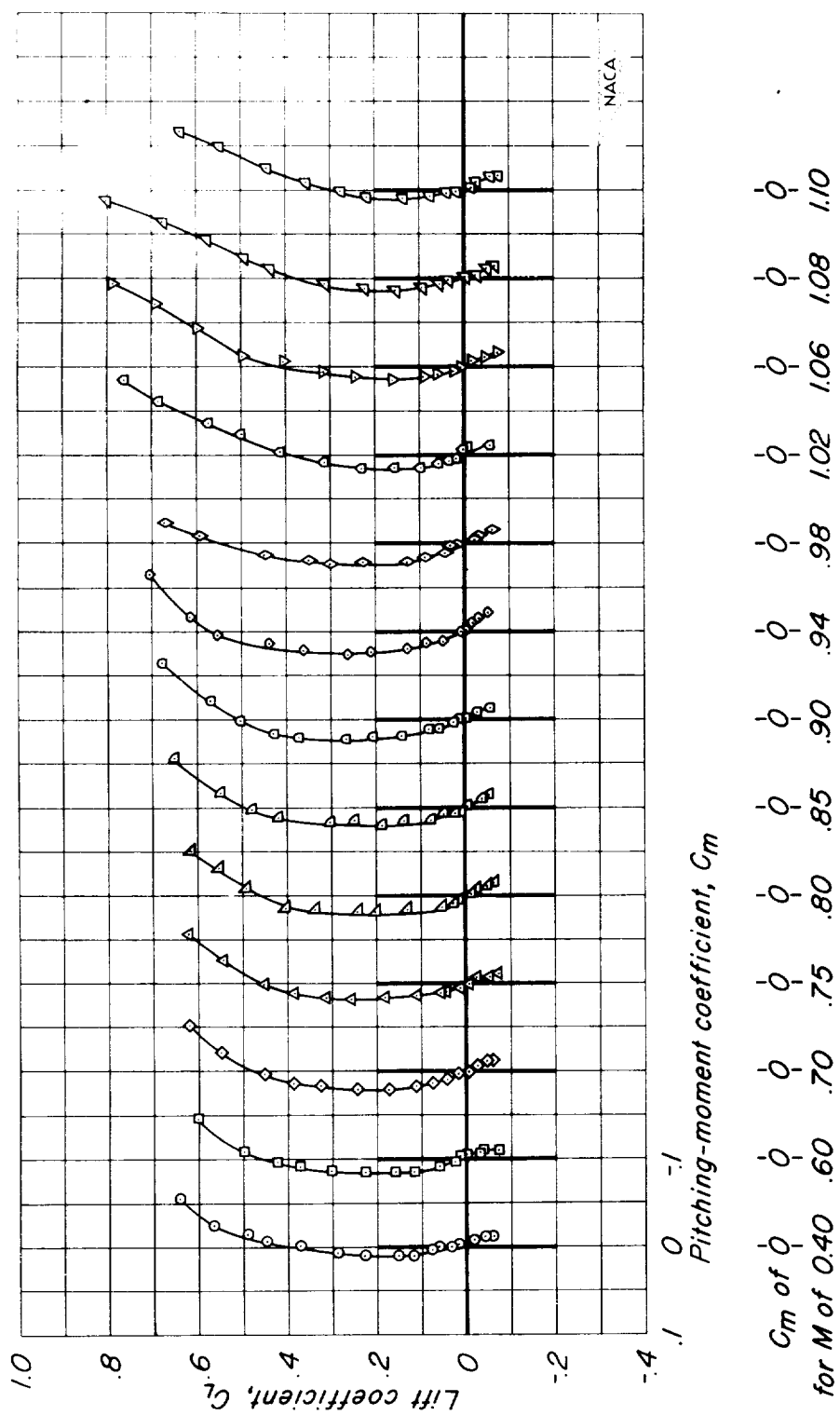
Figure 10.-Continued.



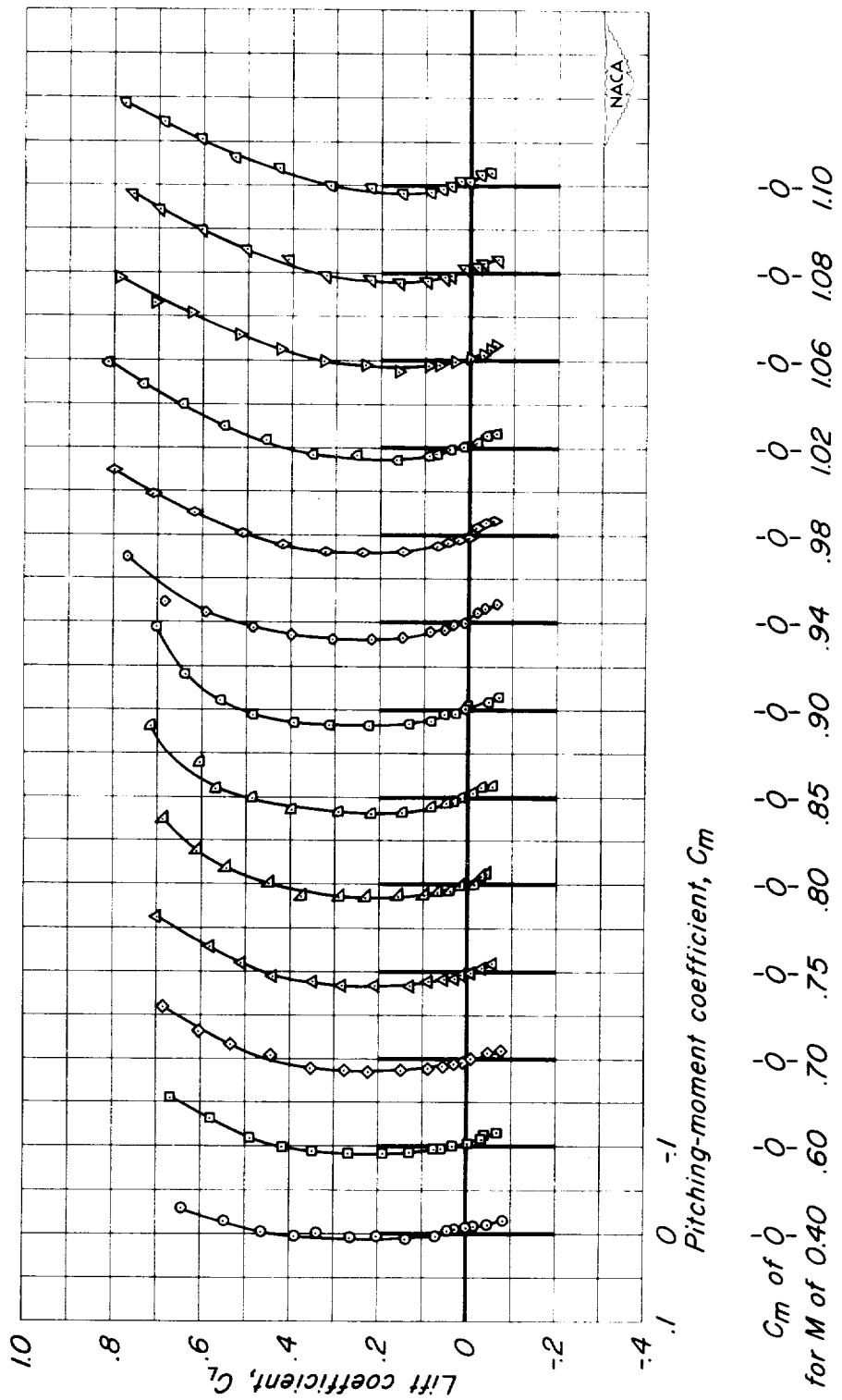
(1) A, 2;  $t/c$ , 0.02.  
Figure 10.-Continued.



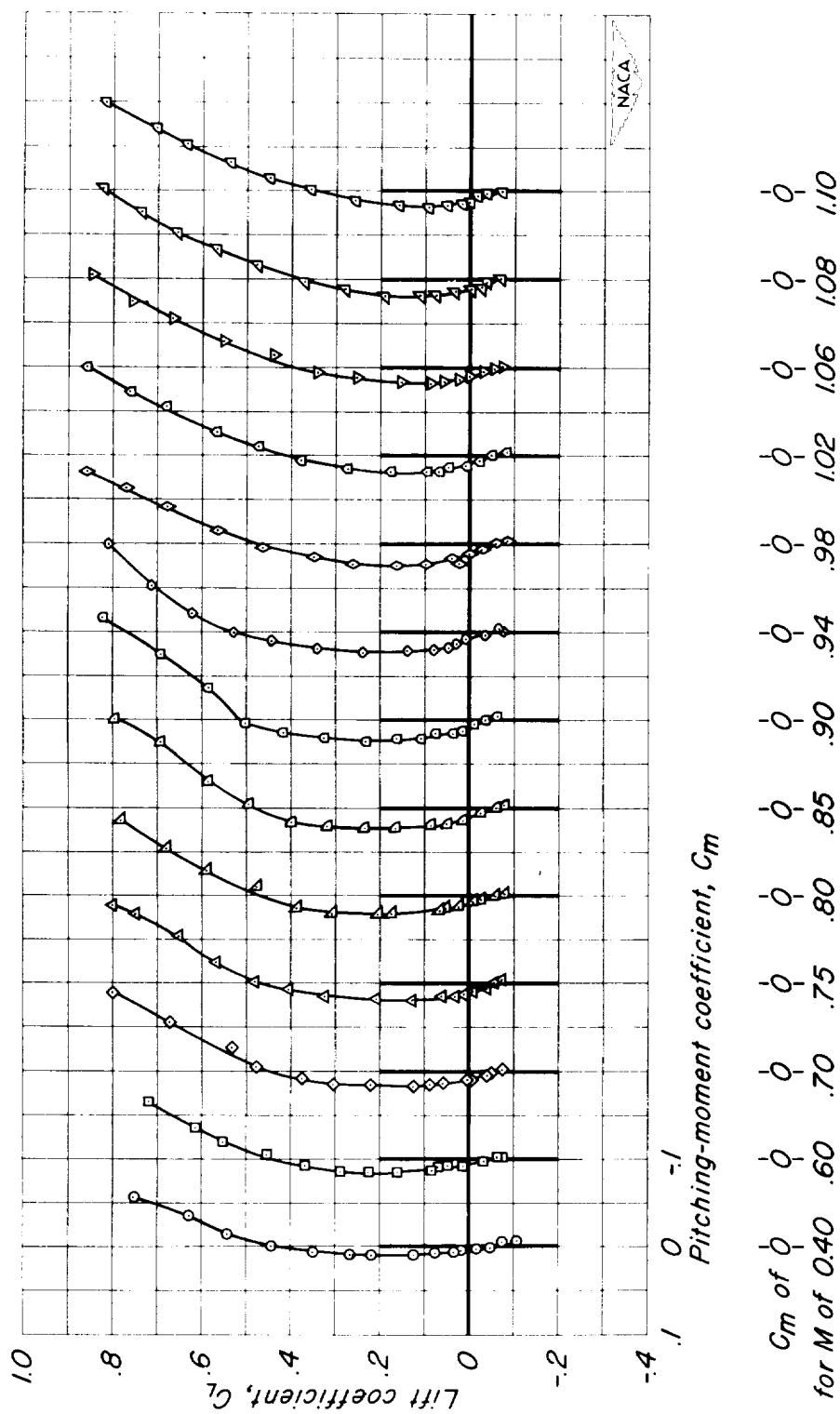
(m)  $A, l; r/c, 0.10$ .  
Figure 10.—Continued.



(n)  $A, l; t/c, 0.008$ .  
Figure 10.—Continued.

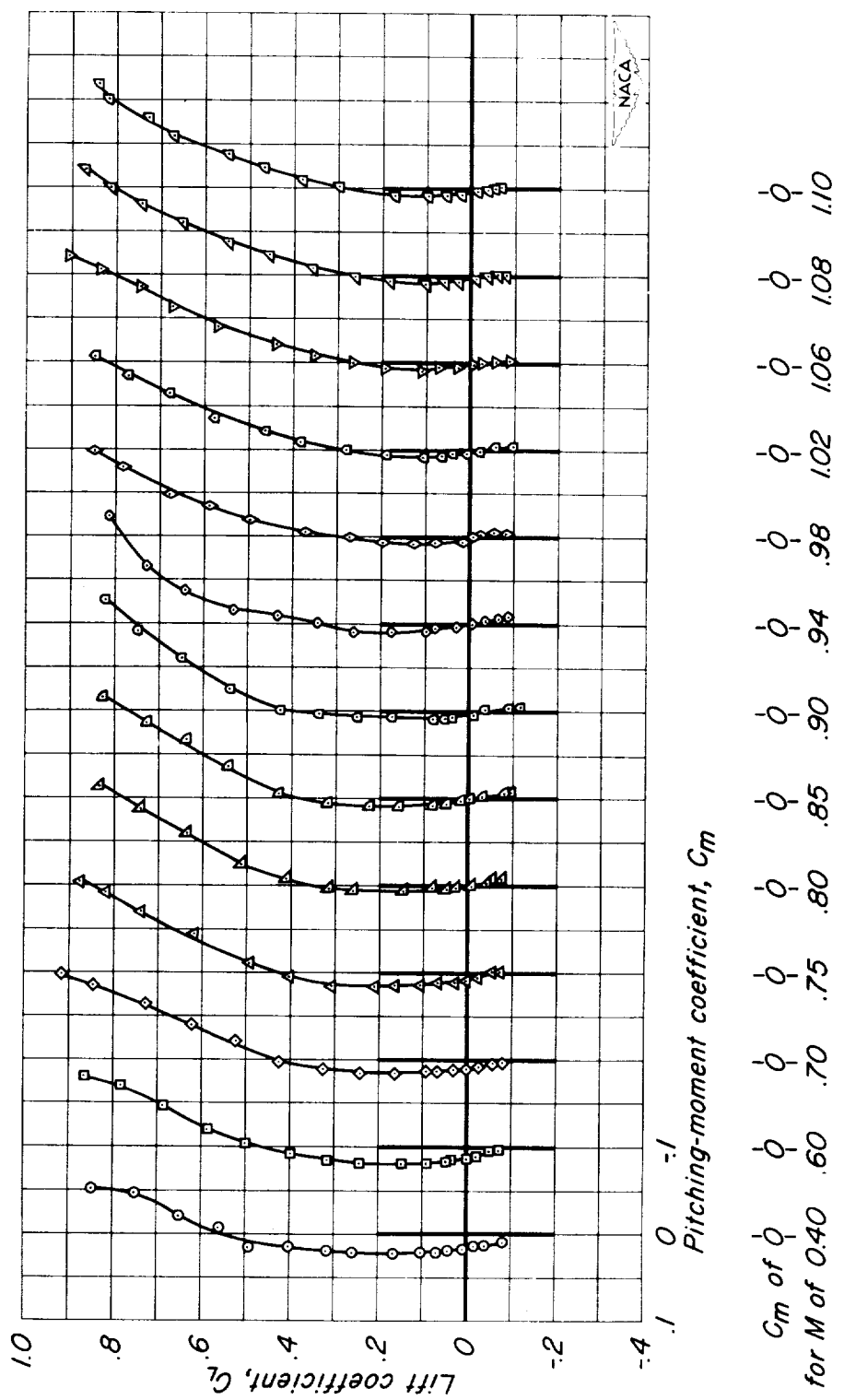


(o)  $A, l; t/c, 0.06$ .  
Figure 10 - Continued.



(p)  $A$ ,  $I$ ;  $t/c$ , 0.04.  
Figure 10.-Continued.

CONFIDENTIAL



(q)  $A, l; t/c, 0.02$ .  
Figure 10.-Concluded.

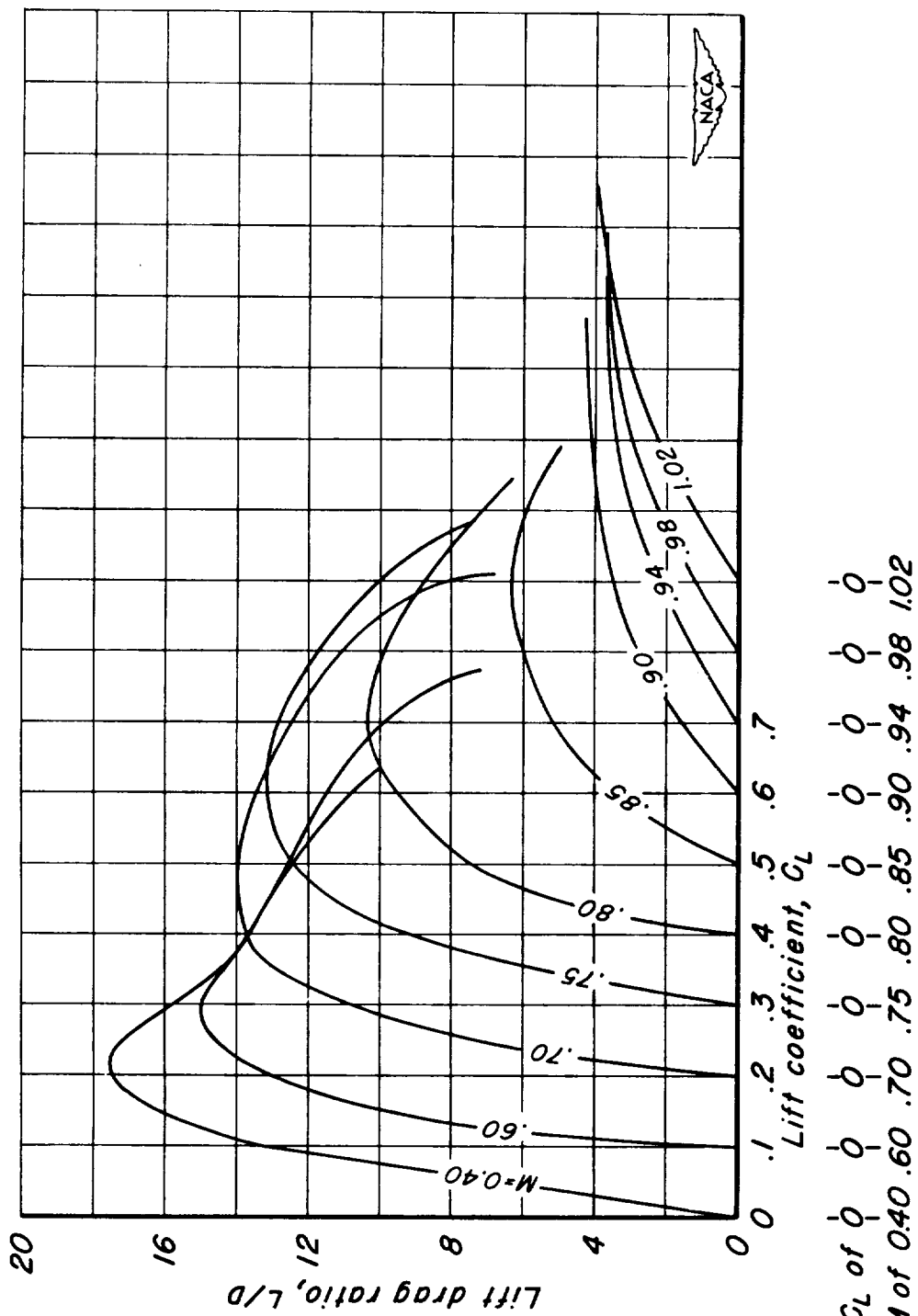
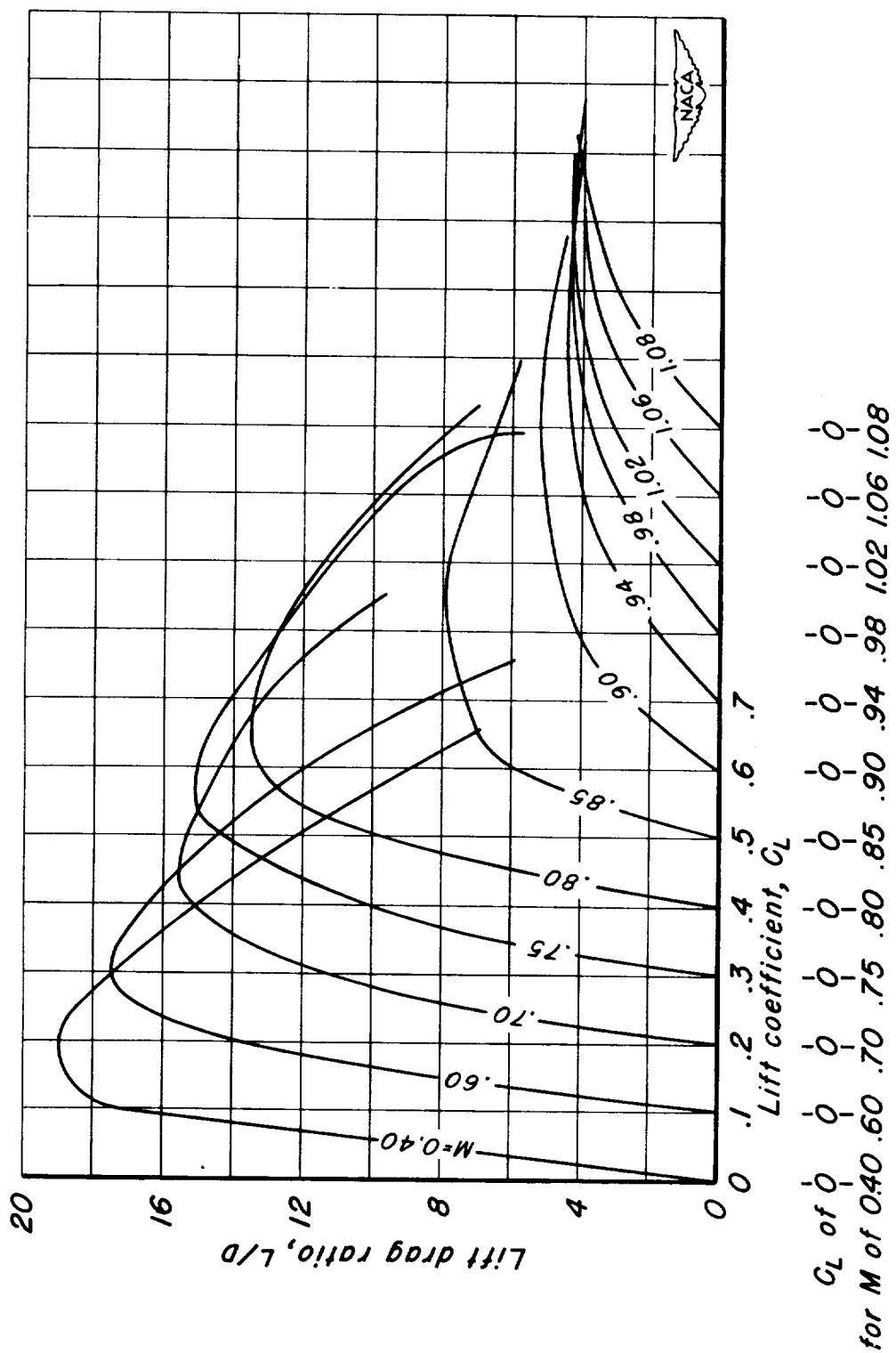
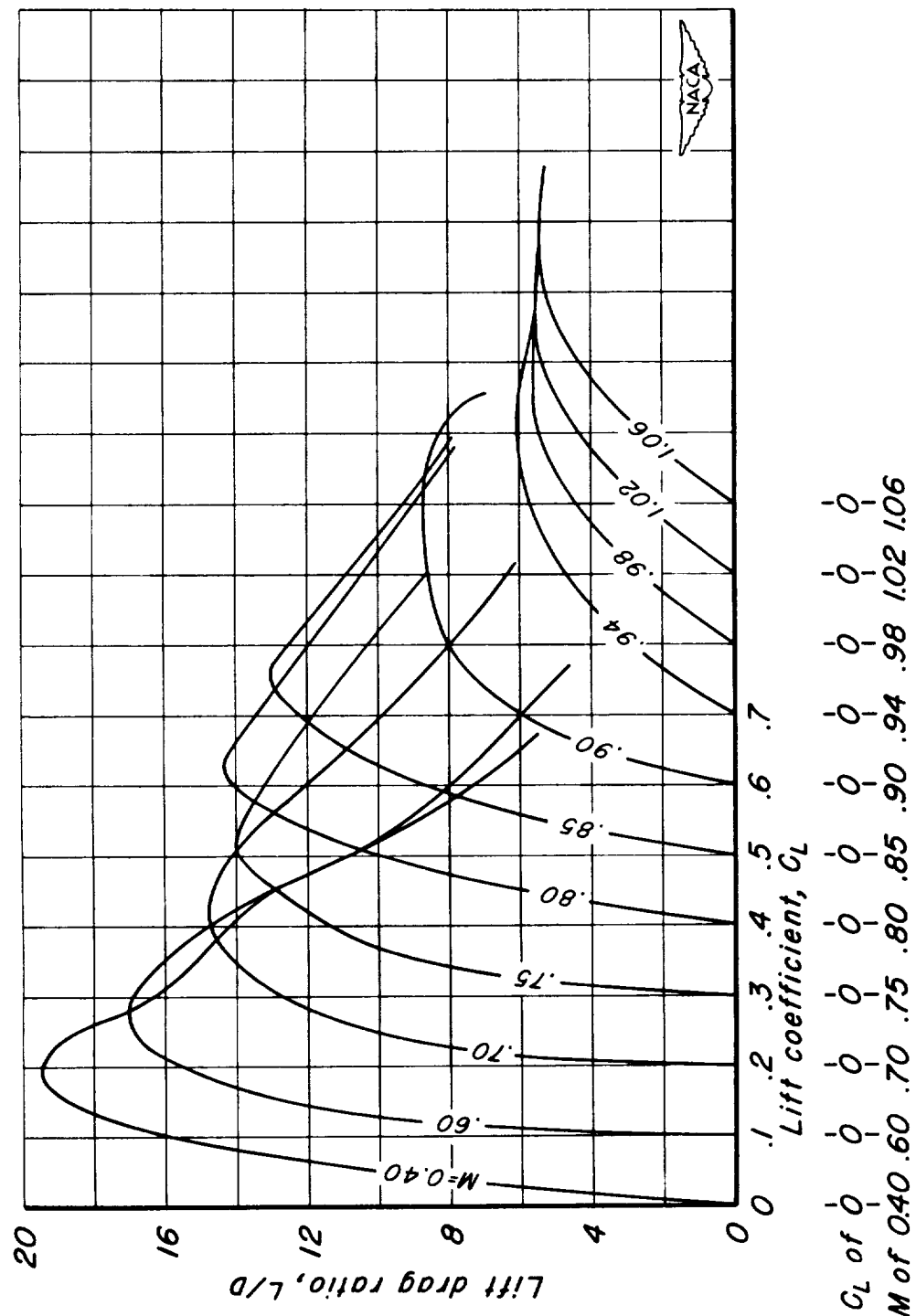


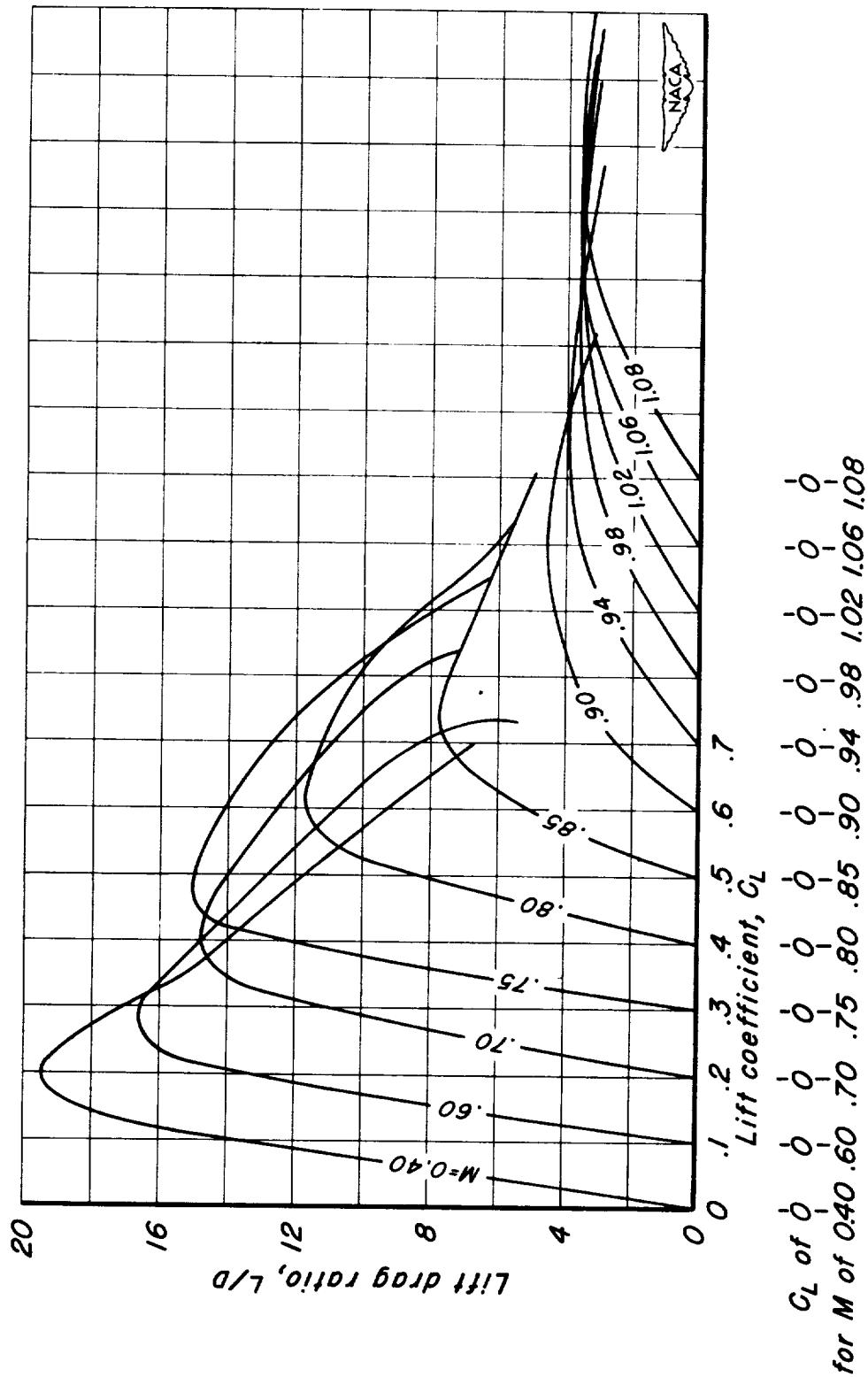
Figure II.- The variation of lift-drag ratio with lift coefficient for the rectangular wings with NACA 63AOXX sections.  
(a)  $A, 6; t/c, 0.10$ .

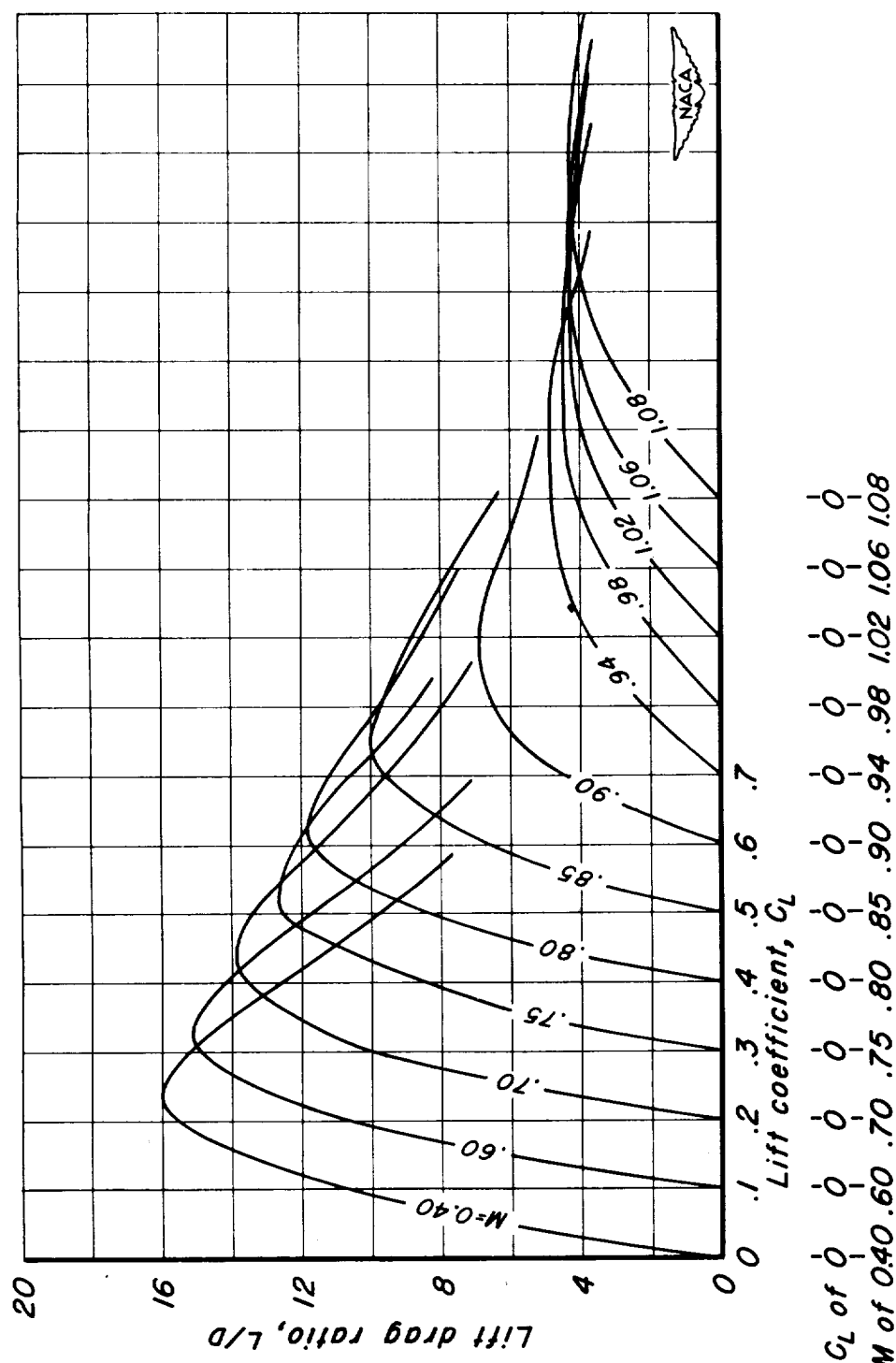


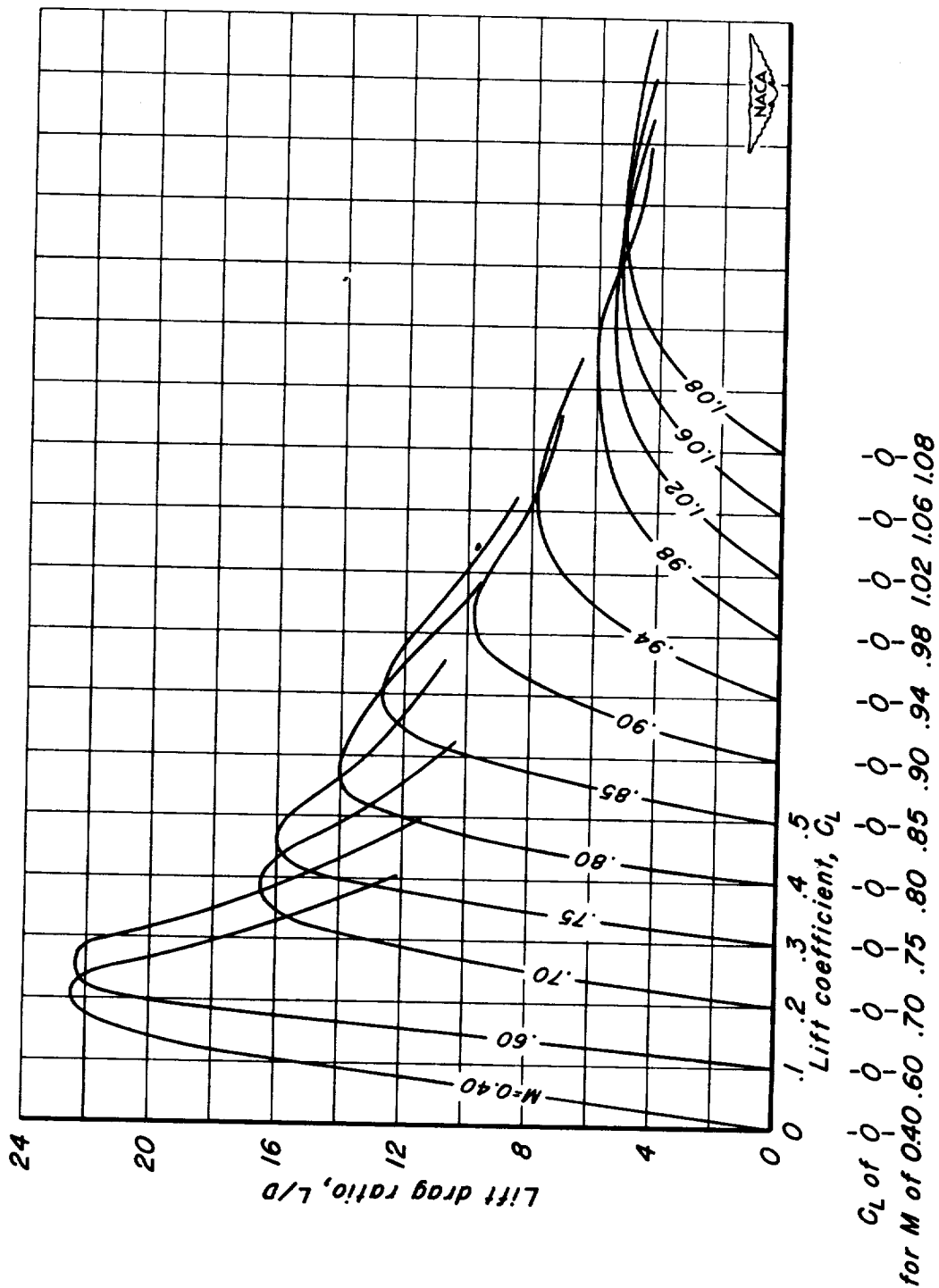
(b)  $A, 6; r/c, 0.08$ .  
Figure II - Continued.

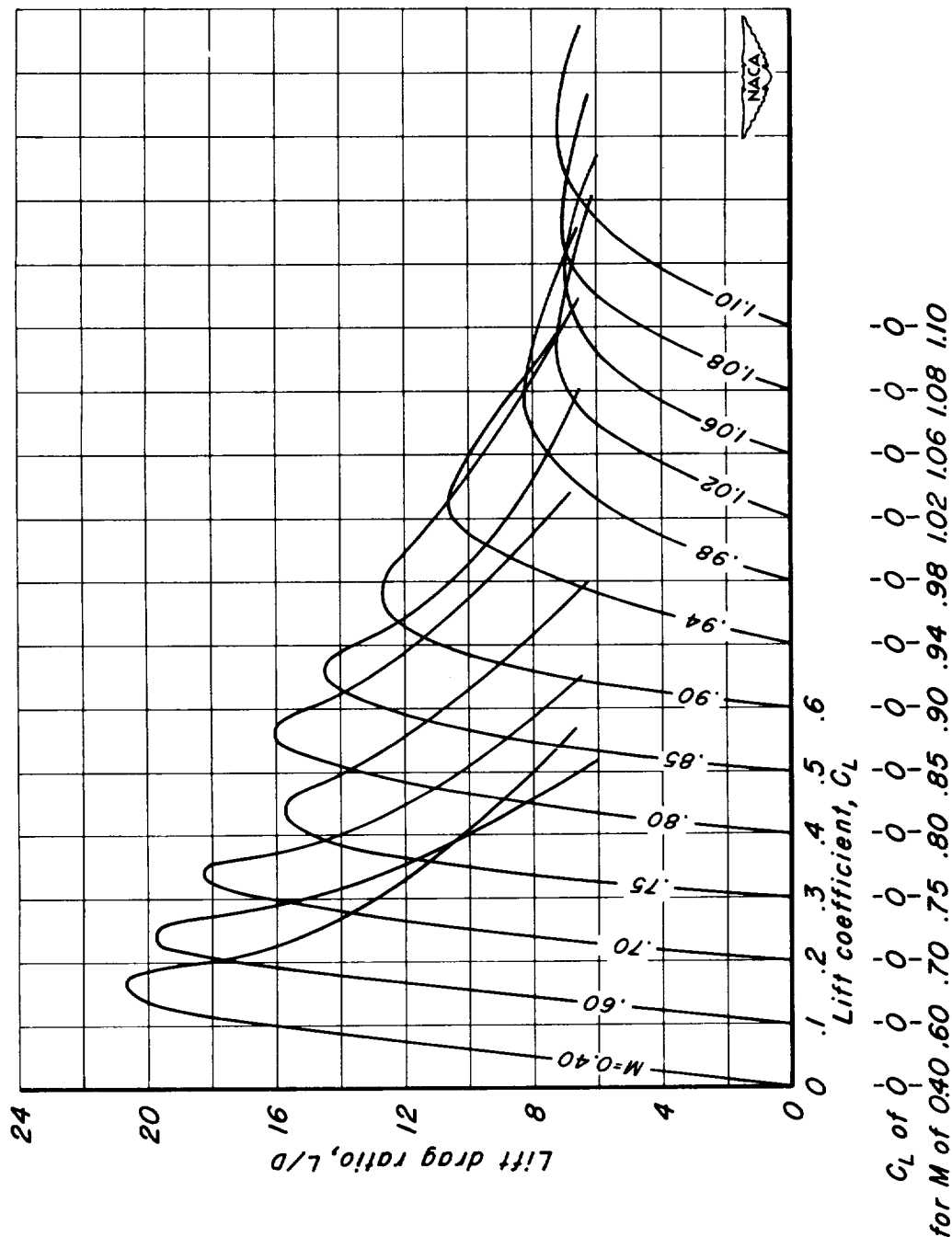


(c) A, 6;  $1/c$ , 0.06.  
Figure II. - Continued.

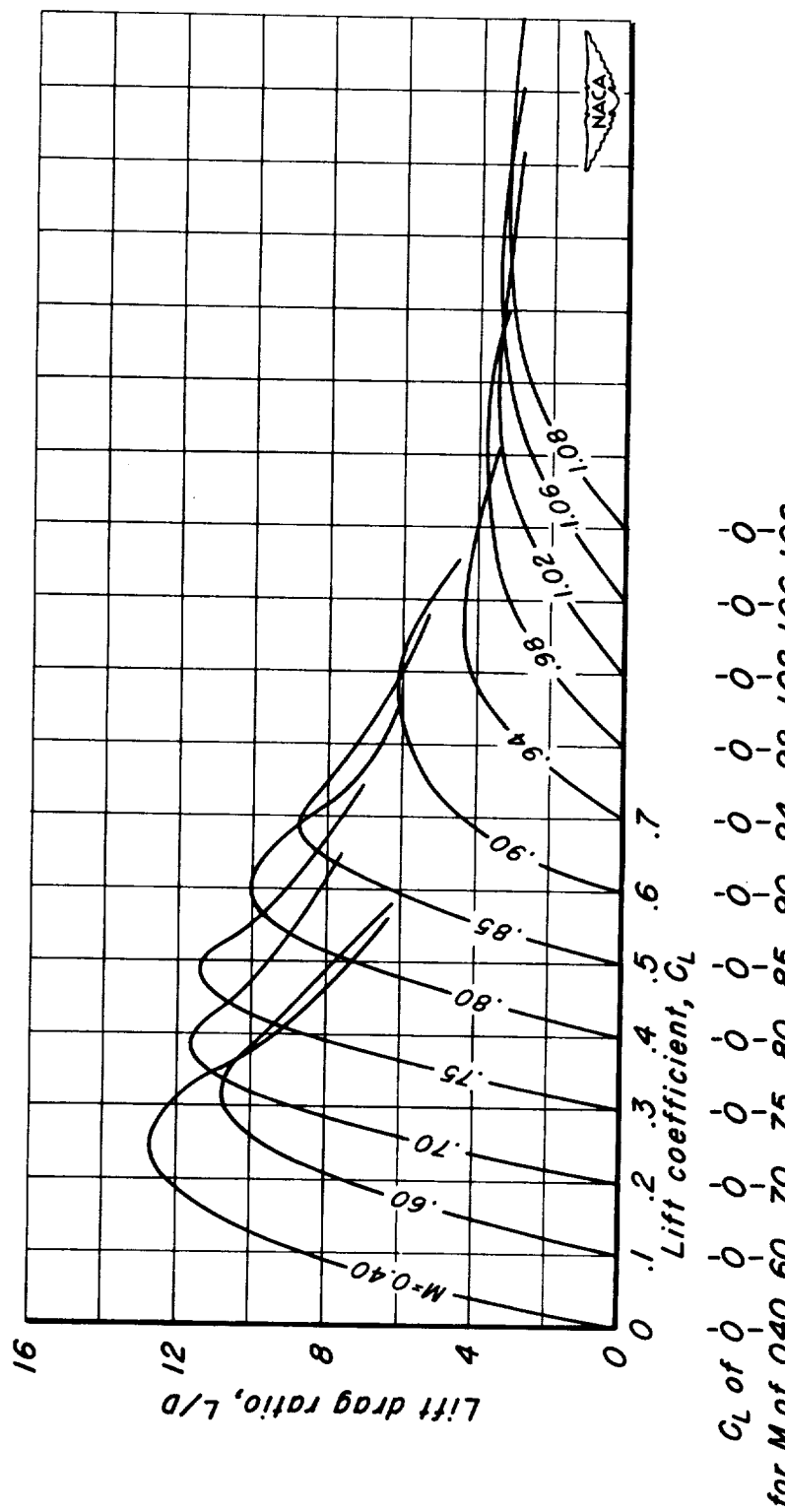




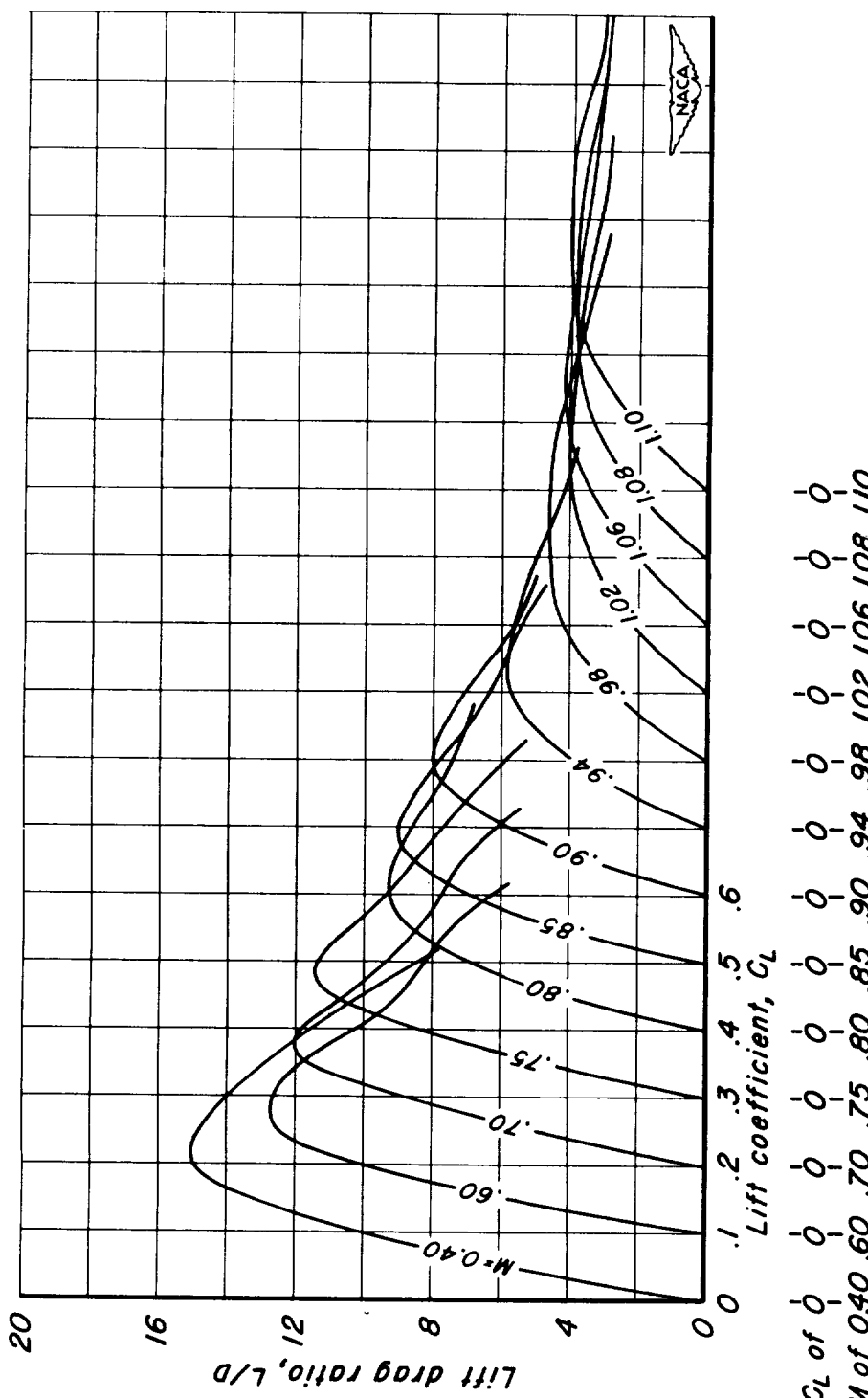




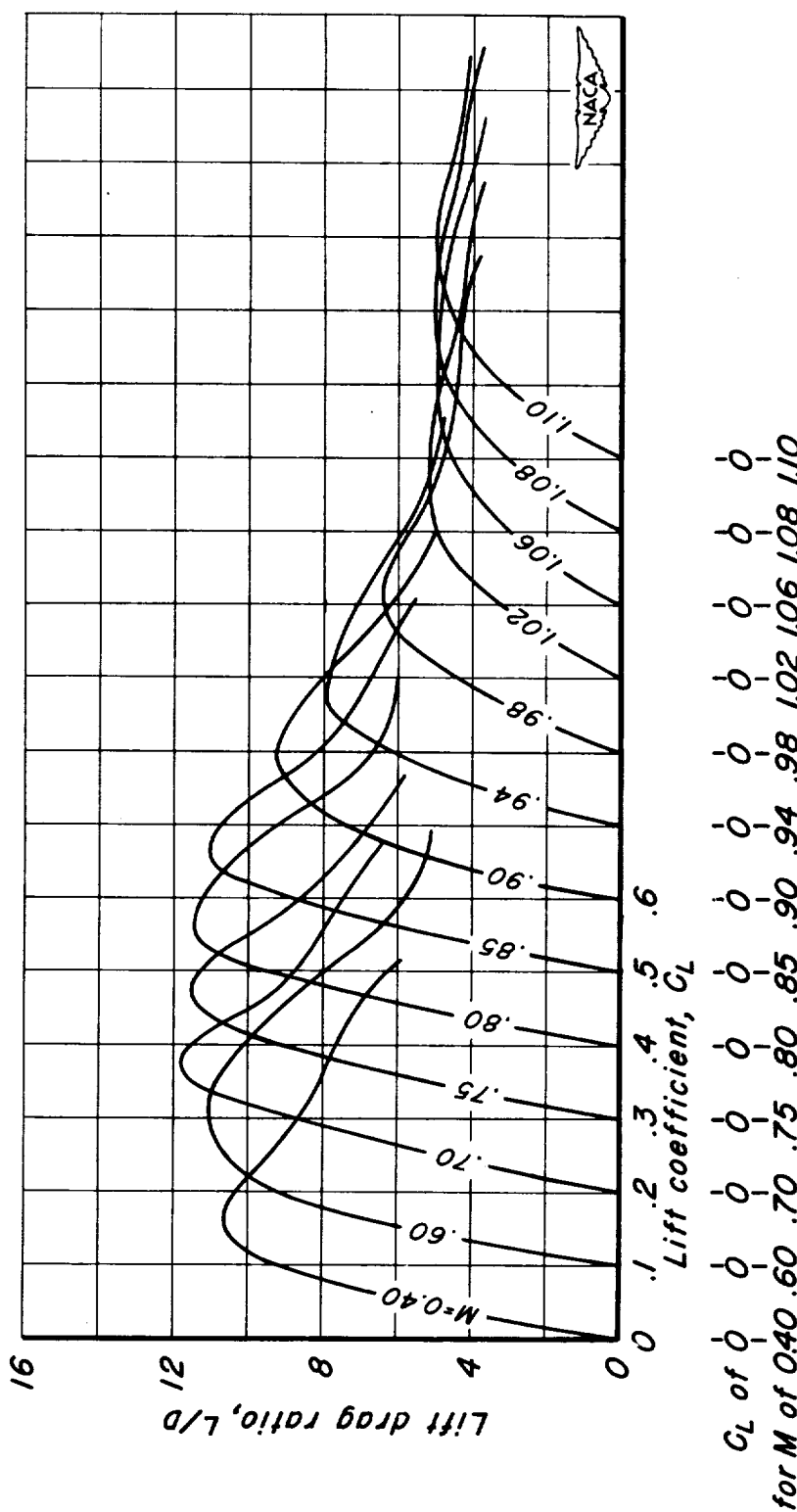
(g)  $A, 4; t/c, 0.04$ .  
Figure 11.- Continued.



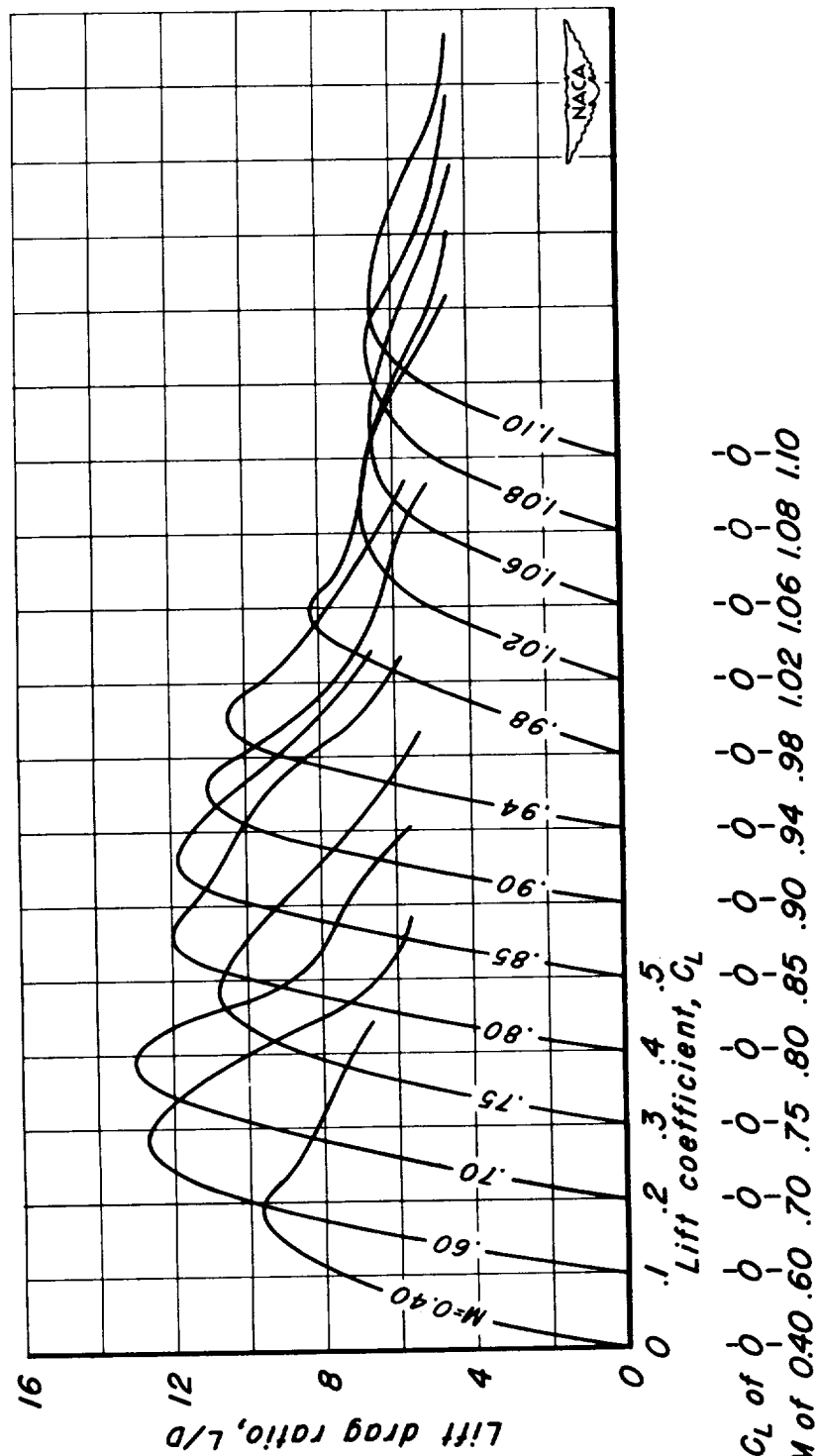
(h)  $A, 2; t/c, 0.10$ .  
Figure II.- Continued.

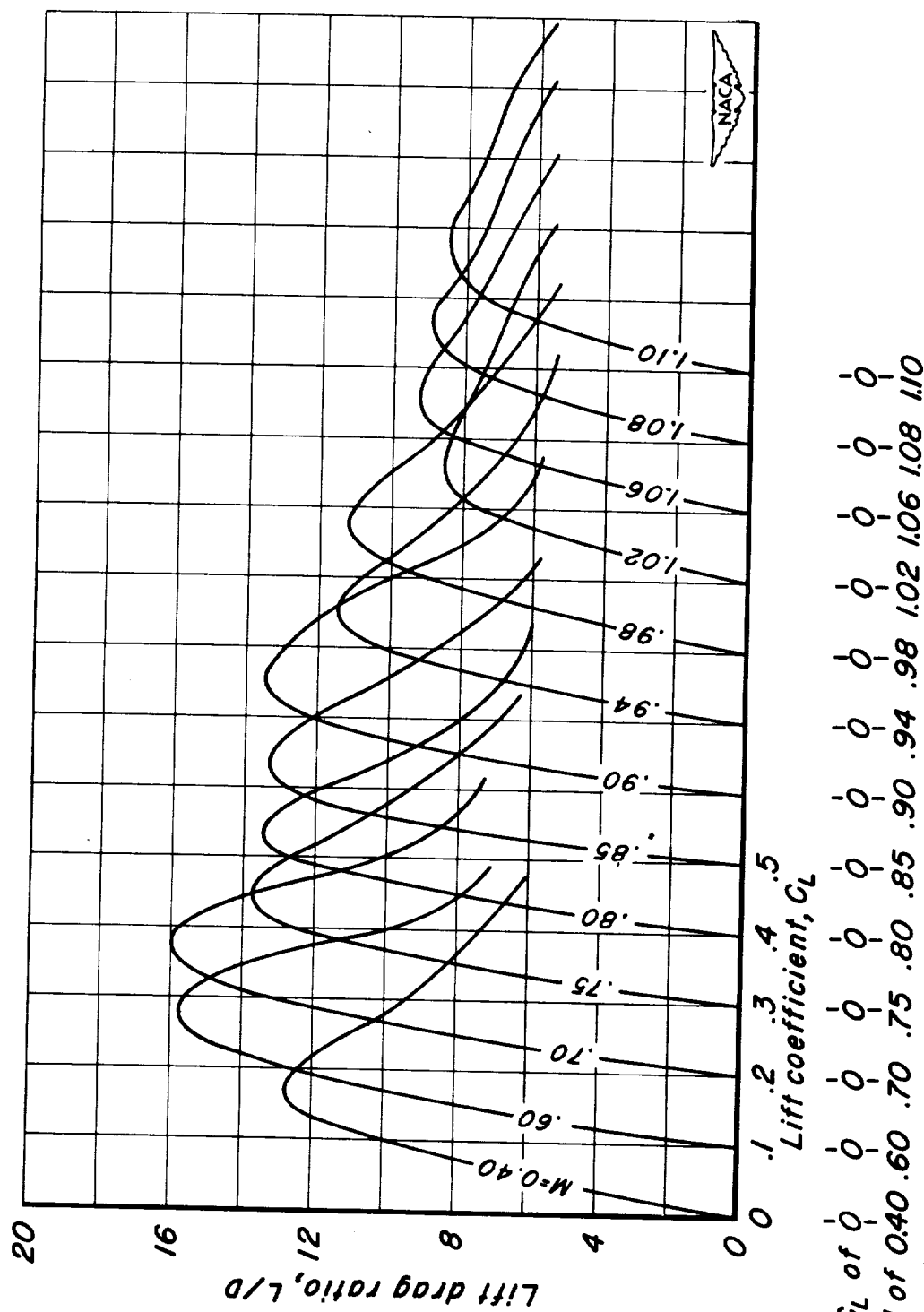


(i)  $A, 2; t/c, 0.08$ .  
Figure II.- Continued.

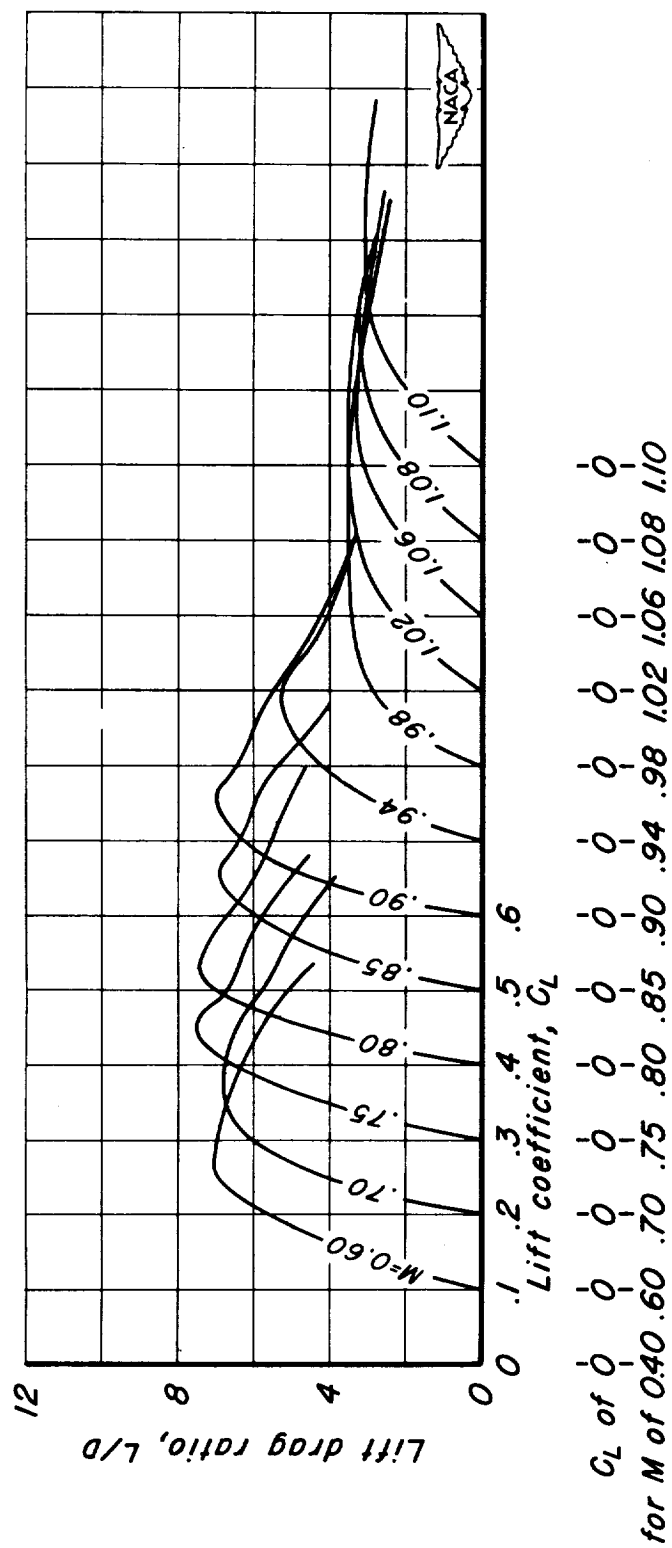


(J)  $A_2; t/c, 0.06$ .  
Figure 11.- Continued.

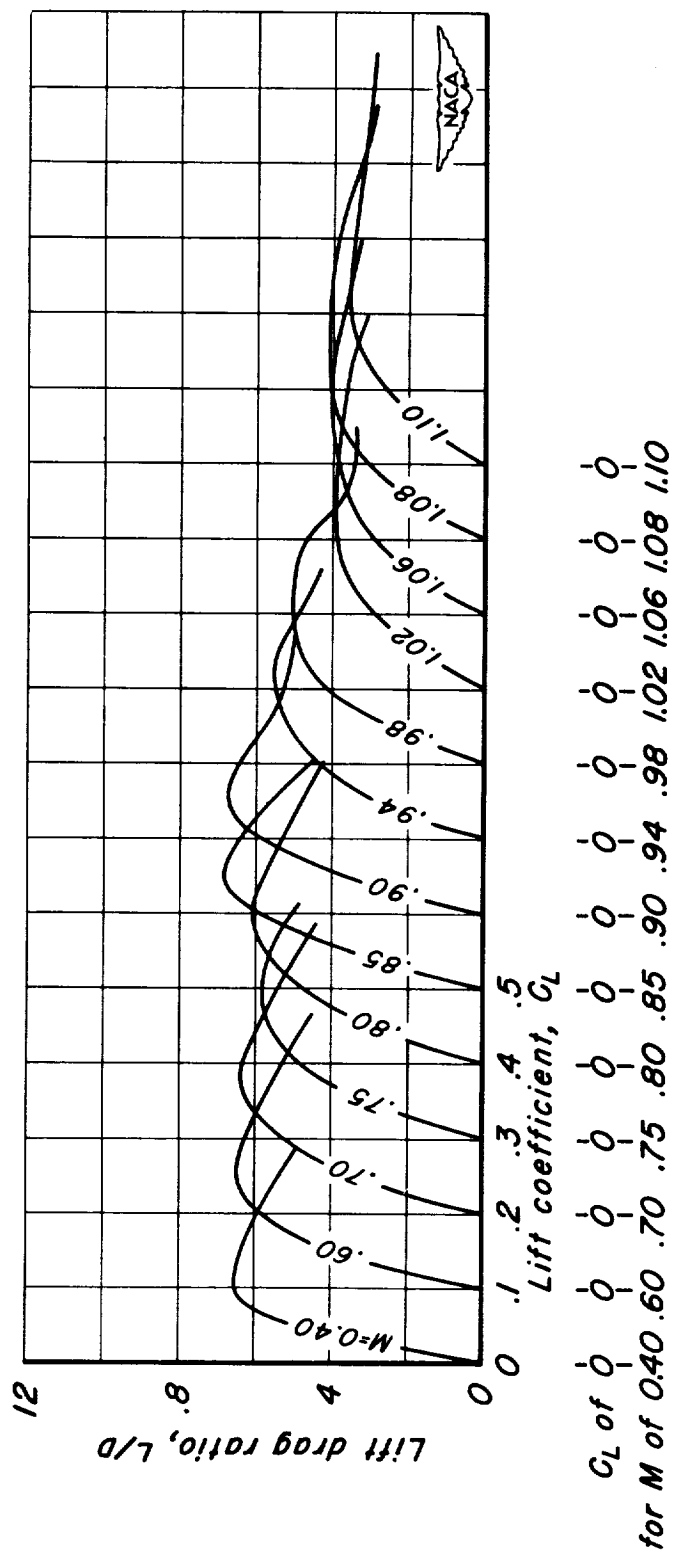




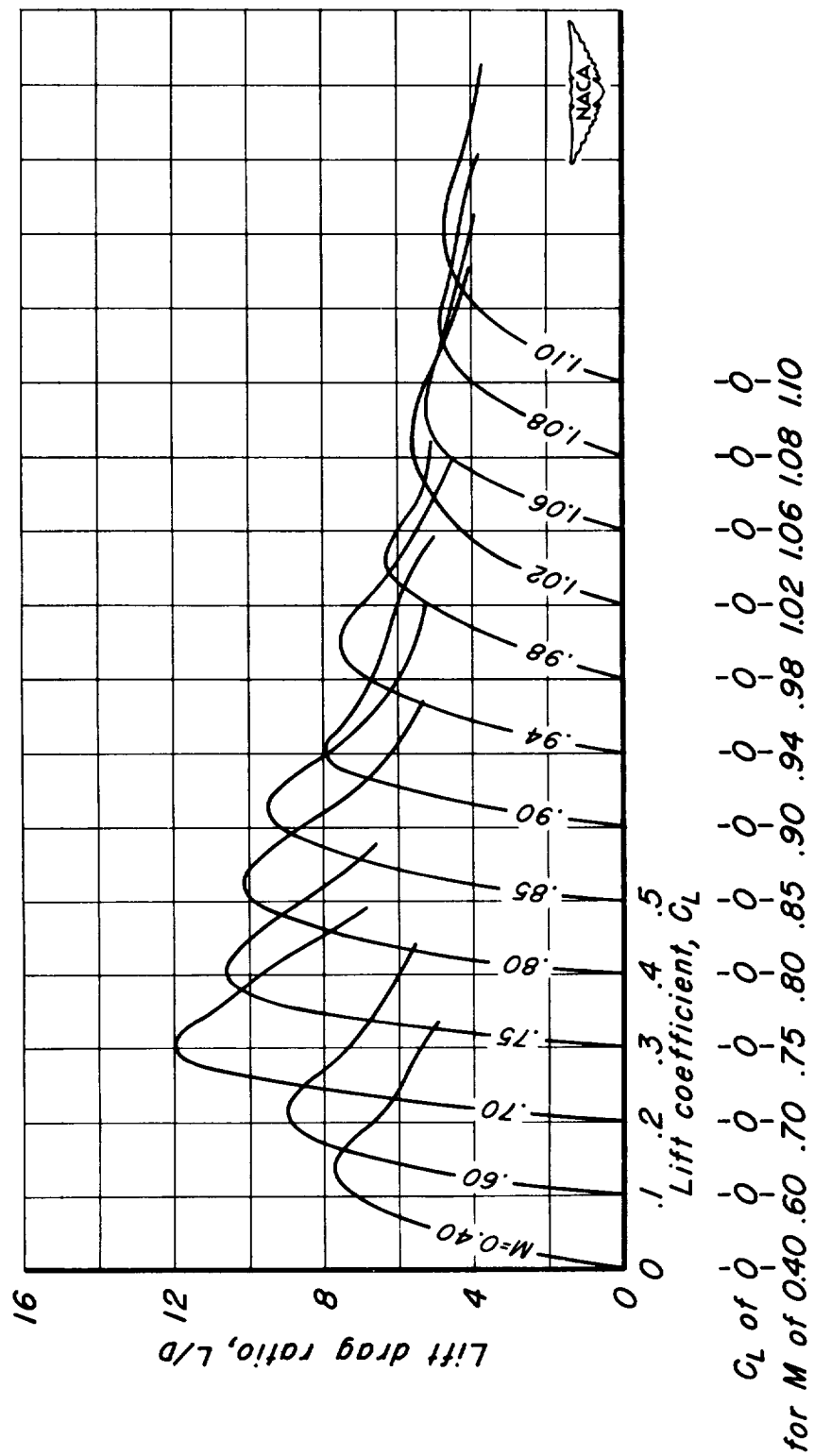
(1)  $A_1, 2; 1/c, 0.02$ .  
Figure II.- Continued.



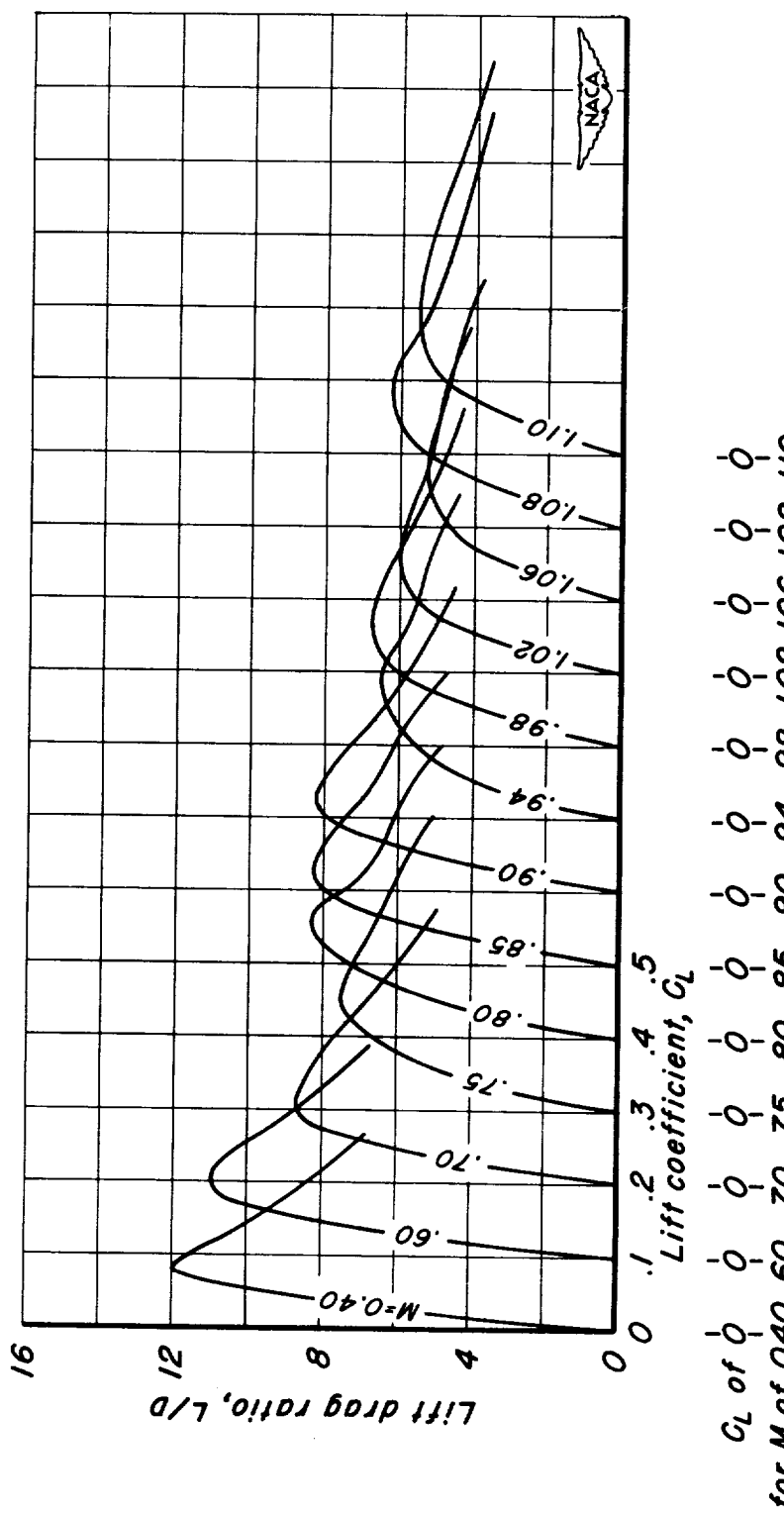
(m)  $A, l; t/c, 0.10$ .  
Figure II.- Continued.



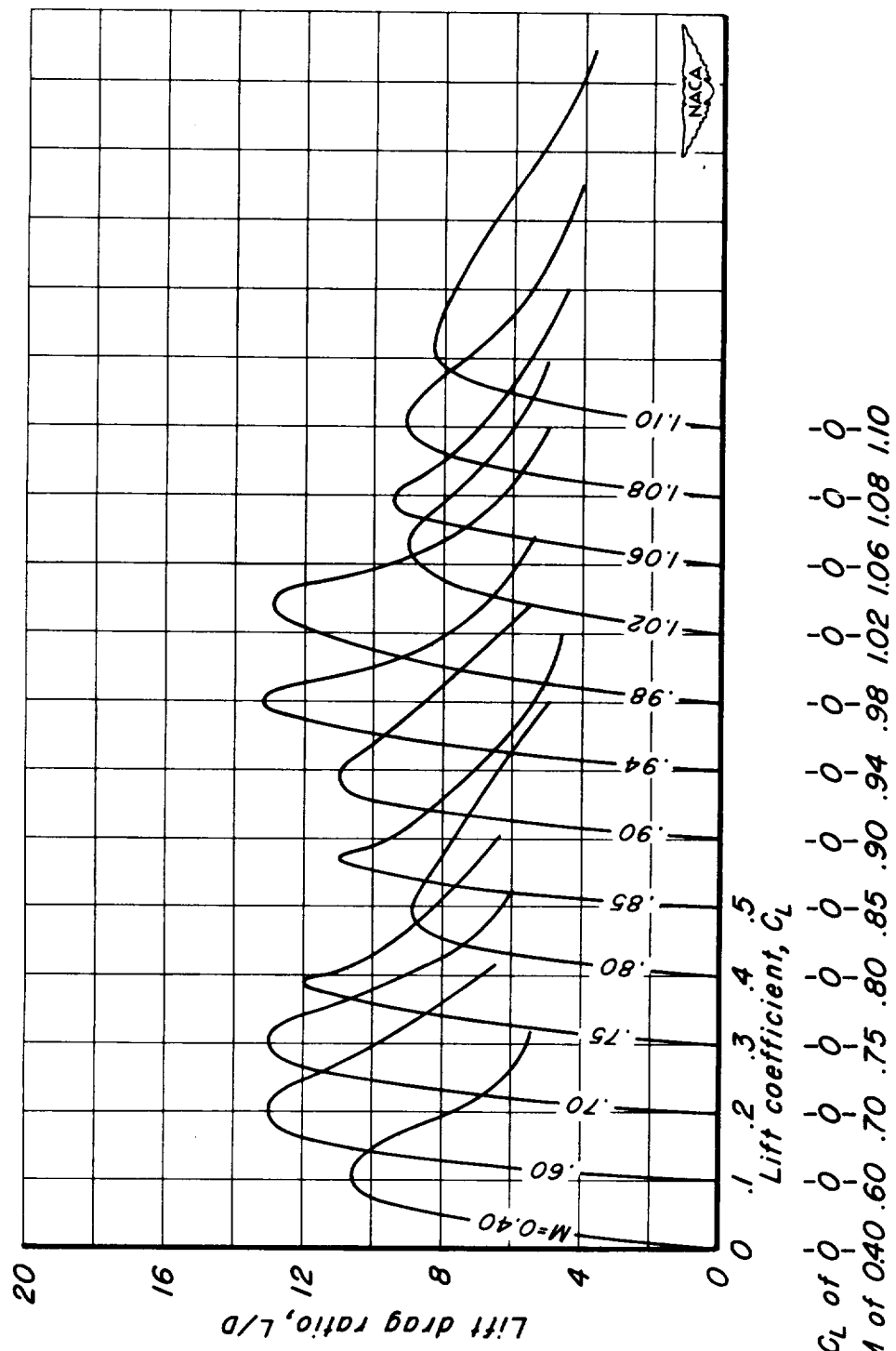
(n)  $A, l; t/c, 0.08$ .  
Figure II.—Continued.



(a)  $A, l_1, t/c, 0.06$ .  
Figure II.- Continued.



(b)  $A, l; t/c, 0.04$ .  
Figure II.- Continued.



(a)  $A, l; t/c, 0.02$ .  
Figure II.- Concluded.

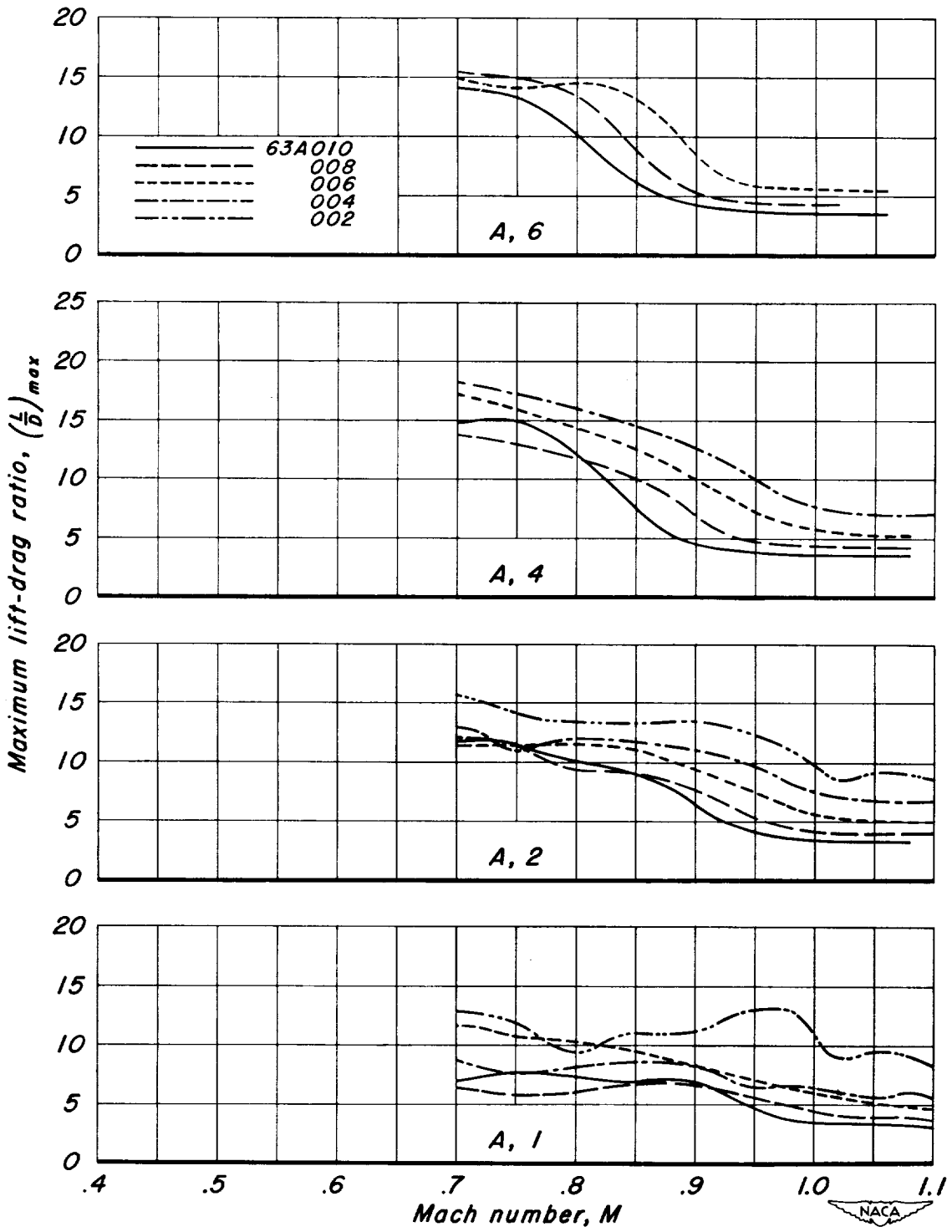


Figure 12.- The variation of maximum lift-drag ratio with Mach number for the rectangular wings with NACA 63AOXX sections.

CONFIDENTIAL

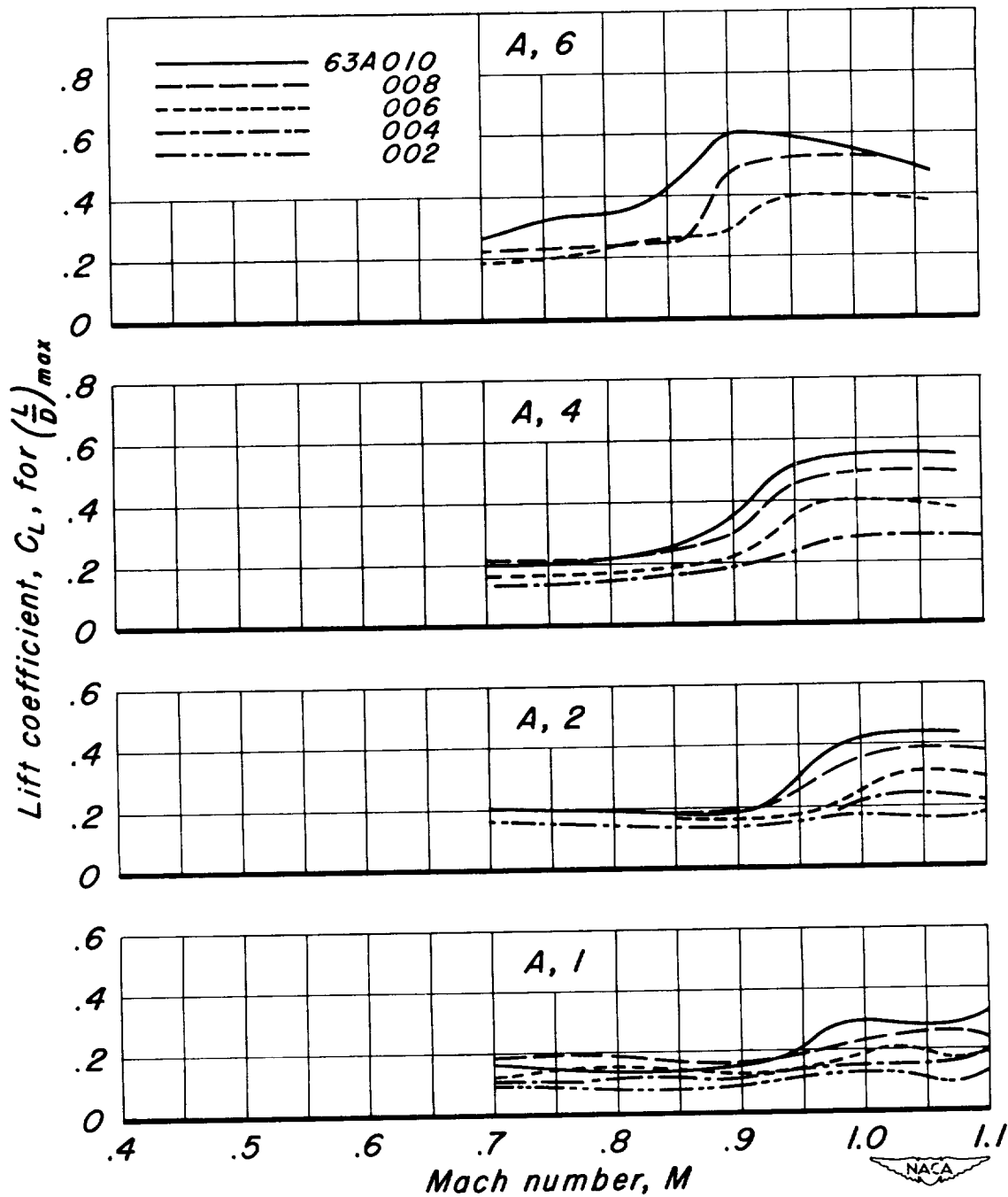


Figure 13.- The variation of lift coefficient for maximum lift-drag ratio with Mach number for the rectangular wings with NACA 63AOXX sections.

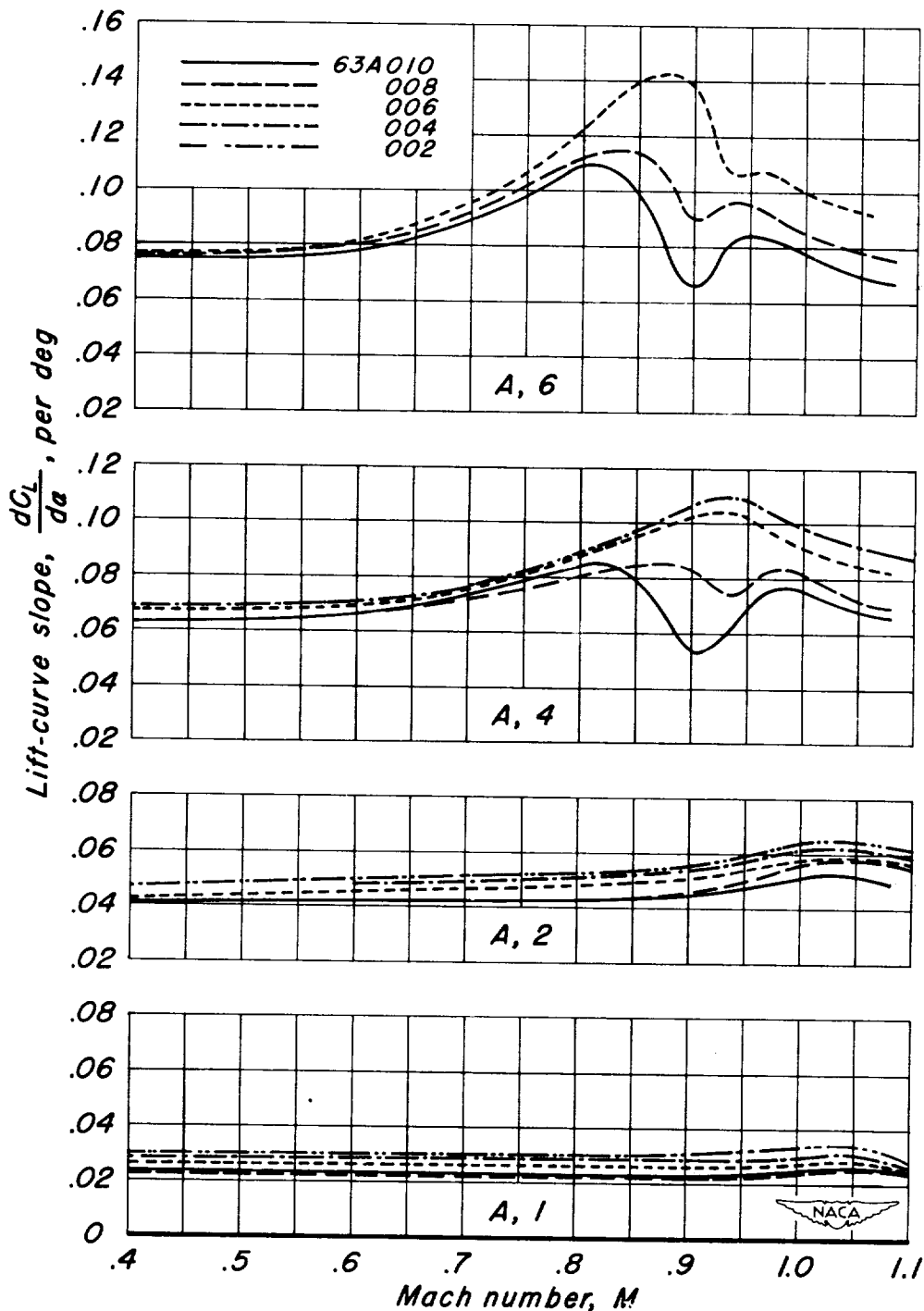


Figure 14.- The variation of lift-curve slope with Mach number for the rectangular wings with NACA 63AOXX sections.

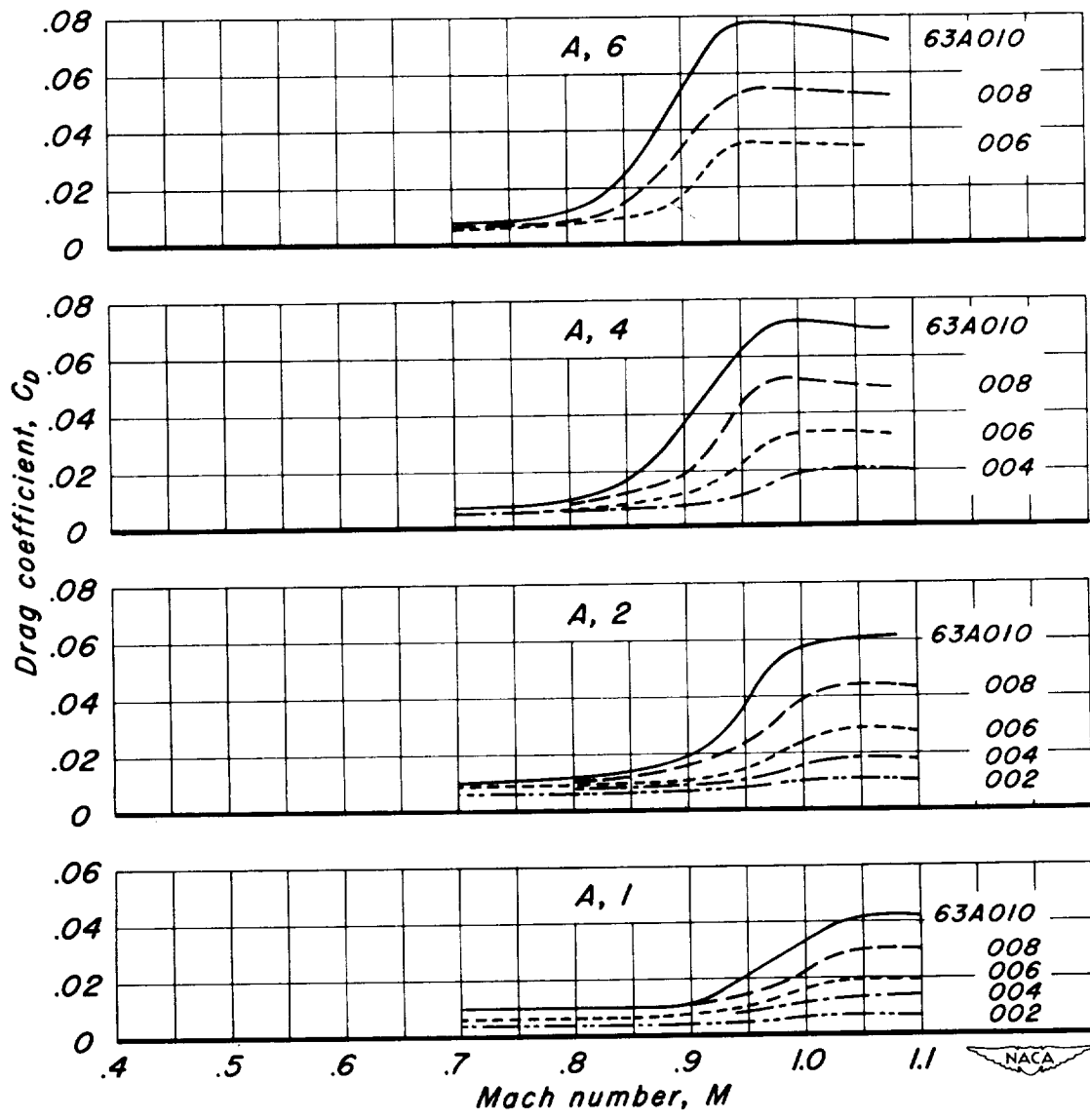
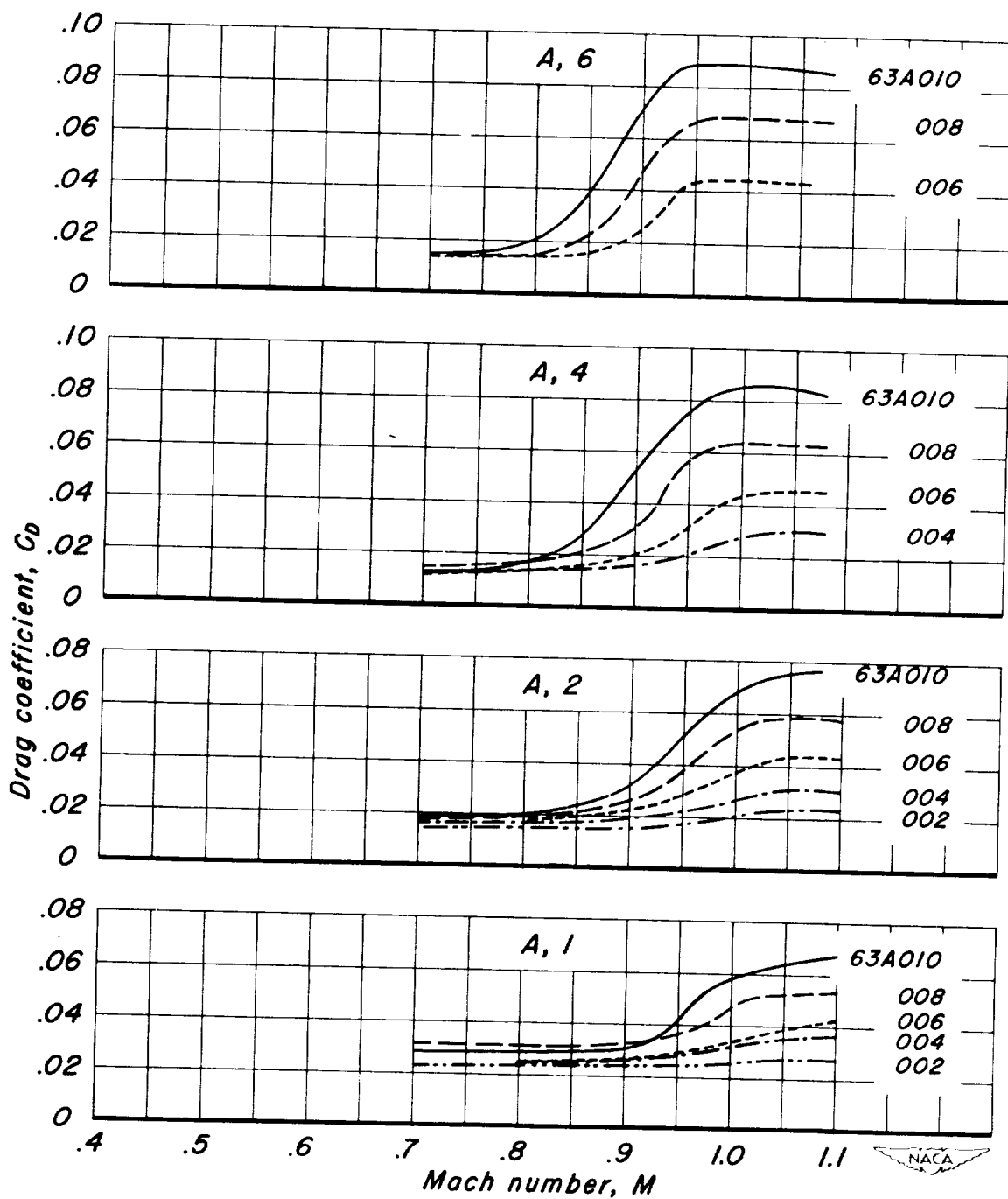
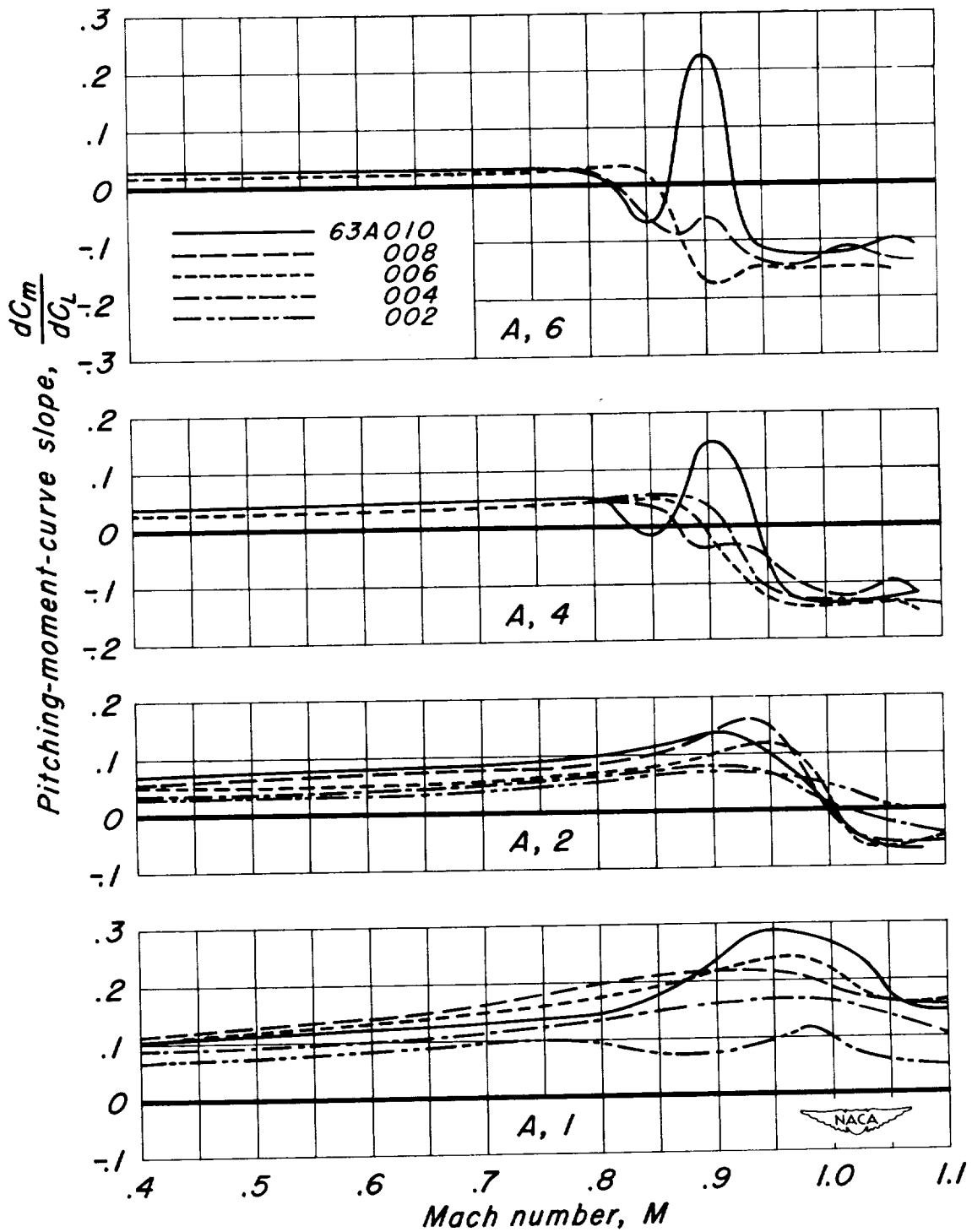
(a)  $C_{L,0}$ .

Figure 15.- The variation of drag coefficient with Mach number for the rectangular wings with NACA 63AOXX sections.



(b)  $C_L, 0.2$ .  
Figure 15.- Concluded



*Figure 16.- The variation of pitching-moment-curve slope with Mach number for the rectangular wings with NACA 63AOXX sections.*

CONFIDENTIAL

